

Est.  
1841

YORK  
ST JOHN  
UNIVERSITY

Lembrechts, Jonas J., van den Hoogen, Johan, Aalto, Juha ORCID: <https://orcid.org/0000-0001-6819-4911>, Ashcroft, Michael B., De Frenne, Pieter, Kemppinen, Julia, Kopecký, Martin, Luoto, Miska, Maclean, Ilya M. D., Crowther, Thomas W., Bailey, Joseph ORCID: <https://orcid.org/0000-0002-9526-7095>, Haesen, Stef, Klinges, David H., Niittynen, Pekka, Scheffers, Brett R., Van Meerbeek, Koenraad, Aartsma, Peter, Abdalaze, Otar, Abedi, Mehdi, Aerts, Rien, Ahmadian, Negar, Ahrends, Antje, Alatalo, Juha M., Alexander, Jake M., Nina Allonsius, Camille, Altman, Jan, Ammann, Christof, Andres, Christian, Andrews, Christopher, Ardö, Jonas, Arriga, Nicola, Arzac, Alberto, Aschero, Valeria, Assis, Rafael L., Johann Assmann, Jakob, Bader, Maaïke Y., Bahalkeh, Khadijeh, Barančok, Peter, Barrio, Isabel C., Barros, Agustina, Barthel, Matti, Basham, Edmund W., Bauters, Marijn, Bazzichetto, Manuele, Belevi Marchesini, Luca, Bell, Michael C., Benavides, Juan C., Luis Benito Alonso, José, Berauer, Bernd J., Bjerke, Jarle W., Björk, Robert G., Björkman, Mats P., Björnsdóttir, Katrin, Blonder, Benjamin, Boeckx, Pascal, Boike, Julia, Bokhorst, Stef, Brum, Bárbara N. S., Bruna, Josef, Buchmann, Nina, Buysse, Pauline, Luís Camargo, José, Campoe, Otávio C., Candan, Onur, Canessa, Rafaella, Cannone, Nicoletta, Carbognani, Michele, Carnicer, Jofre, Casanova-Katny, Angélica, Cesarz, Simone, Chojnicki, Bogdan, Choler, Philippe, Chown, Steven L., Cifuentes, Edgar F., Čiliak, Marek, Contador, Tamara, Convey, Peter, Cooper, Elisabeth J., Cremonese, Edoardo, Curasi, Salvatore R., Curtis, Robin, Cutini, Maurizio, Johan Dahlberg, C., Daskalova, Gergana N., Angel de Pablo, Miguel, Della Chiesa, Stefano, Dengler, Jürgen, Deronde, Bart, Descombes, Patrice, Di Cecco, Valter, Di Musciano, Michele, Dick, Jan, Dimarco, Romina D., Dolezal, Jiri, Dorrepaal, Ellen, Dušek, Jiří, Eisenhauer, Nico, Eklundh, Lars, Erickson, Todd E., Erschbamer, Brigitta, Eugster, Werner, Ewers, Robert M., Exton, Dan A., Fanin, Nicolas, Fazlioglu, Fatih, Feigenwinter, Iris, Fenu, Giuseppe, Ferlian, Olga, Rosa Fernández Calzado, M., Fernández-Pascual, Eduardo, Finckh,

Manfred, Finger Higgins, Rebecca, Forte, T'ai G. W., Freeman, Erika C., Frei, Esther R., Fuentes-Lillo, Eduardo, García, Rafael A., García, María B., Géron, Charly, Gharun, Mana, Ghosn, Dany, Gigauri, Khatuna, Gobin, Anne, Goded, Ignacio, Goeckede, Mathias, Gottschall, Felix, Goulding, Keith, Govaert, Sanne, Jessen Graae, Bente, Greenwood, Sarah, Greiser, Caroline, Grelle, Achim, Guénard, Benoit, Guglielmin, Mauro, Guillemot, Joannès, Haase, Peter, Haider, Sylvia, Halbritter, Aud H., Hamid, Maroof, Hammerle, Albin, Hampe, Arndt, Haugum, Siri V., Hederová, Lucia, Heinesch, Bernard, Helfter, Carole, Hepenstrick, Daniel, Herberich, Maximiliane, Herbst, Mathias, Hermanutz, Luise, Hik, David S., Hoffrén, Raúl, Homeier, Jürgen, Hörtnagl, Lukas, Høye, Toke T., Hrbacek, Filip, Hylander, Kristoffer, Iwata, Hiroki, Antoni Jackowicz-Korczynski, Marcin, Jactel, Hervé, Järveoja, Järvi, Jastrzębowski, Szymon, Jentsch, Anke, Jiménez, Juan J., Jónsdóttir, Ingibjörg S., Jucker, Tommaso, Jump, Alistair S., Juszczak, Radoslaw, Kanka, Róbert, Kašpar, Vít, Kazakis, George, Kelly, Julia, Khuroo, Anzar A., Klemedtsson, Leif, Klisz, Marcin, Kljun, Natascha, Knohl, Alexander, Kobler, Johannes, Kollár, Jozef, Kotowska, Martyna M., Kovács, Bence, Kreyling, Juergen, Lamprecht, Andrea, Lang, Simone I., Larson, Christian, Larson, Keith, Laska, Kamil, le Maire, Gueric, Leihy, Rachel I., Lens, Luc, Liljebladh, Bengt, Lohila, Annalea, Lorite, Juan, Loubet, Benjamin, Lynn, Joshua, Macek, Martin, Mackenzie, Roy, Magliulo, Enzo, Maier, Regine, Malfasi, Francesco, Máliš, František, Man, Matěj, Manca, Giovanni, Manco, Antonio, Manise, Tanguy, Manolaki, Paraskevi, Marciniak, Felipe, Matula, Radim, Clara Mazzolari, Ana, Medinets, Sergiy, Medinets, Volodymyr, Meeussen, Camille, Merinero, Sonia, de Cássia Guimarães Mesquita, Rita, Meusburger, Katrin, Meysman, Filip J. R., Michaletz, Sean T., Milbau, Ann, Moiseev, Dmitry, Moiseev, Pavel, Mondoni, Andrea, Monfries, Ruth, Montagnani, Leonardo, Moriana-Armendariz, Mikel, Morra di Cella, Umberto, Mörsdorf, Martin, Mosedale, Jonathan R., Muffler, Lena, Muñoz-Rojas, Miriam, Myers, Jonathan A., Myers-Smith, Isla H., Nagy, Laszlo, Nardino, Marianna, Naujokaitis-Lewis, Ilona, Newling, Emily, Nicklas, Lena, Niedrist, Georg, Niessner, Armin, Nilsson, Mats B., Normand, Signe, Nosetto, Marcelo D., Nouvellon, Yann, Nuñez, Martin A., Ogaya, Romà, Ogée, Jérôme, Okello, Joseph, Olejnik, Janusz, Eivind Olesen, Jørgen, Opedal, Øystein, Orsenigo,

Simone, Palaj, Andrej, Pampuch, Timo, Panov, Alexey V., Pärtel, Meelis, Pastor, Ada, Pauchard, Aníbal, Pauli, Harald, Pavelka, Marian, Pearse, William D., Peichl, Matthias, Pellissier, Loïc, Penczykowski, Rachel M., Penuelas, Josep, Petit Bon, Matteo, Petraglia, Alessandro, Phartyal, Shyam S., Phoenix, Gareth K., Pio, Casimiro, Pitacco, Andrea, Pitteloud, Camille, Plichta, Roman, Porro, Francesco, Portillo-Estrada, Miguel, Poulenard, Jérôme, Poyatos, Rafael, Prokushkin, Anatoly S., Puchalka, Radoslaw, Puşcaş, Mihai, Radujković, Dajana, Randall, Krystal, Ratier Backes, Amanda, Remmele, Sabine, Remmers, Wolfram, Renault, David, Risch, Anita C., Rixen, Christian, Robinson, Sharon A., Robroek, Bjorn J.M., Rocha, Adrian V., Rossi, Christian, Rossi, Graziano, Rounsard, Olivier, Rubtsov, Alexey V., Saccone, Patrick, Sagot, Clotilde, Sallo Bravo, Jhonatan, Santos, Cinthya C., Sarneel, Judith M., Scharnweber, Tobias, Schmeddes, Jonas, Schmidt, Marius, Scholten, Thomas, Schuchardt, Max, Schwartz, Naomi, Scott, Tony, Seeber, Julia, Cristina Segalin de Andrade, Ana, Seipel, Tim, Semenchuk, Philipp, Senior, Rebecca A., Serra-Diaz, Josep M., Sewerniak, Piotr, Shekhar, Ankit, Sidenko, Nikita V., Siebicke, Lukas, Siegwart Collier, Laura, Simpson, Elizabeth, Siqueira, David P., Sitková, Zuzana, Six, Johan, Smiljanic, Marko, Smith, Stuart W., Smith-Tripp, Sarah, Somers, Ben, Vedel Sørensen, Mia, João L. L. Souza, José, Israel Souza, Bartolomeu, Souza Dias, Arildo, Spasojevic, Marko J., Speed, James D. M., Spicher, Fabien, Stanisci, Angela, Steinbauer, Klaus, Steinbrecher, Rainer, Steinwandter, Michael, Stemkovski, Michael, Stephan, Jörg G., Stiegler, Christian, Stoll, Stefan, Svátek, Martin, Svoboda, Miroslav, Tagesson, Torbern, Tanentzap, Andrew J., Tanneberger, Franziska, Theurillat, Jean-Paul, Thomas, Haydn J. D., Thomas, Andrew D., Tielbörger, Katja, Tomaselli, Marcello, Albert Treier, Urs, Trouillier, Mario, Dan Turtureanu, Pavel, Tutton, Rosamond, Tyystjärvi, Vilna A., Ueyama, Masahito, Ujházy, Karol, Ujházyová, Mariana, Uogintas, Domas, Urban, Anastasiya V., Urban, Josef, Urbaniak, Marek, Ursu, Tudor-Mihai, Primo Vaccari, Francesco, Van de Vondel, Stijn, van den Brink, Liesbeth, Van Geel, Maarten, Vandvik, Vigdis, Vangansbeke, Pieter, Varlagin, Andrej, Veen, G.F., Veenendaal, Elmar, Venn, Susanna E., Verbeeck, Hans, Verbruggen, Erik, Verheijen, Frank G.A., Villar, Luis, Vitale, Luca, Vittoz, Pascal, Vives-Inгла, Maria, von Oppen, Jonathan, Walz,

Josefine, Wang, Runxi, Wang, Yifeng, Way, Robert G., Wedegärtner, Ronja E. M., Weigel, Robert, Wild, Jan, Wilkinson, Matthew, Wilmking, Martin, Wingate, Lisa, Winkler, Manuela, Wipf, Sonja, Wohlfahrt, Georg, Xenakis, Georgios, Yang, Yan, Yu, Zicheng, Yu, Kailiang, Zellweger, Florian, Zhang, Jian, Zhang, Zhaochen, Zhao, Peng, Ziemblińska, Klaudia, Zimmermann, Reiner, Zong, Shengwei, Zyryanov, Viacheslav I., Nijs, Ivan and Lenoir, Jonathan (2021) Global maps of soil temperature. *Global Change Biology*.

Downloaded from: <http://ray.yorks.ac.uk/id/eprint/5803/>

The version presented here may differ from the published version or version of record. If you intend to cite from the work you are advised to consult the publisher's version:

<http://dx.doi.org/10.1111/gcb.16060>

Research at York St John (RaY) is an institutional repository. It supports the principles of open access by making the research outputs of the University available in digital form. Copyright of the items stored in RaY reside with the authors and/or other copyright owners. Users may access full text items free of charge, and may download a copy for private study or non-commercial research. For further reuse terms, see licence terms governing individual outputs. [Institutional Repository Policy Statement](#)

# RaY

Research at the University of York St John

For more information please contact RaY at [ray@yorks.ac.uk](mailto:ray@yorks.ac.uk)

# 1 Global maps of soil temperature

2 *Running head: Global maps of soil temperature*

3

4 Jonas J. Lembrechts<sup>1,\*</sup>, Johan van den Hoogen<sup>2,\*</sup>, Juha Aalto<sup>3,4</sup>, Michael B. Ashcroft<sup>5,6</sup>, Pieter De Frenne<sup>7</sup>, Julia  
5 Kempainen<sup>8</sup>, Martin Kopecký<sup>9,10</sup>, Miska Luoto<sup>11</sup>, Ilya M. D. Maclean<sup>12</sup>, Thomas W. Crowther<sup>2</sup>, Joseph J. Bailey<sup>13</sup>,  
6 Stef Haesen<sup>14</sup>, David H. Klings<sup>15,16</sup>, Pekka Niittynen<sup>11</sup>, Brett R. Scheffers<sup>17</sup>, Koenraad Van Meerbeek<sup>14</sup>, Peter  
7 Aartsma<sup>18</sup>, Otar Abdalaze<sup>19</sup>, Mehdi Abedi<sup>20</sup>, Rien Aerts<sup>21</sup>, Negar Ahmadian<sup>20</sup>, Antje Ahrends<sup>22</sup>, Juha M. Alatalo<sup>23</sup>,  
8 Jake M. Alexander<sup>24</sup>, Camille Nina Allonsius<sup>25</sup>, Jan Altman<sup>9</sup>, Christof Ammann<sup>26</sup>, Christian Andres<sup>27</sup>, Christopher  
9 Andrews<sup>28</sup>, Jonas Ardö<sup>29</sup>, Nicola Arriga<sup>30</sup>, Alberto Arzac<sup>31</sup>, Valeria Aschero<sup>32,33</sup>, Rafael L. Assis<sup>34</sup>, Jakob Johann  
10 Assmann<sup>35,36</sup>, Maaïke Y. Bader<sup>37</sup>, Khadijeh Bahalkeh<sup>20</sup>, Peter Barančok<sup>38</sup>, Isabel C. Barrio<sup>39</sup>, Agustina Barros<sup>40</sup>,  
11 Matti Barthel<sup>27</sup>, Edmund W. Basham<sup>15</sup>, Marijn Bauters<sup>41</sup>, Manuele Bazzichetto<sup>42</sup>, Luca Belelli Marchesini<sup>43</sup>,  
12 Michael C. Bell<sup>44</sup>, Juan C. Benavides<sup>45</sup>, José Luis Benito Alonso<sup>46</sup>, Bernd J. Berauer<sup>47,48</sup>, Jarle W. Bjerke<sup>49</sup>, Robert  
13 G. Björk<sup>50,51</sup>, Mats P. Björkman<sup>50,51</sup>, Katrin Björnsdóttir<sup>52</sup>, Benjamin Blonder<sup>53</sup>, Pascal Boeckx<sup>41</sup>, Julia Boike<sup>54,55</sup>,  
14 Stef Bokhorst<sup>21</sup>, Bárbara N. S. Brum<sup>56</sup>, Josef Brůna<sup>9</sup>, Nina Buchmann<sup>27</sup>, Pauline Buysse<sup>57</sup>, José Luís Camargo<sup>58</sup>,  
15 Otávio C. Campoe<sup>59</sup>, Onur Candan<sup>60</sup>, Rafaella Canessa<sup>61,62</sup>, Nicoletta Cannone<sup>63</sup>, Michele Carbognani<sup>64</sup>, Jofre  
16 Carnicer<sup>65,66</sup>, Angélica Casanova-Katny<sup>67</sup>, Simone Cesarz<sup>68,69</sup>, Bogdan Chojnicki<sup>70,70</sup>, Philippe Choler<sup>71,72</sup>, Steven L.  
17 Chown<sup>73</sup>, Edgar F. Cifuentes<sup>74</sup>, Marek Čiliak<sup>75</sup>, Tamara Contador<sup>76,77</sup>, Peter Convey<sup>78</sup>, Elisabeth J. Cooper<sup>79</sup>,  
18 Edoardo Cremonese<sup>80</sup>, Salvatore R. Curasi<sup>81</sup>, Robin Curtis<sup>12</sup>, Maurizio Cutini<sup>82</sup>, C. Johan Dahlberg<sup>83,84</sup>, Gergana N.  
19 Daskalova<sup>85</sup>, Miguel Angel de Pablo<sup>86</sup>, Stefano Della Chiesa<sup>87</sup>, Jürgen Dengler<sup>88,89,68</sup>, Bart Deronde<sup>90</sup>, Patrice  
20 Descombes<sup>91</sup>, Valter Di Cecco<sup>92</sup>, Michele Di Musciano<sup>93</sup>, Jan Dick<sup>28</sup>, Romina D. Dimarco<sup>94,95</sup>, Jiri Dolezal<sup>9,96</sup>, Ellen  
21 Dorrepaal<sup>97</sup>, Jiří Dušek<sup>98</sup>, Nico Eisenhauer<sup>68,69</sup>, Lars Eklundh<sup>29</sup>, Todd E. Erickson<sup>99,100</sup>, Brigitta Erschbamer<sup>101</sup>,  
22 Werner Eugster<sup>27</sup>, Robert M. Ewers<sup>102</sup>, Dan A. Exton<sup>103</sup>, Nicolas Fanin<sup>104</sup>, Fatih Fazlioglu<sup>60</sup>, Iris Feigenwinter<sup>27</sup>,  
23 Giuseppe Fenu<sup>105</sup>, Olga Ferlian<sup>68,69</sup>, M. Rosa Fernández Calzado<sup>106</sup>, Eduardo Fernández-Pascual<sup>107</sup>, Manfred  
24 Finckh<sup>108</sup>, Rebecca Finger Higgens<sup>109</sup>, T'ai G. W. Forte<sup>64</sup>, Erika C. Freeman<sup>110</sup>, Esther R. Frei<sup>111,112,113</sup>, Eduardo  
25 Fuentes-Lillo<sup>114,1,115</sup>, Rafael A. García<sup>114,116</sup>, María B. García<sup>117</sup>, Charly Géron<sup>118</sup>, Mana Gharun<sup>27</sup>, Dany Ghosn<sup>119</sup>,  
26 Khatuna Gigauri<sup>120</sup>, Anne Gobin<sup>121,122</sup>, Ignacio Goded<sup>30</sup>, Mathias Goeckede<sup>123</sup>, Felix Gottschall<sup>68,69</sup>, Keith  
27 Goulding<sup>124</sup>, Sanne Govaert<sup>7</sup>, Bente Jessen Graae<sup>125</sup>, Sarah Greenwood<sup>126</sup>, Caroline Greiser<sup>83</sup>, Achim Grelle<sup>127</sup>,  
28 Benoit Guénard<sup>128</sup>, Mauro Guglielmin<sup>129</sup>, Joannès Guillemot<sup>130,131</sup>, Peter Haase<sup>132,133</sup>, Sylvia Haider<sup>134,68</sup>, Aud H.  
29 Halbritter<sup>135</sup>, Maroof Hamid<sup>136</sup>, Albin Hammerle<sup>137</sup>, Arndt Hampe<sup>138</sup>, Siri V. Haugum<sup>135,139</sup>, Lucia Hederová<sup>9</sup>,  
30 Bernard Heinesch<sup>140</sup>, Carole Helfter<sup>141</sup>, Daniel Hepenstrick<sup>142</sup>, Maximiliane Herberich<sup>143</sup>, Mathias Herbst<sup>144</sup>, Luise  
31 Hermanutz<sup>145</sup>, David S. Hik<sup>146</sup>, Raúl Hoffrén<sup>147</sup>, Jürgen Homeier<sup>148,149</sup>, Lukas Hörtnagl<sup>127</sup>, Toke T. Høye<sup>150</sup>, Filip  
32 Hrbacek<sup>151</sup>, Kristoffer Hylander<sup>83</sup>, Hiroki Iwata<sup>152</sup>, Marcin Antoni Jackowicz-Korczynski<sup>153,29</sup>, Hervé Jactel<sup>154</sup>, Järvi  
33 Järveoja<sup>155</sup>, Szymon Jastrzębowski<sup>156</sup>, Anke Jentsch<sup>48,157</sup>, Juan J. Jiménez<sup>158</sup>, Ingibjörg S. Jónsdóttir<sup>159</sup>, Tommaso  
34 Jucker<sup>160</sup>, Alistair S. Jump<sup>161</sup>, Radosław Juszczak<sup>70</sup>, Róbert Kanka<sup>38</sup>, Vít Kašpar<sup>9,162</sup>, George Kazakis<sup>119</sup>, Julia Kelly<sup>163</sup>,  
35 Anzar A. Khuroo<sup>136</sup>, Leif Klemetsson<sup>50</sup>, Marcin Klisz<sup>156</sup>, Natascha Kljun<sup>163</sup>, Alexander Knohl<sup>164</sup>, Johannes  
36 Kobler<sup>165</sup>, Jozef Kollár<sup>38</sup>, Martyna M. Kotowska<sup>149</sup>, Bence Kovács<sup>166</sup>, Juergen Kreyling<sup>167</sup>, Andrea Lamprecht<sup>168</sup>,  
37 Simone I. Lang<sup>169</sup>, Christian Larson<sup>170</sup>, Keith Larson<sup>171</sup>, Kamil Laska<sup>151,172</sup>, Gueric le Maire<sup>130,131</sup>, Rachel I. Leihy<sup>173</sup>,  
38 Luc Lens<sup>174</sup>, Bengt Liljebladh<sup>50</sup>, Annalea Lohila<sup>175,176</sup>, Juan Lorite<sup>106,177</sup>, Benjamin Loubet<sup>57</sup>, Joshua Lynn<sup>135</sup>, Martin  
39 Macek<sup>9</sup>, Roy Mackenzie<sup>76</sup>, Enzo Magliulo<sup>178</sup>, Regine Maier<sup>27</sup>, Francesco Malfasi<sup>63</sup>, František Máliš<sup>179</sup>, Matěj Man<sup>9</sup>,  
40 Giovanni Manca<sup>30</sup>, Antonio Manco<sup>180</sup>, Tanguy Manise<sup>140</sup>, Paraskevi Manolaki<sup>181,182,183</sup>, Felipe Marciniak<sup>56</sup>, Radim  
41 Matula<sup>10,184</sup>, Ana Clara Mazzolari<sup>33</sup>, Sergiy Medinets<sup>185,186,187</sup>, Volodymyr Medinets<sup>185</sup>, Camille Meeussen<sup>7</sup>, Sonia  
42 Merinero<sup>83</sup>, Rita de Cássia Guimarães Mesquita<sup>188</sup>, Katrin Meusburger<sup>189</sup>, Filip J. R. Meysman<sup>190</sup>, Sean T.  
43 Michaletz<sup>191</sup>, Ann Milbau<sup>192</sup>, Dmitry Moiseev<sup>193</sup>, Pavel Moiseev<sup>193</sup>, Andrea Mondoni<sup>194</sup>, Ruth Monfries<sup>22</sup>,  
44 Leonardo Montagnani<sup>195</sup>, Mikel Moriana-Armendariz<sup>79</sup>, Umberto Morra di Cella<sup>196</sup>, Martin Mörsdorf<sup>197</sup>,  
45 Jonathan R. Mosedale<sup>198</sup>, Lena Muffler<sup>149</sup>, Miriam Muñoz-Rojas<sup>199,200</sup>, Jonathan A. Myers<sup>201</sup>, Isla H. Myers-  
46 Smith<sup>85</sup>, Laszlo Nagy<sup>202</sup>, Marianna Nardino<sup>203</sup>, Ilona Naujokaitis-Lewis<sup>204</sup>, Emily Newling<sup>205</sup>, Lena Nicklas<sup>101</sup>, Georg

47 Niedrist<sup>206</sup>, Armin Niessner<sup>207</sup>, Mats B. Nilsson<sup>155</sup>, Signe Normand<sup>35,36</sup>, Marcelo D. Noretto<sup>208,209</sup>, Yann  
48 Nouvellon<sup>130,131</sup>, Martin A. Nuñez<sup>210,95</sup>, Romà Ogaya<sup>211,212</sup>, Jérôme Ogée<sup>104</sup>, Joseph Okello<sup>41,213,214</sup>, Janusz  
49 Olejnik<sup>215</sup>, Jørgen Eivind Olesen<sup>216</sup>, Øystein Opedal<sup>217</sup>, Simone Orsenigo<sup>218</sup>, Andrej Palaj<sup>38</sup>, Timo Pampuch<sup>219</sup>,  
50 Alexey V. Panov<sup>220</sup>, Meelis Pärtel<sup>221</sup>, Ada Pastor<sup>222,182</sup>, Aníbal Pauchard<sup>114,116</sup>, Harald Pauli<sup>168</sup>, Marian Pavelka<sup>98</sup>,  
51 William D. Pearse<sup>223,224</sup>, Matthias Peichl<sup>155</sup>, Loïc Pellissier<sup>225,226</sup>, Rachel M. Penczykowski<sup>227</sup>, Josep Penuelas<sup>211,228</sup>,  
52 Matteo Petit Bon<sup>169,79,9</sup>, Alessandro Petraglia<sup>64</sup>, Shyam S. Phartyal<sup>229</sup>, Gareth K. Phoenix<sup>230</sup>, Casimiro Pio<sup>231</sup>,  
53 Andrea Pitacco<sup>232</sup>, Camille Pitteloud<sup>225,226</sup>, Roman Plichta<sup>184</sup>, Francesco Porro<sup>194</sup>, Miguel Portillo-Estrada<sup>1</sup>, Jérôme  
54 Poulenc<sup>233</sup>, Rafael Poyatos<sup>66,234</sup>, Anatoly S. Prokushkin<sup>220,31</sup>, Radosław Puchalka<sup>235,236</sup>, Mihai Pușcaș<sup>237,238,239</sup>,  
55 Dajana Radujković<sup>1</sup>, Krystal Randall<sup>240</sup>, Amanda Ratier Backes<sup>134,68</sup>, Sabine Remmele<sup>207</sup>, Wolfram Remmers<sup>241</sup>,  
56 David Renault<sup>42,242</sup>, Anita C. Risch<sup>243</sup>, Christian Rixen<sup>111</sup>, Sharon A. Robinson<sup>244</sup>, Bjorn J.M. Robroek<sup>245</sup>, Adrian V.  
57 Rocha<sup>246</sup>, Christian Rossi<sup>247,248</sup>, Graziano Rossi<sup>194</sup>, Olivier Rouspard<sup>249,250,251</sup>, Alexey V. Rubtsov<sup>31</sup>, Patrick  
58 Saccone<sup>168</sup>, Clotilde Sagot<sup>252</sup>, Jhonatan Sallo Bravo<sup>253,254</sup>, Cinthya C. Santos<sup>255</sup>, Judith M. Sarneel<sup>256</sup>, Tobias  
59 Scharnweber<sup>219</sup>, Jonas Schmeddes<sup>167</sup>, Marius Schmidt<sup>257</sup>, Thomas Scholten<sup>258</sup>, Max Schuchardt<sup>48</sup>, Naomi  
60 Schwartz<sup>259</sup>, Tony Scott<sup>124</sup>, Julia Seeber<sup>206,137</sup>, Ana Cristina Segalin de Andrade<sup>255</sup>, Tim Seipel<sup>170</sup>, Philipp  
61 Semenchuk<sup>260</sup>, Rebecca A. Senior<sup>261</sup>, Josep M. Serra-Diaz<sup>262</sup>, Piotr Sewerniak<sup>263</sup>, Ankit Shekhar<sup>27</sup>, Nikita V.  
62 Sidenko<sup>220</sup>, Lukas Siebicke<sup>164</sup>, Laura Siegwart Collier<sup>145,264</sup>, Elizabeth Simpson<sup>223</sup>, David P. Siqueira<sup>265</sup>, Zuzana  
63 Sitková<sup>266</sup>, Johan Six<sup>27</sup>, Marko Smiljanic<sup>219</sup>, Stuart W. Smith<sup>267,268</sup>, Sarah Smith-Tripp<sup>269</sup>, Ben Somers<sup>270</sup>, Mia Vedel  
64 Sørensen<sup>267</sup>, José João L. L. Souza<sup>271</sup>, Bartolomeu Israel Souza<sup>272</sup>, Arildo Souza Dias<sup>273,255</sup>, Marko J. Spasojević<sup>274</sup>,  
65 James D. M. Speed<sup>275</sup>, Fabien Spicher<sup>276</sup>, Angela Stanisci<sup>277</sup>, Klaus Steinbauer<sup>168</sup>, Rainer Steinbrecher<sup>278</sup>, Michael  
66 Steinwandter<sup>206</sup>, Michael Stemkovski<sup>223</sup>, Jörg G. Stephan<sup>279</sup>, Christian Stiegler<sup>164</sup>, Stefan Stoll<sup>241,280</sup>, Martin  
67 Svátek<sup>184</sup>, Miroslav Svoboda<sup>10</sup>, Torbern Tagesson<sup>29,281</sup>, Andrew J. Tanentzap<sup>110</sup>, Franziska Tanneberger<sup>282</sup>, Jean-  
68 Paul Theurillat<sup>283,284</sup>, Haydn J. D. Thomas<sup>85</sup>, Andrew D. Thomas<sup>285</sup>, Katja Tielbörger<sup>62</sup>, Marcello Tomaselli<sup>64</sup>, Urs  
69 Albert Treier<sup>35,36</sup>, Mario Trouillier<sup>219</sup>, Pavel Dan Turtureanu<sup>237,286,239</sup>, Rosamond Tutton<sup>287</sup>, Vilna A. Tyystjärvi<sup>11,288</sup>,  
70 Masahito Ueyama<sup>289</sup>, Karol Ujházy<sup>179</sup>, Mariana Ujházyová<sup>75</sup>, Domas Uogintas<sup>290</sup>, Anastasiya V. Urban<sup>220,184</sup>, Josef  
71 Urban<sup>184,31</sup>, Marek Urbaniak<sup>215</sup>, Tudor-Mihai Ursu<sup>291</sup>, Francesco Primo Vaccari<sup>292</sup>, Stijn Van de Vondel<sup>293</sup>, Liesbeth  
72 van den Brink<sup>62</sup>, Maarten Van Geel<sup>294</sup>, Vigdis Vandvik<sup>135</sup>, Pieter Vangansbeke<sup>7</sup>, Andrej Varlagin<sup>295</sup>, G.F. Ciska)  
73 Veen<sup>296</sup>, Elmar Veenendaal<sup>297</sup>, Susanna E. Venn<sup>298</sup>, Hans Verbeeck<sup>299</sup>, Erik Verbruggen<sup>1</sup>, Frank G.A. Verheijen<sup>300</sup>,  
74 Luis Villar<sup>301</sup>, Luca Vitale<sup>302</sup>, Pascal Vittoz<sup>303</sup>, Maria Vives-Inglá<sup>66</sup>, Jonathan von Oppen<sup>35,36</sup>, Josefine Walz<sup>304</sup>, Runxi  
75 Wang<sup>128</sup>, Yifeng Wang<sup>287</sup>, Robert G. Way<sup>287</sup>, Ronja E. M. Wedegärtner<sup>267</sup>, Robert Weigel<sup>149</sup>, Jan Wild<sup>9,162</sup>, Matthew  
76 Wilkinson<sup>44</sup>, Martin Wilmking<sup>219</sup>, Lisa Wingate<sup>104</sup>, Manuela Winkler<sup>168</sup>, Sonja Wipf<sup>247,111</sup>, Georg Wohlfahrt<sup>137</sup>,  
77 Georgios Xenakis<sup>305</sup>, Yan Yang<sup>306</sup>, Zicheng Yu<sup>307,308</sup>, Kailiang Yu<sup>309</sup>, Florian Zellweger<sup>113</sup>, Jian Zhang<sup>310</sup>, Zhaochen  
78 Zhang<sup>310</sup>, Peng Zhao<sup>155</sup>, Klaudia Ziemblińska<sup>215</sup>, Reiner Zimmermann<sup>207,311</sup>, Shengwei Zong<sup>312</sup>, Viacheslav I.  
79 Zyryanov<sup>220</sup>, Ivan Nijs<sup>1,+</sup>, Jonathan Lenoir<sup>276,+x</sup>

80  
81 \*Jonas J. Lembrechts and Johan Van den Hoogen should be considered joint first author

82 + Ivan Nijs and Jonathan Lenoir should be considered joint senior author

83 x Corresponding authors

84 \*\* See end of manuscript for affiliations and ORCIDiDs

85

## 86 Corresponding authors

87 Jonas Lembrechts ([Jonas.lembrechts@uantwerpen.be](mailto:Jonas.lembrechts@uantwerpen.be), <https://orcid.org/0000-0002-1933-0750>, +).

88 Jonathan Lenoir ([jonathan.lenoir@u-picardie.fr](mailto:jonathan.lenoir@u-picardie.fr), <https://orcid.org/0000-0003-0638-9582>).

89

90 **Abstract**

91 Research in global change ecology relies heavily on global climatic grids derived from  
92 estimates of air temperature in open areas at around 2 m above the ground. These climatic  
93 grids do not reflect conditions below vegetation canopies and near the ground surface, where  
94 critical ecosystem functions occur and most terrestrial species reside. Here, we provide global  
95 maps of soil temperature and bioclimatic variables at a 1-km<sup>2</sup> resolution for 0–5 and 5–15 cm  
96 soil depth. These maps were created by calculating the difference (i.e., offset) between *in-*  
97 *situ* soil temperature measurements, based on time series from over 1200 1-km<sup>2</sup> pixels  
98 (summarized from 8500 unique temperature sensors) across all the world’s major terrestrial  
99 biomes, and coarse-grained air temperature estimates from ERA5-Land (an atmospheric  
100 reanalysis by the European Centre for Medium-Range Weather Forecasts). We show that  
101 mean annual soil temperature differs markedly from the corresponding gridded air  
102 temperature, by up to 10°C (mean =  $3.0 \pm 2.1^\circ\text{C}$ ), with substantial variation across biomes and  
103 seasons. Over the year, soils in cold and/or dry biomes are substantially warmer ( $+3.6 \pm 2.3^\circ\text{C}$ )  
104 than gridded air temperature, whereas soils in warm and humid environments are on average  
105 slightly cooler ( $-0.7 \pm 2.3^\circ\text{C}$ ). The observed substantial and biome-specific offsets emphasize  
106 that the projected impacts of climate and climate change on near-surface biodiversity and  
107 ecosystem functioning are inaccurately assessed when air rather than soil temperature is  
108 used, especially in cold environments. The global soil-related bioclimatic variables provided  
109 here are an important step forward for any application in ecology and related disciplines.  
110 Nevertheless, we highlight the need to fill remaining geographic gaps by collecting more *in-*  
111 *situ* measurements of microclimate conditions to further enhance the spatiotemporal  
112 resolution of global soil temperature products for ecological applications.

113

114 **Keywords:** bioclimatic variables, global maps, microclimate, near-surface temperatures, soil-  
115 dwelling organisms, soil temperature, temperature offset, weather stations

## 116 Introduction

117 With the rapidly increasing availability of big data on species distributions, functional traits  
118 and ecosystem functioning (Bond-Lamberty & Thomson, 2018, Bruelheide *et al.*, 2018,  
119 Kissling *et al.*, 2018, Kattge *et al.*, 2019, Lenoir *et al.*, 2020), we can now study biodiversity  
120 and ecosystem responses to global changes in unprecedented detail (Senior *et al.*, 2019,  
121 Steidinger *et al.*, 2019, Van Den Hoogen *et al.*, 2019, Antão *et al.*, 2020). However, despite  
122 this increasing availability of ecological data, most spatially-explicit studies of ecological,  
123 biophysical and biogeochemical processes still have to rely on the same global gridded  
124 temperature data (Soudzilovskaia *et al.*, 2015, Van Den Hoogen *et al.*, 2019, Du *et al.*, 2020).  
125 Thus far, these global gridded products are based on measurements from standard  
126 meteorological stations that record free-air temperature inside well-ventilated protective  
127 shields placed up to 2 m above-ground in open, shade-free habitats, where abiotic conditions  
128 may differ substantially from those actually experienced by most organisms (World  
129 Meteorological Organization, 2008, Lembrechts *et al.*, 2020).

130 Ecological patterns and processes often relate more directly to below-canopy soil  
131 temperature rather than to well-ventilated air temperature inside a weather station. Near-  
132 surface, rather than air, temperature better predicts ecosystem functions like biogeochemical  
133 cycling (e.g., organic matter decomposition, soil respiration and other aspects of the global  
134 carbon balance) (Schimel *et al.*, 2004, Pleim & Gilliam, 2009, Portillo-Estrada *et al.*, 2016,  
135 Hursh *et al.*, 2017, Gottschall *et al.*, 2019, Davis *et al.*, 2020, Perera-Castro *et al.*, 2020, Jian *et al.*,  
136 2021). Similarly, the use of soil temperature in correlative analyses or predictive models  
137 may improve predictions of climate impacts on organismal physiology and behaviour, as well  
138 as on population and community dynamics and species distributions (Körner & Paulsen, 2004,  
139 Schimel *et al.*, 2004, Ashcroft *et al.*, 2008, Kearney *et al.*, 2009, Scherrer *et al.*, 2011, Opedal  
140 *et al.*, 2015, Berner *et al.*, 2020, Zellweger *et al.*, 2020). Given the key role of soil-related  
141 processes for both aboveground and belowground parts of the ecosystem and their  
142 feedbacks to the atmosphere (Crowther *et al.*, 2016), adequate soil temperature data are  
143 critical for a broad range of fields of study, such as ecology, biogeography, biogeochemistry,  
144 agronomy, soil science and climate system dynamics. Nevertheless, existing global soil  
145 temperature products such as those from ERA5-Land (Copernicus Climate Change Service



146 (C3S), 2019), with a resolution of  $0.08 \times 0.08$  degrees ( $\approx 9 \times 9$  km at the equator), remain too  
147 coarse for most ecological applications.

148 The direction and magnitude of the difference or *offset* between *in-situ* soil temperature and  
149 coarse-gridded air temperature products result from a combination of two factors: (i) the  
150 (vertical) microclimatic difference between air and soil temperature, and (ii) the (horizontal)  
151 mesoclimatic difference between air temperature in flat, cleared areas (i.e., where  
152 meteorological stations are located) and air temperature within different vegetation types  
153 (e.g., below a dense canopy of trees) or topographies (e.g., within a ravine or on a ridge)  
154 (Lembrechts *et al.*, 2020, De Frenne *et al.*, 2021). In essence, the offset is thus the combination  
155 of both the vertical and horizontal differences that result from factors affecting the energy  
156 budget at the Earth's surface, principally radiative energy: the ground absorbs radiative  
157 energy, which is transferred to the air by convective heat exchange, evaporation and spatial  
158 variation in net radiation, and lower convective conductance near the Earth's surface results  
159 in horizontal and vertical variation in temperature (Richardson, 1922, Geiger, 1950). Both  
160 these vertical and horizontal differences in temperature vary significantly across the globe  
161 and in time as a result of environmental conditions affecting the radiation budget (e.g., as a  
162 result of topographic orientation, canopy cover or surface albedo), convective heat exchange  
163 and evaporation (e.g., foliage density, variation in the degree of wind shear caused by surface  
164 friction) and the capacity for the soil to store and conduct heat (e.g., water content and soil  
165 structure and texture) (Geiger, 1950, Zhang *et al.*, 2008, Way & Lewkowicz, 2018, De Frenne  
166 *et al.*, 2019).

167 While the physics of soil temperatures have long been well-understood (Richardson, 1922,  
168 Geiger, 1950), the creation of high-resolution global gridded soil temperature products has  
169 not been feasible before, partially due to the absence of detailed global *in-situ* soil  
170 temperature measurements (Lembrechts & Lenoir, 2019, Lembrechts *et al.*, 2020). Recently,  
171 however, the call for microclimate temperature data representative of *in-situ* conditions (i.e.,  
172 microhabitat) as experienced by organisms living close to the ground surface or in the soil has  
173 become more urgent (Bramer *et al.*, 2018). In this paper, we address this issue by generating  
174 global gridded maps of below-canopy and near-surface soil temperature at 1-km<sup>2</sup> resolution  
175 (in line with most existing global air temperature products). These maps are more  
176 representative of the habitat conditions as experienced by organisms living under vegetation

177 canopies, in the topsoil or near the soil surface. They were created using the abovementioned  
178 offset between gridded air temperature data and *in-situ* soil temperature measurements. We  
179 expect these soil temperature maps to be substantially more representative of actual  
180 microclimatic conditions than existing products as they capture relevant near-surface and  
181 below-ground abiotic conditions where ecosystem functions and processes operate (Daly,  
182 2006, Bramer *et al.*, 2018, Körner & Hiltbrunner, 2018). Indeed, the offset between free-air  
183 (macroclimate) and soil (microclimate) temperature, and between cleared areas and other  
184 habitats, can easily reach up to  $\pm 10^{\circ}\text{C}$  annually, even at the  $1\text{-km}^2$  spatial resolution used here  
185 (Zhang *et al.*, 2018, Lembrechts *et al.*, 2019, Wild *et al.*, 2019).

186 To create the global gridded soil temperature maps introduced above, we used over 8500  
187 time series of soil temperature measured *in-situ* across the world's major terrestrial biomes,  
188 which are compiled and stored in the SoilTemp database (Lembrechts *et al.*, 2020) (Fig. 1a,  
189 Supplementary Material Fig. S1) and averaged into 1200 (or 1000 for the second soil layer)  
190 unique  $1\text{-km}^2$  pixels. First, to illustrate the magnitude of the studied effect, we visualized the  
191 global and biome-specific patterns in the mean annual offset between *in-situ* soil temperature  
192 (0–5 cm and 5–15 cm depth) and coarse-scale interpolated air temperature from ERA5-Land  
193 using the average within  $1 \times 1$  km grid cells. Hereafter, we refer to this difference between  
194 soil temperature and air temperature as the *temperature offset* (or *offset*), sensu (De Frenne  
195 *et al.*, 2021); elsewhere called the *surface offset* (Smith & Riseborough, 1996, Smith &  
196 Riseborough, 2002)). Secondly, we used a machine learning approach with 31 environmental  
197 predictor variables (including macroclimate, soil, topography, reflectance, vegetation and  
198 anthropogenic variables) to model the spatial variation in monthly temperature offsets at a  $1$   
199  $\times 1$  km resolution for all continents except Antarctica (as not covered by many of the used  
200 predictor variable layers). Using these offsets, we then calculated relevant soil-related  
201 bioclimatic variables (SBIO), mirroring the existing global bioclimatic variables for air  
202 temperature. Finally, we compare our new global soil temperature product with a similar one  
203 calculated using coarser-resolution soil temperature data ( $0.1 \times 0.1$  degrees) from ERA5-Land  
204 (Copernicus Climate Change Service (C3S), 2019).

## 205 **Methods**

### 206 ***Data acquisition***

207 Analyses are based on SoilTemp, a global database of microclimate time series (Lembrechts  
208 *et al.*, 2020). We compiled soil temperature measurements from 9362 unique sensors (mean  
209 duration 2.9 years, median duration 1.0 year, ranging from 1 month to 41 years) from 60  
210 countries, using both published and unpublished data sources (Fig. 1, Supplementary Material  
211 Fig. S1). Each sensor corresponds to one independent time series.

212 We used time series spanning a minimum of one month, with a temporal resolution of four  
213 hours or less. Sensors of any type were included (Supplementary Material Table S1), as long  
214 as they measured *in situ*. Sensors in experimentally manipulated plots, i.e., plots in which  
215 microclimate has been manipulated, such as in open top chambers, were excluded. Most data  
216 (> 90%) came from low-cost rugged microclimate loggers such as iButtons (Maxim Integrated,  
217 USA) or TMS4-sensors (Wild *et al.*, 2019), with measurement errors of around 0.5–1°C (note  
218 that we are using degree Celsius over Kelvin throughout, for ease of understanding), while in  
219 a minority of cases sensors with higher meteorological specifications such as industrial or  
220 scientific grade thermocouples and thermistors (measurement errors of less than 0.5°C) were  
221 used. Contributing datasets mostly consisted of short-term regional networks of microclimate  
222 measurements, yet also included a set (< 5%) of soil temperature sensors from long-term  
223 research networks equipped with weather stations (e.g., Pastorello *et al.*, 2017). By combining  
224 these two types of data, a much higher spatial density of sensors and broader distribution of  
225 microhabitats could be obtained than by using weather station data only.

226 About 68% of sensors were deployed between 2010 and 2020 and 93% between 2000 and  
227 2020; we thus focus on the latter period in our analyses. Additionally, given the relatively  
228 short time frame covered by most individual sensors and thus the lack of spatially unbiased  
229 long-term time series, we were not able to test for systematic differences in the temperature  
230 offset between old and recent data sets, and thus we did not correct for this in our models.  
231 We strongly urge future studies to assess such temporal dynamics in the offset once long-  
232 term microclimate data have become sufficient and more available.

233 For each of the individual 9362 time series, we calculated monthly mean, minimum (5%  
234 percentile of all monthly values) and maximum (95% percentile) temperature, after checking  
235 all time series for plausibility and erroneous data. These monthly values, while perhaps not  
236 fully intercomparable between the northern and southern hemisphere, are those that have

237 traditionally been used to calculate bioclimatic variables (Fick & Hijmans, 2017). Months with  
238 more than one day of missing data, either at the beginning or end of the measurement period,  
239 or due to logger malfunctioning during measurement, were excluded, resulting in a final  
240 subset of 380,676 months of soil temperature time series that were used for further analyses.  
241 For each sensor with more than twelve months of data, we calculated moving averages of  
242 annual mean temperature, using each consecutive month as a starting month and calculating  
243 the mean temperature including the next eleven months. We used these moving averages to  
244 make maximal use of the full temporal extent covered by each sensor, because each time  
245 series spanned a different time period, often including parts of calendar years only.

246 The selected dataset contained sensors installed strictly belowground, measuring  
247 temperature at depths between 0 and 200 cm below the ground surface. Sensors recording  
248 several measurements at the same site but located at different (vertical) depths were  
249 included separately (the 9362 unique sensors thus came from 7251 unique loggers).

250 Sensors were grouped in different soil depth categories (0–5, 5–15, 15–30, 30–60, 60–100,  
251 100–200 cm, Supplementary Material Table S2) to incorporate the effects of soil temperature  
252 dampening associated with vertical stratification. We limited our analyses to the topsoil (0–5  
253 cm) and the second soil layer (5–15 cm), as we currently lack sufficient global coverage to  
254 make accurate models at deeper soil depths (8519 time series, about 91%, came from the  
255 two upper depth layers). Due to uncertainty in identification of these soil depths between  
256 studies (e.g., due to litter layers), no finer categorisation is used.

257 We tested for potential bias in temporal resolution (i.e., measurement interval) by calculating  
258 mean, minimum and maximum temperature for a selection of 2000 months for data  
259 measured every 15 minutes, and the same data aggregated to 30, 60, 90, 120 and 240  
260 minutes. Monthly mean, minimum and maximum temperature calculated with any of the  
261 aggregated datasets differed on average less than 0.2°C from the ones with the highest  
262 temporal resolution. We were thus confident that pooling data with different temporal  
263 resolutions of 4 hours or finer would not significantly affect our results.

#### 264 ***Temperature offset calculation***

265 For each monthly value at each sensor location (see Supplementary Material Table S3 for  
266 number of data points per month), we extracted the corresponding monthly means of the 2  
267 m air temperature from the European Centre for Medium-Range Weather (ECMWF)  
268 Forecast's 5<sup>th</sup> reanalysis (ERA5) (from 1979–1981) and ERA5-Land from 1981–2020  
269 (Copernicus Climate Change Service (C3S), 2019), hereafter called ERA5L. The latter dataset  
270 models the global climate with a spatial resolution of  $0.08 \times 0.08$  degrees ( $\approx 9 \times 9$  km at the  
271 equator) with an hourly resolution, converted into monthly means using daily means for the  
272 whole month. Similarly, monthly minima and maxima were obtained from TerraClimate  
273 (Abatzoglou *et al.*, 2018) for the period 2000 to 2020 at a  $0.04 \times 0.04$  degrees ( $\approx 4 \times 4$  km at  
274 the equator) resolution. Monthly means for TerraClimate were not available, and we  
275 therefore estimated them by averaging the monthly minima and maxima. Finally, we also  
276 obtained monthly mean temperatures from CHELSA (Karger *et al.*, 2017a, Karger *et al.*, 2017b)  
277 for the period 2000 to 2013 at a  $30 \times 30$  arc second ( $\approx 1 \times 1$  km at the equator) resolution. In  
278 our modelling exercises (see section '*Integrative modelling*' below), we opted to use the mean  
279 temperature offsets as calculated based on ERA5L rather than on CHELSA. While CHELSA's  
280 higher spatial resolution is definitely an advantage, its time period (stopping in 2013)  
281 insufficiently overlapped with the time period covered by our *in-situ* measurements (2000 to  
282 2020), soil temperature offsets based on the CHELSA dataset were only used for comparative  
283 purposes. We used TerraClimate to model offsets in monthly minimum and maximum  
284 temperature.

285 We calculated moving annual averages of the gridded air temperature data in the same way  
286 as for soil temperature. These were used to create annual temperature offset values following  
287 the same approach as above.

288 The offset between the *in situ* measured soil temperature in the SoilTemp database and the  
289 2 m free-air temperature obtained from the air-temperature grids (ERA5L, TerraClim and  
290 CHELSA, hereafter called 'gridded air temperature') was calculated by subtracting the  
291 monthly or annual mean air temperature from the monthly or annual mean soil temperature.  
292 Positive offset values indicate a measured soil temperature higher than gridded air  
293 temperature, while negative offset values represent cooler soils. Similarly, monthly minimum  
294 and maximum air temperature were subtracted from minimum and maximum soil  
295 temperature, respectively. Monthly minima and maxima of the soil temperature were

296 calculated as, respectively, the 5% lowest and highest instantaneous measurement in that  
297 month, to correct for outliers, which can be especially pronounced at the soil surface (Speak  
298 *et al.*, 2020). As a result, patterns in minima and maxima are more conservative estimates  
299 than if we had used the absolute lowest and highest values.

300 Importantly, the temperature offset calculated here is a result of three key groups of drivers:  
301 (1) height effects (2 m versus 0–15 cm below the soil surface); (2) environmental or habitat  
302 effects (e.g., spatial variability in vegetation, snow or topography); and (3) spatial scale effects  
303 (resolution of gridded air temperature) (Lembrechts *et al.*, 2020). We investigated the  
304 potential role of scale effects by comparing gridded air temperature data sources with  
305 different resolutions (ERA5L, TerraClimate and CHELSA, see below). Height effects and  
306 environmental effects are however not disentangled here, as the offset we propose  
307 incorporates both the difference between air and soil temperature (vertically), as well as the  
308 difference between free-air macroclimate and *in situ* microclimate (horizontally) in one  
309 measure (Lembrechts *et al.*, 2020). While it can be argued that it would be better to treat  
310 both vertical and horizontal effects separately, this would require a similar database of  
311 coupled *in-situ* air and soil temperature measurements, which is not yet available. Using *in*  
312 *situ* measured air temperature could also solve spatial mismatches (i.e., spatially averaged air  
313 temperature represents the whole 1 to 81 km<sup>2</sup> pixel, depending on pixel size, not only the  
314 exact location of the sensor). However, coupled air and soil temperature measurements are  
315 not only rare, but the air temperature measurements also have large measurement errors,  
316 especially in open habitats (Maclean *et al.*, 2021). These errors can be up to several degrees  
317 in open habitats when using non-standardized sensors, loggers and shielding (Holden *et al.*,  
318 2013, Terando *et al.*, 2017, Maclean *et al.*, 2021). Hence, using *in situ* measured air  
319 temperature without correcting for these measurement errors would be misleading.

### 320 ***Global and biome-level analyses***

321 For the purpose of visualization, annual offsets were first averaged in hexagons with a  
322 resolution of approximately 70,000 km<sup>2</sup>, using the dggridR-package (version 2.0.4) in R  
323 (Barnes *et al.*, 2017) (Fig. 1). Next, we plotted mean, minimum and maximum annual soil  
324 temperature as a function of corresponding gridded air temperature from ERA5, TerraClimate  
325 and CHELSA and used generalized additive models (GAMs, package mgcv 1.8-31; Wood, 2012)

326 to visualise deviations from the 1:1-line (i.e., temperature offsets deviating from zero,  
327 Supplementary Figs. S4-5).

328 All annual and monthly values within each soil depth category and falling within the same 1-  
329 km<sup>2</sup> pixel were aggregated as a mean, resulting in a total of c. 1200 unique pixels at 0–5 cm,  
330 and c. 1000 unique pixels at 5–15 cm each month, across the globe (Supplementary Material  
331 Table S3). This averaging includes summarizing the data over space, i.e., multiple sensors  
332 within the same 1-km<sup>2</sup> pixel, and time, i.e., data from multi-year time series from a certain  
333 sensor, to reduce spatial and temporal autocorrelation and sampling bias. We assigned these  
334 1-km<sup>2</sup> averages to the corresponding Whittaker biome of their georeferenced location, using  
335 the package *plotbiomes* (version 0.0.0.9901) in R (Fig. 1 c, d, Supplementary Material Table  
336 S4-5 (Stefan & Levin, 2018)). We ranked biomes based on their offset and compared this with  
337 the mean annual precipitation in each biome (Fig. 1b). This was done separately for each air  
338 temperature data source (ERA5L, TerraClimate and CHELSA), soil depth (0–5 cm, 5–15 cm)  
339 and timeframe (ERA5L 1979–2020, 2000–2020), as well as for the offset between monthly  
340 minimum and maximum soil temperature and the minimum and maximum gridded air  
341 temperature from TerraClimate. Our analyses showed that patterns were robust to variation  
342 in spatial resolution, sensor depth, climate interpolation method and temporal scale  
343 (Supplementary Material Figs. S2–5).

#### 344 ***Acquisition of global predictor variables***

345 To create spatial predictive models of the offset between *in-situ* soil temperature and gridded  
346 air temperature, we first sampled a stack of global map layers at each of the logger locations  
347 within the dataset. These layers included long-term macroclimatic conditions, soil texture and  
348 physiochemical information, vegetation, radiation, and topographic indices as well as  
349 anthropogenic variables. Details of all layers, including descriptions, units, and source  
350 information, are described in Supplementary Data S1. In short, information about soil texture,  
351 structure and physiochemical properties was obtained from SoilGrids (version 1 (Hengl *et al.*,  
352 2017)), limited to the upper soil layer (top 5 cm). Long-term averages of macroclimatic  
353 conditions (i.e., monthly mean, maximum and minimum temperature, monthly precipitation)  
354 was obtained from CHELSA (version 2017 (Karger *et al.*, 2017a)), which includes climate data  
355 averaged across 1979–2013, and from WorldClim (version 2 (Fick & Hijmans, 2017)). Monthly

356 snow probability is based on a pixel-wise frequency of snow occurrence (snow cover >10%)  
357 in MODIS daily snow cover products (MOD10A1 & MYD10A1 (Hall *et al.*, 2002)) in 2001–2019.  
358 Spectral vegetation indices (i.e., averaged MODIS NDVI product MYD13Q1) and surface  
359 reflectance data (i.e., MODIS MCD43A4) were obtained from the Google Earth Engine Data  
360 Catalog ([developers.google.com/earth-engine/datasets](https://developers.google.com/earth-engine/datasets)) and averaged from 2015 to 2019.  
361 Landcover and topographic information were obtained from EarthEnv (Amatulli *et al.*, 2018).  
362 Aridity index (AI) and potential evapotranspiration (PET) layers were obtained from CGIAR  
363 (Zomer *et al.*, 2008). Anthropogenic information (population density) was obtained from the  
364 EU JRC ([ghsl.jrc.ec.europa.eu/ghs\\_pop2019.php](https://ghsl.jrc.ec.europa.eu/ghs_pop2019.php)). Aboveground biomass data were obtained  
365 from GlobBiomass (Santoro, 2018). RESOLVE ecoregion classifications were used to  
366 categorize sampling locations into biomes (Dinerstein *et al.*, 2017). With this set of predictor  
367 variables, we included information on all different categories of drivers of soil temperature.  
368 An important variable that had to be excluded was snow depth, due to the lack of a relevant  
369 1-km<sup>2</sup> resolution global product. The final set of predictor variables included 24 ‘static’  
370 variables and eight monthly layers (i.e., maximum, mean, and minimum temperature,  
371 precipitation, cloud cover, solar radiation, water vapour pressure, and snow cover). As cloud  
372 cover estimates were not available for high-latitude regions in the Northern Hemisphere in  
373 January and December due to a lack of daylight, we excluded cloud cover as an explanatory  
374 variable for these months (i.e., ‘EarthEnvCloudCover\_MODCF\_monthlymean\_XX’, with XX  
375 representing the months in two-digit form Supplementary Data S1).

376 All variable map layers were reprojected and resampled to a unified pixel grid in EPSG:4326  
377 (WGS84) at 30 arc-sec resolution ( $\approx 1 \times 1$  km at the equator). Areas covered by permanent  
378 snow or ice (e.g., the Greenland ice cap or glaciated mountain ranges, identified using  
379 SoilGrids) were excluded from the analyses. Antarctic sampling points were excluded from  
380 the modelling data set owing to the limited coverage of several covariate layers in the region.

### 381 **Modelling**

382 To generate global maps of monthly temperature offsets (Fig. 2), we trained Random Forest  
383 (RF) models for each month, using the temperature offsets as the response variables and the  
384 global variable layers as predictors (Breiman, 2001, Hengl *et al.*, 2018). We used a geospatial  
385 RF modelling pipeline as developed by van den Hoogen *et al.* (2021). RF models are machine



386 learning models that combine many classification trees using randomized subsets of the data,  
387 with each tree iteratively dividing data into groups of most closely related data points (Hengl  
388 *et al.*, 2018). They are particularly valuable here due to their capacity to uncover nonlinear  
389 relationships (e.g., due to increased decoupling of soil from air temperature in colder and thus  
390 snow-covered areas) and their ability to capture complex interactions among covariates (e.g.,  
391 between snow and vegetation cover) (Olden *et al.*, 2008). Furthermore, they may currently  
392 have advantages over mechanistic microclimate models for global modelling (Maclean &  
393 Klinges, 2021), as the latter require highly detailed physical input parameters for calibration,  
394 and current computational barriers preclude global assessments at a 1 km<sup>2</sup> resolution and  
395 over multiple decades. Nevertheless, we urge future endeavours to compare and potentially  
396 improve our results with estimates based on such mechanistic models.

397 We performed a grid search procedure to tune the RF models across a range of 52  
398 hyperparameter settings (variables per split: 2–14, minimum leaf population: 2–5, in all  
399 combinations adding up to 52 models, each time with 250 trees). During this procedure, we  
400 assessed each of the 52 model's performance using k-fold cross-validation (k = 10; folds  
401 assigned randomly, stratified per biome). The models' mean and standard deviation values  
402 were the basis for choosing the best of all evaluated models. This procedure was repeated for  
403 each month separately for the two soil depth layers (0–5 cm, 5–15 cm), for offsets in mean,  
404 minimum and maximum temperature. The importance of predictor variables was assessed  
405 using the variable importance and ordered by mean variable importance across all models.  
406 This variable importance adds up the decreases in the impurity criterion (i.e., the measure on  
407 which the local optimal condition is chosen) at each split of a node for each individual variable  
408 over all trees in the forest (van den Hoogen *et al.*, 2021).

#### 409 ***Soil bioclimatic variables***

410 The resulting global maps of the annual and monthly offsets between mean, minimum and  
411 maximum soil and air temperature were used to calculate relevant bioclimatic variables  
412 following the definition used in CHELSA, BIOCLIM, ANUCLIM and WorldClim (Xu & Hutchinson,  
413 2011, Booth *et al.*, 2014, Fick & Hijmans, 2017, Karger *et al.*, 2017a)(Fig. 3–4). First, we  
414 calculated monthly soil mean, maximum and minimum temperature by adding monthly  
415 temperature offsets to the respective CHELSA monthly mean, maximum and minimum

416 temperature (Karger *et al.*, 2017a). Next, we used these soil temperature layers to compute  
417 11 soil bioclimatic layers (SBIO, Table 1) (O'Donnell & Ignizio, 2012). Wettest and driest  
418 quarters were identified for each pixel based on CHELSA's monthly values.

### 419 **Model uncertainty**

420 To assess the uncertainty in the monthly models, we performed a stratified bootstrapping  
421 procedure, with total size of the bootstrap samples equal to the original training data (van  
422 den Hoogen *et al.*, 2021). Using biomes as a stratification category, we ensured the samples  
423 included in each of the bootstrap training collections were proportionally representative of  
424 each biome's total area. Next, we trained RF models (with the same hyperparameters as  
425 selected during the grid-search procedure) using each of 100 bootstrap iterations. Each of  
426 these trained RF models was then used to classify the predictor layer stack, to generate per-  
427 pixel 95% confidence intervals and standard deviation for the modelled monthly offsets (Fig.  
428 5a, Supplementary Material Fig. S6a). The mean  $R^2$  value of the RF models for the monthly  
429 mean temperature offset was 0.70 (from 0.64 to 0.78) at 0–5 cm and 0.76 (0.63–0.85) at 5 to  
430 15 cm across all twelve monthly models. Mean RMSE of the models was 2.20°C (1.94–2.51°C)  
431 at 0–5 cm, and 2.06°C (1.67–2.35°C) at 5–15 cm.

432 Importantly, model uncertainty as reported in Fig. 5a and Supplementary Material Fig. S6a  
433 comes on top of existing uncertainties in (1) *in-situ* soil temperature measurements and (2)  
434 the ERA5L macroclimate models as used in our models. However, both of those are usually  
435 under 1°C (Copernicus Climate Change Service (C3S), 2019, Wild *et al.*, 2019).

436 To assess the spatial extent of extrapolation, which is necessary due to the incomplete global  
437 coverage of the training data, we first performed a Principal Component Analysis (PCA) on the  
438 full environmental space covered by the monthly training data, including all explanatory  
439 variables as used in the models, and then transformed the composite image into the same PC  
440 spaces as of the sampled data (Van Den Hoogen *et al.*, 2019). Next, we created convex hulls  
441 for each of the bivariate combinations from the first 10 to 12 PCs, covering at least 90% of the  
442 sample space variation, with the number of PCs depending on the month. Using the  
443 coordinates of these convex hulls, we assessed whether each pixel fell within or outside each  
444 of these convex hulls, and calculated the percentage of bivariate combinations for which this

445 was the case (Fig. 5b, Supplementary Material Fig. S6b). This process was repeated for each  
446 month, and for each of the two soil depths separately.

447 These uncertainty maps are important because one should be careful with extrapolation  
448 beyond the range of conditions covered by the environmental variables included in the  
449 original calibration dataset, especially in the case of non-linear patterns such as modelled  
450 here. The maps are provided as spatial masks to remove or reduce the weighting of the pixels  
451 for which predictions are beyond the range of values covered by the models during  
452 calibration. To assess this further, we used a spatial leave-one-out cross-validation analysis to  
453 test for spatial autocorrelation in the data set (Supplementary Material Fig. S7) (van den  
454 Hoogen *et al.*, 2021). This approach trains a model for each sample in the data set on all  
455 remaining samples, excluding data points that fall within an increasingly large buffer around  
456 that focal sample. Results show lowest confidence for May to September at 5–15 cm, likely  
457 driven by uneven global coverage of data points.

458 Finally, we compared the modelled mean annual temperature (SBIO1, topsoil layer) with a  
459 similar product based on monthly ERA5L topsoil (0–7 cm) temperature with a spatial  
460 resolution of  $0.1 \times 0.1$  degrees (Copernicus Climate Change Service (C3S), 2019). The  
461 corresponding SBIO1 based on ERA5L was calculated using the means of the monthly  
462 averages for each month over the period 1981 to 2016, and averaging these 12 monthly  
463 values into one annual product. We then visualized spatial differences between SBIO1 and  
464 ERA5, as well as differences across the macroclimatic gradient, to identify mismatches  
465 between both datasets.

466 All geospatial modelling was performed using the Python API in Google Earth Engine (Gorelick  
467 *et al.*, 2017). The R statistical software, version 4.0.2 (R Core Team, 2020), was used for data  
468 visualisations. All maps were plotted using the Mollweide projection, which preserves relative  
469 areas, to avoid large distortions at high latitudes.

#### 470 ***Sources of uncertainty***

471 The temporal mismatch between the period covered by CHELSA (1979-2013) and our *in-situ*  
472 measurements (2000-2020) prevented us from directly using CHELSA climate to calculate the  
473 temperature offsets used in our models. This temporal mismatch might affect the offsets

474 calculated here because the relationship between temperature offset and macroclimate will  
475 change through time as the climate warms. Similarly, inter-annual differences in offsets due  
476 to specific weather conditions cannot be implemented in the used approach. However, we  
477 are confident that, at the relatively coarse spatial (1 km<sup>2</sup>) and temporal (monthly averages)  
478 resolution we are working at, our results are sufficiently robust to withstand these temporal  
479 issues, given that we found high consistency in offset patterns between the different  
480 timeframes and air temperature datasets examined (Supplementary Material Figs. S2–5).  
481 Nevertheless, we strongly urge future research to disentangle these potential temporal  
482 dynamics, especially given the increasing rate at which the climate is warming (Xu *et al.*, 2018,  
483 GISTEMP Team, 2021).

484 Similarly, a potential bias could result from the mismatch in method and resolution between  
485 ERA5L – used to calculate the temperature offsets – and CHELSA, which was used to create  
486 the bioclimatic variables. However, even though temperature offsets have slightly larger  
487 variation when based on the coarser-grained ERA5L-data than on the finer-grained CHELSA-  
488 data, Supplementary Material Figs. S2–5 show that relationships between soil and air  
489 temperature are largely consistent in all biomes and across the whole global temperature  
490 gradient. Therefore, the larger offsets created additional random scatter, yet no consistent  
491 bias.

492 Finally, we acknowledge that the 1-km<sup>2</sup> resolution gridded products might not be  
493 representative of conditions at the *in-situ* measurement locations within each pixel. This issue  
494 could be particularly significant for different vegetation types (here proxied at the pixel level  
495 using total aboveground biomass (unit: tons/ha i.e., Mg/ha, for the year 2010; Santoro, 2018)  
496 and NDVI (MODIS NDVI product MYD13Q1, averaged over 2015–2019)). To verify this, we  
497 compared a pixel’s estimated aboveground biomass with the dominant *in-situ* habitat (forest  
498 versus open) surrounding the sensors in that pixel (Supplementary Table S6). Importantly, all  
499 sensors installed in forests fell indeed in pixels with more than 1 ton/ha aboveground  
500 biomass. Similarly, 75% or more of sensors in open terrain fell in pixels with biomass estimates  
501 of less than 1 ton/ha. Only in the temperate woodland biome was the match between *in-situ*  
502 habitat estimates and pixel-level aboveground biomass lower, with less than 95% of sensors  
503 in forested locations correctly placed in pixels with more than 1 ton/ha biomass, and less than  
504 50% of open terrain sensors in pixels with less than 1 ton/ha biomass. While our predictions

505 will thus not be accurate for locations within a pixel that largely deviate from average  
506 conditions (e.g., open terrain in pixels identified as largely forested, or vice versa), they should  
507 be largely representative for those pixel-level averages.

## 508 **Results**

### 509 ***Biome-wide patterns in the temperature offset***

510 We found positive and negative temperature offsets of up to 10°C between *in situ* measured  
511 mean annual topsoil temperature and gridded air temperature (mean =  $3.0 \pm 2.1^\circ\text{C}$  standard  
512 deviation, Fig. 1, 0–5 cm depth; 5–15 cm is available in Supplementary Material Figs. S2, 5).  
513 The magnitude and direction of these temperature offsets varied considerably within and  
514 across biomes. Mean annual topsoil temperature was on average  $3.6 \pm 2.3^\circ\text{C}$  higher than  
515 gridded air temperature in cold and/or dry biomes, namely tundra, boreal forests, temperate  
516 grasslands, and subtropical deserts. In contrast, offsets were slightly negative in warm and  
517 wet biomes (tropical savannas, temperate forests, and tropical rainforests) where soils were,  
518 on average,  $0.7 \pm 2.7^\circ\text{C}$  cooler than gridded air temperature (Fig. 1b, Supplementary Material  
519 Figs. S2 and 5; note, however, the lower spatial coverage in these biomes in Fig. 1a, c, d,  
520 Supplementary Material Table S4). Temperature offsets in annual minimum and maximum  
521 temperature amounted to c. 10°C maximum. While annual soil temperature minima were on  
522 average higher than corresponding gridded air temperature minima in all biomes,  
523 temperature offsets of annual maxima followed largely the same biome-related trends as  
524 seen for the annual means, albeit with the higher variability expected for temperature  
525 extremes (Supplementary Material Figs. S2g, S2h, S4g, S4h). Using different air temperature  
526 data sources did not alter the annual temperature offset and biome-related patterns (see  
527 Methods and Supplementary Material Figs. S2–5).

528 Soils in the temperate seasonal forest biome were on average  $0.8^\circ\text{C}$  ( $\pm 2.2^\circ\text{C}$ ) cooler than air  
529 temperature within 1-km<sup>2</sup> grid cells of forested habitats, and  $1.0^\circ\text{C}$  ( $\pm 4.0^\circ\text{C}$ ) warmer than the  
530 air within 1-km<sup>2</sup> grid cells of non-forested habitats, resulting in a biome-wide average of  $0.5^\circ\text{C}$   
531 (Supplementary Material Table S7). Similar patterns were observed in other biomes.

### 532 ***Temporal and spatial variation in temperature offsets***

533 Our Random Forest outputs highlighted a strong seasonality in monthly temperature offsets,  
534 especially towards higher latitudes (Fig. 2). High-latitude soils were found to be several  
535 degrees warmer than the air (monthly offsets of up to 25°C) during their respective winter  
536 months, and cooler (up to 10°C) in summer months, both at 0–5 cm (Fig. 2) and 5–15 cm  
537 (Supplementary Material Fig. S8) soil depths. In the tropics and subtropics, soils in dry biomes  
538 (e.g., in the Sahara Desert or southern Africa) were predicted to be warmer than air  
539 throughout most of the year, whilst soils in mesic biomes (e.g., tropical biomes in South  
540 America, central Africa and Southeast Asia) were modelled to be consistently cooler, at both  
541 soil depths. These global gridded products were then used to create temperature-based  
542 global bioclimatic variables for soils (SBIO, Fig. 3, Supplementary Material Fig. S9).

### 543 ***Global variation in soil temperature***

544 We observed 17% less spatial variation in mean annual soil temperature globally (expressed  
545 by the standard deviation) than in air temperature, largely driven by the positive offset  
546 between soil and air temperature in cold environments (Fig. 4). Importantly, our machine  
547 learning models slightly (up to 1°C, or around 10% of variation) underestimated temperature  
548 offsets at both extremes of the temperature gradient at the 1-km<sup>2</sup> resolution (Supplementary  
549 Material Fig. S10) and likely even more in comparison with finer-resolution products.  
550 Estimates of the reduction in variation across space are thus conservative, especially in the  
551 coldest biomes. The reduction in spatial temperature variation was observed in all cold and  
552 cool biomes, with tundra and boreal forests having both a significant positive mean  
553 temperature offset and a reduction of 20% and 22% in variation, respectively (Fig. 4c). In the  
554 warmest biomes (e.g., tropical savanna and subtropical desert), however, we found an  
555 increase in variation of, on average, 10%.

556 Our bootstrap approach to validate modelled monthly offsets indicated high consistency  
557 among the outcomes of 100 bootstrapped models (Fig. 5, Supplementary Material Fig. S6a),  
558 with standard deviations in most months and across most parts of the globe around or below  
559  $\pm 1^\circ\text{C}$ . One exception to this was the temperature offset at high latitudes of the northern  
560 hemisphere during winter months (standard deviation up to  $\pm 5^\circ\text{C}$  in the 0–5 cm layer).  
561 Predictive performance was comparable across biomes, although with large variation in data  
562 availability (Supplementary Material Fig. S11).

563 The importance of predictor variables in the RF models was largely consistent across months.  
564 Macroclimatic variables such as incoming solar radiation as well as long-term averages in air  
565 temperature and precipitation were by far the most influential explanatory variables in the  
566 spatial models of the monthly temperature offset (Supplementary Material Figs. S12, 13).

567 We highlight that the current availability of *in-situ* soil temperature measurements is  
568 significantly lower in the tropics (Supplementary Material Table S5), where our model had to  
569 extrapolate temperatures beyond the range used to calibrate the model (Fig. 5b,  
570 Supplementary Material Fig. S6b).

571 Finally, our comparison with a mean annual soil temperature product derived from the  
572 coarse-resolution ERA5L topsoil temperature showed that spatial variability, e.g., driven by  
573 topographic heterogeneity, is much better captured here than in the coarser resolution of the  
574 ERA5L-based product (Fig. 6c-e). Nevertheless, our predictions at the coarse scale showed to  
575 be condensed within a 5°C range of values from the ERA5L-predictions, for more than 95% of  
576 pixels globally. Noteworthy, our predictions resulted in consistently cooler soil temperature  
577 predictions than topsoil conditions provided by ERA5L across large areas, such as the boreal  
578 and tropical forest biomes (Fig. 6a, b). Additionally, our models predicted lower values for  
579 SBIO1 than ERA5L in all regions with mean annual soil temperature below 0°C, except for a  
580 few locations around Greenland and Svalbard (Fig. 6a, b).

## 581 **Discussion**

### 582 ***Global patterns in soil temperature***

583 We observed large spatiotemporal heterogeneity in the global offset between soil and air  
584 temperature, often in the order of several degrees annually and up to more than 20°C during  
585 winter months at high latitudes. These values are in line with empirical data from regional  
586 studies (Zhang *et al.*, 2018, Lembrechts *et al.*, 2019, Obu *et al.*, 2019). Both annual and  
587 monthly offsets showed clear discrepancies between cold and dry versus warm and wet  
588 biomes. The modelled monthly offsets covaried strongly negatively with both long-term  
589 averages in free-air temperature and solar radiation, linking to the well-known decoupling of  
590 soil from air temperature due to snow (for cold extremes in cold and cool biomes) (Grundstein  
591 *et al.*, 2005). However, the secondary importance of variables related to precipitation and soil

592 structure hints to the additional distinction between wet and dry biomes at the warm end of  
593 the temperature gradient. There, buffering due to shading, evapotranspiration and the  
594 specific heat of water (mostly against warm extremes in warm and wet biomes) results in  
595 cooler soil temperature (Geiger, 1950, Grundstein *et al.*, 2005, Hennon *et al.*, 2010, Wang &  
596 Dickinson, 2012, De Frenne *et al.*, 2013, Grünberg *et al.*, 2020), while such buffering is not as  
597 strong in warm and dry biomes due to the lower water availability (Wang & Dickinson, 2012,  
598 Greiser *et al.*, 2018, Zhou *et al.*, 2021). As such, these results highlight strong macroclimatic  
599 impacts on the soil microclimate across the globe (see also De Frenne *et al.*, 2019), yet with  
600 soil temperature importantly non-linearly related to air temperature at the global scale. This  
601 confirms that the latter is not sufficient as a proxy for temperature conditions near or in the  
602 soil. With our soil-specific global bioclimatic products, we have provided the means to correct  
603 for these important region-specific, non-linear differences between soil and air temperature  
604 at an unprecedented spatial resolution.

#### 605 ***Drivers of the temperature offset***

606 Our empirical modelling approach enabled us to accurately map global patterns in soil  
607 temperature. In doing so we did not aim to disentangle the mechanisms governing the  
608 temperature offset: such an endeavour would require modelling the biophysics of energy  
609 exchange at the soil surface across biomes (Kearney *et al.*, 2019, Maclean *et al.*, 2019,  
610 Maclean & Klings, 2021). Importantly, many of the predictor variables used in our study (e.g.,  
611 long-term averages in macroclimatic conditions or solar radiation) are unlikely to represent  
612 direct causal relationships underlying the temperature offset, but may rather indirectly relate  
613 to many ensuing factors that affect the functioning of ecosystems at fine spatial scales which,  
614 in turn, feedback on local temperature offsets, such as energy and water balances, snow  
615 cover, wind intensity and vegetation cover (De Frenne *et al.*, 2021). For example, while  
616 increased solar radiation itself would theoretically result in soils warming more than the air,  
617 high solar radiation at the global scale often coincides with high vegetation cover blocking  
618 radiation input to the soil, thus correlating with relatively cooler soils (De Frenne *et al.*, 2021).  
619 Our results highlight, however, that the complex relationship between microclimatic soil  
620 temperature and macroclimatic air temperature is predictable across large spatial extents  
621 thanks to broad scale patterns, even if this is governed by a multitude of local-scale factors  
622 involving fine spatiotemporal resolutions. Nevertheless, the predictive quality of our models



623 was lower in high latitude regions, where high variation in the *in situ* measured offsets – likely  
624 driven by the interactions between snow, local topography and vegetation – reduced  
625 predictive power of the models at the 1-km<sup>2</sup> resolution (Greiser *et al.*, 2018, Way &  
626 Lewkowicz, 2018, Grünberg *et al.*, 2020, Myers-Smith *et al.*, 2020, Niittynen *et al.*, 2020).

### 627 **Implications for microclimate warming**

628 Our results highlight clear biome-specific differences in mean annual temperature between  
629 air and soil temperatures, as well as a significant reduction in the spatial variation in  
630 temperature in the soil or near the soil surface, especially in cold and cool biomes (Fig. 4).  
631 These patterns remain even despite the presence of often strongly opposing monthly offset  
632 trends (Fig. 2). The observed correlation between long-term averages in macroclimatic  
633 conditions and the annual temperature offset illustrates that soil temperature is unlikely to  
634 warm at the same rate as air temperature when macroclimate warms. Indeed, one degree of  
635 air temperature warming could result in either a bigger or smaller soil temperature change,  
636 depending on where along the macroclimatic gradient this is happening. These effects might  
637 be seen in cold biome soils most strongly, as they not only experience the largest (positive)  
638 temperature offsets and reductions in climate range compared to air temperature (Fig. 4b, c),  
639 but they are also expected to experience the strongest magnitude of macroclimate warming  
640 (Cooper, 2014, Overland *et al.*, 2014, Chen *et al.*, 2021, GISTEMP Team, 2021). As a result,  
641 mean annual temperatures in cold climate soils can be expected to warm slower than the  
642 corresponding macroclimate as offsets shrink with increasing macroclimate warming.

643 Contrastingly, predicted climate warming in hot and dry biomes could be amplified in the  
644 topsoil, where we show soils to become increasingly warmer than the air at higher  
645 temperatures. Similarly, changes in precipitation regimes – and thus soil moisture – can  
646 significantly alter the relationship between air and soil temperature, with critical implications  
647 for soil moisture-atmosphere feedbacks, especially in hot biomes (Zhou *et al.*, 2021). Indeed,  
648 as precipitation decreases, offsets could turn more positive and soil temperatures might  
649 warm even faster than the observed macroclimate warming. Therefore, future research  
650 should not only use soil temperature data as provided here to study belowground ecological  
651 processes (De Frenne *et al.*, 2013, Lembrechts *et al.*, 2020), it should also urgently investigate  
652 future scenarios of soil climate warming in light of changing air temperature and precipitation,

653 at ecologically relevant spatial and temporal resolutions to incorporate the non-linear  
654 relationships exposed so far (Lembrechts & Nijs, 2020).

### 655 **Within-pixel heterogeneity**

656 We chose to use a 1-km<sup>2</sup> resolution spatial grid to model mismatches between soil and air  
657 temperature, aggregating all values from different microhabitats within the same 1-km<sup>2</sup> grid  
658 cell (e.g., sensors in forested versus open patches) as well as all daily and diurnal variation  
659 within a month. Additionally, we used coarse-grained free-air temperature rather than in-situ  
660 measured air temperatures. We are aware that higher spatiotemporal resolutions would  
661 likely reveal the importance of locally heterogeneous variables. Finer-scale factors that affect  
662 the local radiation balance and wind (e.g., topography, snow and vegetation cover,  
663 urbanization) at the landscape to local scales and those that directly affect neighbouring  
664 locations (e.g. topographic shading and cold-air drainage, Whiteman, 1982, Ashcroft & Gollan,  
665 2012, Lembrechts *et al.*, 2020) would probably have emerged as more important drivers at  
666 regional scales and with higher spatiotemporal resolutions than those used here  
667 (Supplementary Material Fig. S12). The latter is illustrated by the multi-degree Celsius  
668 difference in mean annual temperature between forested and non-forested locations within  
669 the same biome (Supplementary Material Table S7), as well as the lower accuracy obtained  
670 during winter months at high latitudes, where and when fine-scale spatial heterogeneity in  
671 snow cover and depth probably lowers models' predictability at the 1-km<sup>2</sup> resolution. *In-situ*  
672 measurements were largely from areas with a representative vegetation type, supporting the  
673 reliability of our predictions for the dominant habitat type within a pixel. However, improved  
674 accuracy at high latitudes will depend on the future development of high-resolution snow  
675 depth and/or snow water equivalent estimates (Luoju *et al.*, 2010).

676 The SoilTemp database (Lembrechts *et al.*, 2020) will facilitate the necessary steps towards  
677 mapping soil temperature at higher spatiotemporal resolutions in the future, with its  
678 georeferenced time series of *in situ* measured soil and near-surface temperature and  
679 associated metadata. Nevertheless, when compared to existing soil temperature products  
680 such as those from ERA5L (Copernicus Climate Change Service (C3S), 2019), we emphasize  
681 that the increased resolution of our data products already provides a major technical  
682 advance, even though substantial finer within-pixel variation is still lost through  
683 spatiotemporal aggregation.

## 684 **Conclusions**

685 The spatial (biome-specific) and temporal (seasonally variable) offsets between air and soil  
686 temperature quantified here likely bias predictions of current and future climate impacts on  
687 species and ecosystems (Körner & Paulsen, 2004, Kearney *et al.*, 2009, Cooper, 2014, Opedal  
688 *et al.*, 2015, Graae *et al.*, 2018, Zellweger *et al.*, 2020, Bergstrom *et al.*, 2021). Temperature  
689 in the topsoil rather than in the air ultimately defines the distribution and performance of  
690 most terrestrial species, as well as many ecosystem functions at or below the soil surface  
691 (Pleim & Gilliam, 2009, Portillo-Estrada *et al.*, 2016, Hursh *et al.*, 2017, Gottschall *et al.*, 2019).  
692 As many ecosystem functions are highly correlated with temperature (yet often non-linear,  
693 Johnston *et al.*, 2021), soil temperature rather than air temperature should in those instances  
694 be the preferred predictor for estimating their rates and temperature thresholds (Rosenberg  
695 *et al.*, 1990, Coûteaux *et al.*, 1995, Schimel *et al.*, 1996). Correcting for the non-linear  
696 relationship between air and soil temperature identified here is thus vital for all fields  
697 investigating abiotic and biotic processes relating to terrestrial environments (White *et al.*,  
698 2020). Indeed, soil temperature, macroclimate and land-use change will interact to define the  
699 future climate as experienced by organisms, and high-resolution soil temperature data is  
700 needed to tackle current and future challenges.

701 By making our global soil temperature maps and the underlying monthly offset data openly  
702 available, we offer gridded soil temperature data for climate research, ecology, agronomy  
703 and other life and environmental sciences. Future research has the important task of further  
704 improving the spatial and temporal resolution of global microclimate products as  
705 microclimate operates at much higher temporal resolutions, with temporal variation over  
706 hours, days, seasons and years (Potter *et al.*, 2013, Bütikofer *et al.*, 2020), as well as to confirm  
707 accuracy of predictions in undersampled regions in the underlying maps (Lembrechts *et al.*,  
708 2021). However, we are convinced that the maps presented here bring us one step closer to  
709 having accessible climate data exactly where it matters most for many terrestrial organisms  
710 (Kearney & Porter, 2009, Ashcroft *et al.*, 2014, Pincebourde *et al.*, 2016, Niittynen & Luoto,  
711 2018, Lembrechts & Lenoir, 2019). We nevertheless highlight that there is still a long way to  
712 go towards global soil microclimate data with an optimal spatiotemporal resolution. We  
713 therefore urge all scientists to submit their microclimate time series to the SoilTemp database

714 to fill data gaps and help to increase the spatial resolution until it matches with the scale at  
715 which ecological processes take place (Bütikofer *et al.*, 2020, Lembrechts *et al.*, 2020).

716

## 717 **Data availability**

718 All monthly data to train the models and reproduce the figures, sampled covariate data, and  
719 models are available at <https://doi.org/10.5281/zenodo.4558663>. Soil bioclim layers SBIO1-  
720 11 are also directly available in Google Earth Engine under  
721 projects/crowtherlab/soil\_bioclim/soil\_bioclim\_0\_5cm and  
722 projects/crowtherlab/soil\_bioclim/soil\_bioclim\_5\_15cm.

723

## 724 **Code availability**

725 All source code is available at <https://doi.org/10.5281/zenodo.4558663>.

726

## 727 **Acknowledgements**

728 JLL received funding from the Research Foundation Flanders (grant nr. 12P1819N) The project received funding from the Research  
729 Foundation Flanders (grants nrs, G018919N, W001919N). JA received funding from the University of Helsinki, Faculty of Science  
730 (MICROCLIM, grant nr. 7510145) and Academy of Finland Flagship (grant no. 337552). PDF, CM and PV received funding from the  
731 European Research Council (ERC) under the European Union's Horizon 2020 research and innovation programme (ERC Starting Grant  
732 FORMICA 757833). JK received funding from the Arctic Interactions at the University of Oulu and Academy of Finland (318930, Profi 4),  
733 Maa- ja vesitekniiikan tuki ry., Tiina and Antti Herlin Foundation, Nordenskiöld Samfundet and Societas pro Fauna et Flora Fennica. MK  
734 received funding from the Czech Science Foundation (grant nr. 20-28119S) and the Czech Academy of Sciences (grant nr. RVO 67985939).  
735 TC received funding from DOB Ecology. National Geographic Society grant no. 9480-14 and WW-240R-17. MA recieved funding from CISSC  
736 ( program ICRP (grant nr:2397) and INSF (grant nr: 96005914). The Royal Botanic Garden Edinburgh is supported by the Scottish  
737 Government's Rural and Environment Science and Analytical Services Division. JMA received funding from the Funding Org. Qatar  
738 Petroleum (grant nr. QUEx-CAS-QP-RD-18/19). JMA received funding from the European Union's Horizon 2020 research and innovation  
739 program (grant no. 678841) and from the Swiss National Science Foundation (grant no. 31003A\_176044). JA was supported by research  
740 grants LTAUSA19137 (program INTER-EXCELLENCE, subprogram INTER-ACTION) provided by Czech Ministry of Education, Youth and Sports  
741 and 20-05840Y of the Czech Science Foundation. AA was supported by the Ministry of Science and Higher Education of the Russian  
742 Federation (grant FSRZ-2020-0014). SN, UAT, JJA, and JvO received funding from the Independent Research Fund Denmark (7027-00133B).  
743 Lvdb, KT, MYB and RC acknowledge funding from the German Research Foundation within the Priority Program SPP-1803 "EarthShape:  
744 Earth Surface Shaping by Biota" (grant TI 338/14-1&2 and BA 3843/6-1). PB was supported by grant project VEGA of the Ministry of  
745 Education of the Slovak Republic and the Slovak Academy of Sciences No. 2/0132/18. Forest Research received funding from the Forestry  
746 Commission (climate change research programme). JCB acknowledges the support of Universidad Javeriana. JLBA received funding from  
747 the Dirección General de Cambio Climático del Gobierno de Aragón; JLBA acknowledges fieldwork assistance by Ana Acín, the Ordesa y  
748 Monte Perdido National Park, and the Servicio de Medio Ambiente de Soria de la Junta de Castilla y León. RGB and MPB received funding  
749 from BECC - Biodiversity and Ecosystem services in a Changing Climate. MPB received funding from The European Union's Horizon 2020  
750 research and innovation program under the Marie Skłodowska-Curie Grant Agreement No. 657627 and The Swedish Research Council  
751 FORMAS – future research leaders No. 2016-01187. JB received funding from the Czech Academy of Sciences (grant nr. RVO 67985939).  
752 NB received funding from the SNF (grant numbers 40FA40\_154245, 20FI21\_148992, 20FI20\_173691, 407340\_172433) and from the EU  
753 (contract no. 774124). ICOS EU research infrastructure. EU FP7 NitroEurope. EU FP7 ECLAIRE. The authors from Biological Dynamics of  
754 Forest Fragments Project, PDBFF, Instituto Nacional de Pesquisas da Amazônia, Brazil were supported by the MCTI/CNPq/FNDCT – Ação  
755 Transversal n°68/2013 – Programa de Grande Escala da Biosfera-Atmosfera na Amazônia – LBA; Project "Como as florestas da Amazônia  
756 Central respondem às variações climáticas? Efeitos sobre dinâmica florestal e sinergia com a fragmentação florestal." This is the study 829  
757 of the BDFFP Technical Series. to The EUCFLUX Cooperative Research Program and Forest Science and Research Institute-IPEF. NC  
758 acknowledges funding by Stelvio National Park. JC was funded by the Spanish government grant CGL2016-78093-R. ANID-FONDECYT

759 1181745 AND INSTITUTO ANTARTICO CHILENO (INACH FR-0418). SC received funding from the German Research Foundation (grant no.  
760 DFG– FZT 118, 202548816). The National Science Foundation, Poland (grant no. UMO-2017/27/B/ST10/02228), within the framework of  
761 the “Carbon dioxide uptake potential of sphagnum peatlands in the context of atmospheric optical parameters and climate  
762 changes”(KUSCO2) project. SLC received funding from the South African National Research Foundation and the Australian Research  
763 Council. FM, MČ, KU and MU received funding from Slovak Research and Development Agency (no. APVV-19-0319). Instituto Antartico  
764 Chileno (INACH\_RT-48\_16), Iniciativa Científica Milenio Núcleo Milenio de Salmónidos Invasores INVASAL, Institute of Ecology and  
765 Biodiversity (IEB), CONICYT PIA APOYO CCTE AFB170008. PC is supported by NERC core funding to the BAS 'Biodiversity, Evolution and  
766 Adaptation Team. EJC received funding from the Norwegian Research Council (grant number 230970). GND was supported by NERC E3  
767 doctoral training partnership grant (NE/L002558/1) at the University of Edinburgh and the Carnegie Trust for the Universities of Scotland.  
768 Monitoring stations on Livingston Island, Antarctica were funded by different research projects of the Govern of Spain (PERMAPLANET  
769 CTM2009-10165-E; ANTARPERMA CTM2011-15565-E; PERMASNOW CTM2014-52021-R), and the PERMATHERMAL arrangement between  
770 the University of Alcalá and the Spanish Polar Committee. GN received funding from the Autonomous Province of Bolzano (ITA). The  
771 infrastructure, part of the UK Environmental Change Network, was funded historically in part by ScotNature and NERC National  
772 Capability LTS-S: UK-SCAPE; NE/R016429/1). JD was supported by the Czech Science Foundation (GA17-19376S) and MSMT  
773 (LTAUSA18007). ED received funding from the Kempe Foundation (JCK-1112 and JCK-1822). The infrastructure was supported by the  
774 Ministry of Education, Youth and Sports of the Czech Republic within the National Sustainability Programme I (NPU I), grant number  
775 LO1415 and by the project for national infrastructure support CzeCOS/ICOS Reg.No. LM2015061. NE received funding from the German  
776 Research Foundation (DFG– FZT 118, 202548816). BE received funding from the GLORIA-EU project no EVK2-CT2000-00056, the  
777 Autonomous Province of Bolzano (ITA), from the Tiroler Wissenschaftsfonds and from the University of Innsbruck. RME was supported by  
778 funding to the SAFE Project from the Sime Darby Foundation. OF received funding from the German Research Foundation (DFG– FZT 118,  
779 202548816). EFP was supported by the Jardín Botánico Atlántico (SV-20-GIJON-JBA). MF was funded by the German Federal Ministry of  
780 Education and Research (BMBF) in the context of The Future Okavango (Grant No. 01LL0912) and SASSCAL (01LG1201M; 01LG1201N)  
781 projects. EFL received funding from ANID PIA / BASAL FB210006. RAG received funding from Fondecyt 11170516, CONICYT PIA AFB170008  
782 and ANID PIA / BASAL FB210006. MBG received funding from National Parks (DYNBIO, #1656/2015) and The Spanish Research Agency  
783 (VULBIMON, #CGL2017-90040-R). MG received funding from the Swiss National Science Foundation (ICOS-CH Phase 2 20FI20\_173691). FG  
784 received funding from the German Research Foundation (DFG– FZT 118, 202548816). KG and TS received funding from the UK  
785 Biotechnology and Biological Research Council (grant = 206/D16053). SG was supported by the Research Foundation Flanders (FWO)  
786 (project G0H1517N). KJ and PH received funding from the EU Horizon2020 INFRAIA project eLTER-PLUS (871128), the project LTER-CWN  
787 (FFG, F&E Infrastrukturförderung, project number 858024) and the Austrian Climate Research Program (ACRP7 – CentForCSink –  
788 KR14AC7K11960). SH and ARB received funding through iDiv funded by the German Research Foundation (DFG– FZT 118, 202548816). LH  
789 received funding from the Czech Science Foundation (grant nr. 20-28119S) and the Czech Academy of Sciences (grant nr. RVO 67985939).  
790 MH received funding from the Baden-Württemberg Ministry of Science, Research and Arts via the project DRiER (Drought impacts,  
791 processes and resilience: making the in-visible visible). LH received funding from International Polar Year, Weston Foundation, and  
792 ArcticNet. DH received funding from Natural Sciences and Engineering Council (Canada) (RGPIN-06691). TTH received funding from  
793 Independent Research Fund Denmark (grant no. 8021-00423B) and Villum Foundation (grant no. 17523). Ministry of Education, Youth and  
794 Sports of the Czech Republic (projects LM2015078, VAN2020/01 and CZ.02.1.01/0.0/0.0/16\_013/0001708). KH, CG and CJD received  
795 funding from Bolin Centre for Climate Research, Stockholm University and from the Swedish research council Formas [grant n:o 2014-  
796 00530 to KH]. JJ received funding from the Funding Org. Swedish Forest Society Foundation (grant nr. 2018-485-Steg 2 2017) and Swedish  
797 Research Council FORMAS (grant nr. 2018-00792). AJ received funding from the German Federal Ministry of Education and Research BMBF  
798 (Grant Nr. FKZ 031B0516C SUSALPS) and the Oberfrankenstiftung (Grant Nr. OFS FP00237). ISJ received funding from the Energy Research  
799 Fund (NÝR-11 - 2019, NÝR-18 - 2020). TJ was supported by a UK NERC Independent Research Fellowship (grant number: NE/S01537X/1). RJ  
800 received funding from National Science Centre of Poland (grant number: 2016/21/B/ST10/02271) and Polish National Centre for Research  
801 and Development (grant number: Pol-Nor/203258/31/2013). VK received funding from the Czech Academy of Sciences (grant nr. RVO  
802 67985939). AAK received funding from MoEFCC, Govt of India (AICOPTAX project F. No. 22018/12/2015/RE/Tax). NK received funding  
803 from FORMAS, VR, support from the research infrastructure ICOS. BK received funding from the National Research, Development and  
804 Innovation Fund of Hungary (grant nr. K128441). Ministry of Education, Youth and Sports of the Czech Republic (projects LM2015078 and  
805 CZ.02.1.01/0.0/0.0/16\_013/0001708). Project B1-RNM-163-UGR-18-Programa Operativo FEDER 2018, partially funded data collection.  
806 Norwegian Research Council (NORKLIMA grants #184912 and #244525) awarded to Vigdis Vandvik. MM received funding from the Czech  
807 Science Foundation (grant nr. 20-28119S) and the Czech Academy of Sciences (grant nr. RVO 67985939). Project CONICYT-PAI 79170119  
808 and ANID-MPG 190029 awarded to Roy Mackenzie. This work was partly funded by project MIUR PON Cluster OT4CLIMA. RM received  
809 funding from the SNF project number 407340\_172433. FM received funding from the Stelvio National Park. PM received funding from  
810 AIAS-COFUND fellowship programme supported by the Marie Skłodowska- Curie actions under the European Union’s Seventh Framework  
811 Pro-gramme for Research, Technological development and Demonstration (grant agreement no 609033) and the Aarhus University  
812 Research Foundation, Denmark. RM received funding from the Ministry of Education, Youth and Sports of the Czech Republic (project  
813 LTT17033). SM and VM received funding from EU FP6 NitroEurope (grant nr. 17841), EU FP7 ÉCLAIRE (grant nr. 282910), the Ministry of  
814 Education and Science of Ukraine (projects nr. 505, 550, 574, 602), GEF-UNEP funded “Toward INMS” project (grant nr. NEC05348) and ENI  
815 CBC BSB PONTOS (grant nr. BSB 889). The authors from Biological Dynamics of Forest Fragments Project, PDBFF, Instituto Nacional de  
816 Pesquisas da Amazônia, Brazil were supported by the MCTI/CNPq/FNDCT – Ação Transversal n°68/2013 – Programa de Grande Escala da  
817 Biosfera-Atmosfera na Amazônia – LBA; Project “Como as florestas da Amazônia Central respondem às variações climáticas? Efeitos sobre  
818 dinâmica florestal e sinergia com a fragmentação florestal.”. FJRM was financially supported by the Netherlands Organization for Scientific  
819 Research (VICI grant 016.VICI.170.072) and Research Foundation Flanders (FWO-SBO grant S000619N). STM received funding from New  
820 Frontiers in Research Fund-Exploration (grant nr. NFRF-2018-02043) and NSERC Discovery. MMR received funding from the Australian  
821 Research Council Discovery Early Career Research Award (grant nr. DE180100570). JAM received funding from the National Science  
822 Foundation (DEB 1557094), International Center for Advanced Renewable Energy and Sustainability (I-CARES) at Washington University in  
823 St. Louis, ForestGEO, and Tyson Research Center. IM-S was funded by the UK Natural Environment Research Council through the  
824 ShrubTundra Project (NE/M016323/1). MBN received funding from FORMAS, VR, Kempe Foundations support from the research

825 infrastructures ICOS and SITES. MDN received funding from CONICET (grant nr. PIP 112-201501-00609). Spanish Ministry of Science grant  
826 PID2019-110521GB-I00 and Catalan government grant 2017-1005. French National Research Agency (ANR) in the frame of the Cluster of  
827 Excellence COTE (project HydroBeech, ANR-10-LABX-45). VLIR-OUS, under the Institutional University Cooperation programme (IUC) with  
828 Mountains of the Moon University. Project LAS III 77/2017/B entitled: "Estimation of net carbon dioxide fluxes exchanged between the  
829 forest ecosystem on post-agricultural land and between the tornado-damaged forest area and the atmosphere using spectroscopic and  
830 numerical methods", source of funding: General Directorate of State Forests, Warsaw, Poland. Max Planck Society (Germany), RFBR,  
831 Krasnoyarsk Territory and Krasnoyarsk Regional Fund of Science, project number 20-45-242908. Estonian Research Council (PRG609), and  
832 the European Regional Development Fund (Centre of Excellence EcolChange). Canada-Denmark Arctic Research Station Early Career  
833 Scientist Exchange Program, from Polar Knowledge Canada (POLAR) and the Danish Agency for Science and Higher Education. AP received  
834 funding from Fondecyt 1180205, CONICYT PIA AFB170008 and ANID PIA / BASAL FB210006. MP received funding from the Funding Org.  
835 Knut and Alice Wallenberg Foundation (grant nr. 2015.0047), and acknowledges funding from the Swedish Research Council (VR) with  
836 contributing research institutes to both the SITES and ICOS Sweden infrastructures. JP and RO were funded by the Spanish Ministry of  
837 Science grant PID2019-110521GB-I00, the fundación Ramón Areces grant ELEMENTAL-CLIMATE, and the Catalan government grant 2017-  
838 1005. MPB received funding from the Svalbard Environmental Protection Fund (grant project number 15/128) and the Research Council of  
839 Norway (Arctic Field Grant, project number 269957). RP received funding from the Ministry of Education, Youth and Sports of the Czech  
840 Republic (grant INTER-TRANSFER nr. LTT20017). LTSEr Zone Atelier Alpes; Fédération FREE-Alpes. RP received funding from a Humboldt  
841 Fellowship for Experienced Researchers. Prokushkin AS and Zyryanov VI contribution has been supported by the RFBR grant #18-05-60203-  
842 Arktika. RPU received funding from the Polish National Science Centre (grant project number 2017/27/B/NZ8/00316). ODYSSEE project  
843 (ANR-13-ISV7-0004, PN-II-ID-JRP-RO-FR-2012). KR was supported through an Australian Government Research Training Program  
844 Scholarship. Fieldwork was supported by the Global Challenges program at the University of Wollongong, the ARC the Australian Antarctic  
845 Division and INACH. Project SUBANTECO IPEV 136 (French Polar Institute Paul-Emile Victor), Zone Atelier CNRS Antarctique et Terres  
846 Australes, SAD Région Bretagne (Project INFLECT), BiodivERsa 2019-2020 BioDivClim call 'ASICS' (ANR-20-EBIS-0004). SAR received funding  
847 from the Australian Research Council. NSF grant #1556772 to the University of Notre Dame. Pavia University (Italy). OR received funding  
848 from EU-LEAP-Agri (RAMSES II), EU-DESIRA (CASSECS), EU-H2020 (SustainSahel), AGROPOLIS and TOTAL Foundations (DSCATT), CGIAR  
849 (GLDC). AR was supported by the Russian Science Foundation (Grant 18-74-10048). Parc national des Ecrins. JS received funding from  
850 Vetenskapsrådet grant nr (No: 2014-04270), ALTER-net multi site grant, River LIFE project (LIFE08 NAT/S/000266), Flexpeil. Helmholtz  
851 Association long-term research program TEREÑO (Terrestrial Environmental Observatories). PS received funding from the Polish Ministry  
852 of Science and Higher Education (grant nr. N N305 304840). AS acknowledges funding by ETH Zürich project FEVER ETH-27 19-1. LSC  
853 received funding from NSERC Canada Graduate Scholarship (Doctoral) Program; LSC was also supported by ArcticNet-NCE (insert grant #).  
854 Conselho Nacional de Desenvolvimento Científico e Tecnológico (141513/2017-9); Fundação Carlos Chagas Filho de Amparo à Pesquisa do  
855 Estado do Rio de Janeiro (E26/200.84/2019). ZS received funding from the SRDA (grants nos. APVV-16-0325 and APVV-20-0365) and from  
856 the ERDF (grant no. ITMS 313011S735, CE LignoSilva). JS, MB, and CA received funding from core budget of ETH Zurich. State excellence  
857 Program M-V "WETSCAPES". AfricanBioServices project funded by the EU Horizon 2020 grant number 641918. The authors from  
858 KIT/IMK-IFU acknowledge the funding received within the German Terrestrial Environmental Observatories (TERENO) research program of  
859 the Helmholtz Association and from the Bavarian Ministry of the Environment and Public Health (UGV06080204000). Deutsche  
860 Forschungsgemeinschaft (DFG, German Research Foundation), project number 192626868, in the framework of the collaborative German-  
861 Indonesian research project CRC 990 (SFB): "EFForTS, Ecological and Socioeconomic Functions of Tropical Lowland Rainforest  
862 Transformation Systems (Sumatra, Indonesia)". MS received funding from the Ministry of Education, Youth and Sports of the Czech  
863 Republic (grant nr. INTER-TRANSFER LTT19018). TT received funding from the Swedish National Space Board (SNSB Dnr 95/16) and the  
864 CASSECS project supported by the European Union. HJDT received funding from the UK Natural Environment Research Council (NERC  
865 doctoral training partnership grant NE/L002558/1). German Science Foundation (DFG) GraKo 2010 "Response". PDT received funding  
866 from the MEMOIRE project (PN-III-P1-1.1-PD2016-0925). Arctic Challenge for Sustainability II (ArCS II; JPMXD1420318865). JU received  
867 funding from Czech Science Foundation (grant nr. 21-114875). TU received funding from the Romanian Ministry of Education and Research  
868 (CCCDI - UEFISCDI -project PN-III-P2-2.1-PED-2019-4924 and PN2019-2022/19270201-Ctr. 25N BIODIVERS 3-BIOSERV). AV acknowledge  
869 funding from RSF, project 21-14-00209. GFV received funding from the Dutch Research Council NWO (Veni grant, no. 863.14.013).  
870 Australian Research Council Discovery Early Career Research Award DE140101611. FGAV received funding from the Portuguese Science  
871 Foundation (FCT) under CEECIND/02509/2018, CESAM (UIDP/50017/2020+UIDB/50017/2020), FCT/MCTES through national funds, and  
872 the co-funding by the FEDER, within the PT2020 Partnership Agreement and Compete 2020. Ordesa y Monte Perdido National Park. MVI  
873 received funding from the Spanish Ministry of Science and Innovation through a doctoral grant (FPU17/05869). JW received funding from  
874 the Czech Science Foundation (grant nr. 20-28119S) and the Czech Academy of Sciences (grant nr. RVO 67985939). CR and SW received  
875 funding from the Swiss Federal Office for the Environment (FOEN) and the de Giacomo foundation. YY received funding from the National  
876 Natural Science Foundation of China (Grant no. 41861134039 and 41941015). ZY received funding from the National Natural Science  
877 Foundation of China (grant nr. 41877458). FZ received funding from the Swiss National Science Foundation (grant nr. 172198 and 193645).  
878 PZ received funding from the Funding Org. Knut and Alice Wallenberg Foundation (grant no. 2015.0047). JL received funding from: (i) the  
879 Agence Nationale de la Recherche (ANR), under the framework of the young investigators (JCJC) funding instrument (ANR JCJC Grant  
880 project N°ANR-19-CE32-0005-01: IMPRINT); (ii) the Centre National de la Recherche Scientifique (CNRS) (Défi INFINITI 2018: MORFO); and  
881 the Structure Fédérative de Recherche (SFR) Condorcet (FR CNRS 3417: CREUSE)

882 Fieldwork in the Arctic got facilitated by funding from the EU INTERACT program. SN, UAT, JJA, and JVo would like to thank the field team  
883 of the Vegetation Dynamics group for their efforts and hard work. We acknowledge Dominique Tristan for letting access to the field. for  
884 the logistic support the crew of INACH and Gabriel de Castilla Station team on Deception Island. We thank the Inuvialuit and Klwane First  
885 Nations for the opportunity to work on their land. MadP acknowledges fieldwork assistance and logistics support to Unidad de Tecnología  
886 Marina CSIC, and the crew of Juan Carlos I and Gabriel de Castilla Spanish Antarctic Stations, as well as to the different colleagues from  
887 UAH that helped on the instruments maintenance. ERF acknowledges fieldwork assistance by Martin Heggli. MBG acknowledges fieldwork  
888 and technical assistance by P Abadía, C Benedé, P Bravo, J Gómez, M Grasa, R Jimenez, H Miranda, B Ponz, J Revilla and P Tejero, and the  
889 Ordesa and Monte Perdido National Park staff. LH acknowledges field assistance by John Jacobs, Andrew Trant, Robert Way, Darroch

890 Whitaker; I acknowledge the Inuit of Nunatsiavut, and the Cooperative Management Board of Torngat Mountains National Park for their  
891 support of this project and acknowledge that the field research was conducted on their traditional lands. We thank our many bear guides,  
892 especially Boonie, Eli, Herman, John, and Maria Merkuratsuk. AAK acknowledges field support of Akhtar Malik, Rameez Ahmad. Part of  
893 microclimatic records from Saxony was funded by the Saxon Switzerland National Park Administration. Tyson Research Center. JP  
894 acknowledges field support of Emmanuel Malet (Edytem) and Rangers of Réserves Naturelles de Haute-Savoie (ASTERS). practical help:  
895 Roel H. Janssen, N. Huij, E. Bakker, Schools in the tepåseförsöket, Forskar fredag, Erik Herberg. The support by the Bavarian Forest  
896 National Park administration is highly appreciated. Liesbeth acknowledges CONAF and onsite support from the park rangers from PN Pan  
897 de Azucar, PN La Campana, PN Nahuelbuta and from comunidad agrícola Quebrada de Talca. JL and FS acknowledge Manuel Nicolas and  
898 all forest officers from the Office National des Forêts (ONF) who are in charge of the RENECOFOR network and who provided help and  
899 local support for the installation and maintenance of temperature loggers in the field.

## 900 Author contributions

901 JLL and JL conceptualized the project, JLL, JvdH, MBA, PDF, MK, ML, IMDM, TWC, IN and JL designed  
902 the paper, the SoilTemp consortium acquired the data, JLL, JVDH, JK, and PN analysed the data, JLL,  
903 JvdH, JA, MBA, PDF, JK, MK, ML, IMDM, TWC, JJB, SH, DHK, PN, BRS and KVM interpreted the  
904 analyses. All authors significantly revised the manuscript and approved it for submission.

## 905 The authors declare no competing interests.

## 906 Affiliations

907 1) Research Group PLECO (Plants and Ecosystems), University of Antwerp, 2610 Wilrijk, Belgium, 2) Department of Environmental Systems  
908 Science, Institute of Integrative Biology, ETH Zürich, Zürich, Switzerland, 3) Finnish Meteorological Institute, P.O. Box 503, FI-00101  
909 Helsinki, Finland, 4) Department of Geosciences and Geography, Gustaf Hällströmin katu 2a, FIN-00014 University of Helsinki, Finland, 5)  
910 Centre for Sustainable Ecosystem Solutions, School of Biological Sciences, University of Wollongong, Wollongong, Australia, 6) Australian  
911 Museum, Sydney, Australia, 7) Forest & Nature Lab, Department of Environment, Ghent University, Geraardsbergsesteenweg 267, 9090  
912 Melle-Gontrode, Belgium, 8) Geography Research Unit, University of Oulu, Oulu, Finland, 9) Institute of Botany of the Czech Academy of  
913 Sciences, Zámek 1, CZ-25243, Průhonice, Czech Republic, 10) Faculty of Forestry and Wood Sciences, Czech University of Life Sciences  
914 Prague, Kamýcká 129, CZ-165 21, Prague 6 - Suchbát, Czech Republic, 11) Dept of Geosciences and Geography, Gustaf Hällströmin katu 2a,  
915 FIN-00014 Univ. of Helsinki, Finland, 12) Environment and Sustainability Institute, University of Exeter, Penryn Campus, Penryn, UK, TR10  
916 9FE, 13) Department of Geography, York St John University, Lord Mayor's Walk, York, YO31 7EX, United Kingdom, 14) Department of Earth  
917 and Environmental Sciences, KU Leuven, Celestijnenlaan 200E, 3001 Leuven, Belgium, 15) School of Natural Resources and Environment,  
918 University of Florida, Gainesville, FL 32611, USA, 16) Smithsonian Environmental Research Center, Edgewater MD 21037 USA, 17)  
919 Department of Wildlife Ecology and Conservation, University of Florida, Gainesville, FL 32611, USA, 18) Department of Natural Sciences  
920 and Environmental Health, University of South-Eastern Norway, Gullbringvegen 36, NO-3800, Bø, Norway, 19) Alpine Ecosystems Research  
921 Program, Institute of Ecology, Ilia State University, Tbilisi, Georgia, 20) Department of Range Management, Faculty of Natural Resources  
922 and Marine Sciences, Tarbiat Modares University, Noor, Mazandaran Province, I. R. Iran, 21) Department of Ecological Science, Vrije  
923 Universiteit Amsterdam, The Netherlands., 22) Royal Botanic Garden Edinburgh, 20A Inverleith Row, EH3 5LR, Edinburgh, UK, 23)  
924 Environmental Science Center, Qatar University, Doha, Qatar, 24) Department of Environmental Systems Science, Institute of Integrative  
925 Biology, ETH Zurich, Universitätsstrasse 16, CH-8092 Zürich, Switzerland, 25) Research group ECOBE, University of Antwerp, 2610 Wilrijk,  
926 Belgium, 26) Department of Agroecology and Environment, Agroscope Research Institute, Reckenholzstrasse 191, 8046 Zürich,  
927 Switzerland, 27) Department of Environmental Systems Science, ETH Zurich, Universitaetstrasse 2, 8092 Zurich, Switzerland, 28) UK Centre  
928 for Ecology & Hydrology, Bush Estate, Penicuik, Midlothian, EH26 0QB, United Kingdom, 29) Department of Physical Geography and  
929 Ecosystem Science, Lund University, Sölvegatan 12, 223 62 Lund, Sweden, 30) European Commission, Joint Research Centre (JRC), Ispra,  
930 Italy, 31) Siberian Federal University, 660041 Krasnoyarsk, Russia, 32) Instituto Argentino de Nivología, Glaciología y Ciencias Ambientales  
931 (IANIGLA), CONICET, CCT-Mendoza; Facultad de Ciencias Exactas y Naturales, Universidad Nacional de Cuyo, 33) Instituto Argentino de  
932 Nivología, Glaciología y Ciencias Ambientales (IANIGLA), CONICET, CCT-Mendoza, 34) Natural History Museum, University of Oslo, 0318,  
933 Oslo, Norway, 35) Section for Ecoinformatics & Biodiversity, Department of Biology, Aarhus University, Aarhus C, Denmark, 36) Center for  
934 Biodiversity Dynamics in a Changing World, Department of Biology, Aarhus University, Aarhus C, Denmark, 37) Ecological Plant Geography,  
935 Faculty of Geography, University of Marburg, Deutschhausstrasse 10, 35032, Marburg, Germany, 38) Institute of Landscape Ecology Slovak  
936 Academy of Sciences, Štefánikova 3, 81499 Bratislava, Slovakia, 39) Faculty of Environmental and Forest Sciences, Agricultural University of  
937 Iceland, Árleyni 22, 112 Reykjavík, Iceland, 40) Instituto Argentino de Nivología, Glaciología y Ciencias Ambientales (IANIGLA), CONICET,  
938 CCT-Mendoza, 41) Isotope Bioscience Laboratory - ISOFYS, Ghent University, Coupure Links 653, 9000 Gent, Belgium, 42) Université de  
939 Rennes, CNRS, EcoBio (Ecosystèmes, biodiversité, évolution) - UMR 6553, F-35000 Rennes, France, 43) Department of Sustainable Agro-  
940 ecosystems and Bioresources, Research and Innovation Centre, Fondazione Edmund Mach, Via E. Mach 1, 38010 San Michele all'Adige,  
941 Italy, 44) Forest Research, Alice Holt Lodge, Wrecclesham, Farnham, UK, 45) Department of Ecology, Pontificia Universidad Javeriana,  
942 Bogota, Colombia, 46) Jolube Consultor Botánico. C/Mariano R de Ledesma, 4. E-22700 Jaca, Huesca, SPAIN, 47) Institute of Landscape and  
943 Plant Ecology, Department of Plant Ecology, University of Hohenheim, Ottilie-Zeller\_weg 2, 70599 Stuttgart, Germany, 48) Disturbance  
944 Ecology, BayCEER, University of Bayreuth, Universitätsstr. 30, 95447 Bayreuth, Germany, 49) Norwegian Institute for Nature Research,  
945 FRAM - High North Research Centre for Climate and the Environment, P.O. Box 6606 Langnes, N-9296 Tromsø, Norway, 50) Department of  
946 Earth Sciences, University of Gothenburg, P.O. Box 460, SE-40530 Gothenburg, Sweden, 51) Gothenburg Global Biodiversity Centre, P.O.  
947 Box 461, SE-405 30 Gothenburg, Sweden, 52) Department of Biological and Environmental Sciences, University of Gothenburg, P.O. Box  
948 461, 43 Gothenburg SE-405 30, Sweden, 53) Department of Environmental Science, Policy, and Management, University of California,

949 Berkeley, CA 94720 USA, 54) Alfred Wegener Institute Helmholtz Center for Polar and Marine Research, Telegrafenberg A45, 14473  
950 Potsdam, Germany, 55) Geography Department, Humboldt-Universität zu Berlin, Germany, 56) Pós-Graduação em Ciências de Florestas  
951 Tropicais, Instituto Nacional de Pesquisas da Amazônia, Manaus, Brasil, CEP: 69060-001, 57) UMR ECOSYS INRAE, AgroParisTech,  
952 Université Paris Saclay, France, 58) Biological Dynamics of Forest Fragments Project, BDFFP, Instituto Nacional de Pesquisas da Amazônia,  
953 Av. André Araujo, 2936 - Petrópolis, Manaus, Amazonas, 69067-375, Brazil, 59) Department of Forest Sciences, Federal University of  
954 Lavras, 37.200-900, Lavras, MG, Brazil, 60) Faculty of Arts and Sciences, Department of Molecular Biology and Genetics, Ordu University,  
955 52200, Ordu, Turkey, 61) Ecological Plant Geography, Faculty of Geography, University of Marburg, Deutschhausstrasse 10, 35032,  
956 Marburg, Germany., 62) Plant Ecology Group, Department of Evolution and Ecology, University of Tübingen, Auf der Morgenstelle 5, 72076  
957 Tübingen, Germany, 63) Department of Science and High Technology, Insubria University, Via Valleggio 11, 22100 Como, Italy, 64)  
958 Department of Chemistry, Life Sciences and Environmental Sustainability, University of Parma, Parco Area delle Scienze 11/A, 43124  
959 Parma, Italy, 65) Department of Evolutionary Biology, Ecology and Environmental Sciences, Biodiversity Research Institute (IRBio),  
960 University of Barcelona, 08028 Barcelona, Catalonia, Spain, 66) CREA, E08193 Bellaterra (Cerdanyola del Vallès), Catalonia, Spain, 67)  
961 Laboratorio de Ecofisiología Vegetal y Cambio Climático, Laboratorio de Ecofisiología Vegetal y Cambio Climático, Departamento de  
962 Ciencias Veterinarias y Salud Pública, Universidad Católica de Temuco, Campus Luis Rivas del Canto and Núcleo de Estudios Ambientales  
963 (NEA), Facultad de Recursos Naturales, Universidad Católica de Temuco, Temuco, 4780000, Chile, 68) German Centre for Integrative  
964 Biodiversity Research (iDiv) Halle-Jena-Leipzig, Leipzig, Germany, 69) Institute of Biology, Leipzig University, Leipzig, Germany, 70)  
965 Laboratory of Bioclimatology, Department of Ecology and Environmental Protection, Poznan University of Life Sciences, ul. Piatkowska 94,  
966 60-649, Poznan, Poland, 71) Univ. Grenoble Alpes, Univ. Savoie Mont Blanc, CNRS, LECA, F-38000 Grenoble, France, 72) Univ. Grenoble  
967 Alpes, Univ. Savoie Mont Blanc, CNRS, LTSER Zone Atelier Alpes, F-38000 Grenoble, France, 73) Securing Antarctica's Environmental  
968 Future, School of Biological Sciences, Monash University, Victoria 3800, Australia, 74) Forest Ecology and Conservation Group, Department  
969 of Plant Sciences, University of Cambridge, Cambridge CB23EA, UK, 75) Faculty of Ecology and Environmental Sciences, Technical  
970 University in Zvolen, T. G. Masaryka 24, 960 01 Zvolen, Slovakia, 76) Sub-Antarctic Biocultural Conservation Program, Universidad de  
971 Magallanes, Pde. Manuel Bulnes 01855, Punta Arenas, Magallanes y la Antártica Chilena, 77) Núcleo Milenio de Salmónidos Invasores,  
972 INVASAL, Concepción, Chile, 78) British Antarctic Survey, NERC, High Cross, Madingley Road, Cambridge CB3 0ET, United Kingdom, 79)  
973 Department of Arctic and Marine Biology, Faculty of Biosciences Fisheries and Economics, UiT-The Arctic University of Norway, N-9037  
974 Tromsø, Norway, 80) Climate Change Unit, Environmental Protection Agency of Aosta Valley, Italy, 81) Department of Biological Sciences,  
975 University of Notre Dame, Notre Dame, IN 46556, USA, 82) Department of Science, University of Roma Tre, 00146 Rome, Italy, 83)  
976 Department of Ecology, Environment and Plant Sciences and Bolin Centre for Climate Research, Stockholm University, 106 91 Stockholm,  
977 Sweden, 84) the County Administrative Board of Västra Götaland, SE-403 40 Gothenburg, Sweden, 85) School of GeoSciences, University  
978 of Edinburgh, King's Buildings, Edinburgh, EH9 3FF, United Kingdom, 86) Department of Geology, Geography and Environment. University  
979 of Alcalá. 28805 Alcalá de Henares, Madrid, Spain., 87) Chair of Geoinformatics, Technische Universität Dresden, Dresden, Germany, 88)  
980 Vegetation Ecology, Institute of Natural Resource Sciences (IUNR), ZHAW Zurich University of Applied Sciences, Grüentalstr. 14, 8820  
981 Wädenswil, Switzerland, 89) Plant Ecology, Bayreuth Center of Ecology and Environmental Research (BayCEER), University of Bayreuth,  
982 Universitätsstr. 30, 95447 Bayreuth, Germany, 90) VITO-TAP, Boeretang 200, 2400-Mol, Belgium, 91) Swiss Federal Research Institute WSL,  
983 8903 Birmensdorf, Switzerland, 92) Majella Seed Bank, Majella National Park, Colle Madonna, 66010 Lama dei Peligni, Italy, 93)  
984 Department of Life, Health and Environmental Sciences, University of L'Aquila, Piazzale Salvatore Tommasi 1, 67100 L'Aquila, Italy, 94)  
985 Grupo de Ecología de Poblaciones de Insectos, IFAB (INTA - CONICET), Modesta Victoria 4450, Bariloche, Argentina, 95) Department of  
986 Biology and Biochemistry, University of Houston, Houston, Texas, 77204 USA, 96) Faculty of Science, Department of Botany, University of  
987 South Bohemia, Na Zlaté Stoe 1, 37005 České Budějovice, Czech Republic, 97) Climate Impacts Research Centre, Department of Ecology  
988 and Environmental Science, Umeå University, Abisko, Sweden, 98) Global Change Research Institute, Academy of Sciences of the Czech  
989 Republic, 99) School of Biological Sciences, The University of Western Australia, Crawley, WA 6009, Australia, 100) Kings Park Science,  
990 Department of Biodiversity, Conservation & Attractions, Kings Park, 6005 WA, Australia, 101) Department of Botany, Faculty of Biology,  
991 University of Innsbruck, Sternwartestraße 15, 6020 Innsbruck, Austria, 102) Imperial College London, Silwood Park Campus, Ascot SL5 7PY,  
992 UK, 103) Operation Wallacea, Wallace House, Old Bolingbroke, Lincolnshire, PE23 4EX, UK, 104) INRAE, Bordeaux Sciences Agro, UMR  
993 1391 ISPA, F-33140 Villenave d'Ornon, France, 105) Department of Life and Environmental Sciences, University of Cagliari, Viale  
994 Sant'Ignazio da Laconi 13, 09123, Cagliari, Italy., 106) Department of Botany, University of Granada, 18071, Granada, Spain, 107) IMIB –  
995 Biodiversity Research Institute, University of Oviedo, Mieres, Spain, 108) Institute for Plant Science and Microbiology, University of  
996 Hamburg, Ohnhorststr. 18, 22609 Hamburg, Germany, 109) Dartmouth College, Hanover, NH, USA, 110) Ecosystems and Global Change  
997 Group, Department of Plant Sciences, University of Cambridge, Cambridge, CB2 3EA, United Kingdom, 111) WSL Institute for Snow and  
998 Avalanche Research SLF, 7260 Davos, Switzerland, 112) Climate Change, Extremes and Natural Hazards in Alpine Regions Research Center  
999 CERC, Flüelastrasse 11, 7260 Davos Dorf, Switzerland, 113) Swiss Federal Research Institute for Forest, Snow and Landscape Research WSL,  
1000 8903 Birmensdorf, Switzerland, 114) Laboratorio de Invasiones Biológicas (LIB), Facultad de Ciencias Forestales, Universidad de  
1001 Concepción, Concepción, Chile, 115) School of Education and Social Sciences, Adventist University of Chile, Chile, 116) Instituto de Ecología  
1002 y Biodiversidad (IEB), Santiago, Chile, 117) Pyrenean Institute of Ecology (CSIC), Av. Montañana 1005, 50059 Zaragoza, Spain, 118)  
1003 Biodiversity and Landscape, TERRA research centre, Gembloux Agro-Bio Tech, University of Liège, Gembloux, 5032, Belgium ; Research  
1004 Group PLECO (Plants and Ecosystems), University of Antwerp, 2610 Wilrijk, Belgium, 119) Department of Geo-information in  
1005 Environmental Management, Mediterranean Agronomic Institute of Chania, PO Box 85, 73100 Chania, Greece, 120) Georgian Institute of  
1006 Public Affairs, department of Environmental management ad policy, Tbilisi, Georgia, 121) Flemish Institute for Technological Research,  
1007 2400 Mol, Belgium, 122) Department of Earth and Environmental Science, Faculty of BioScience Engineering, KULeuven, Belgium, 123)  
1008 Max Planck Institute for Biogeochemistry, Department of Biogeochemical Signals, Jena, Germany, 124) Sustainable Agricultural Sciences  
1009 Department, Rothamsted Research, Harpenden, AL5 2JQ, UK, 125) Department of Biology, Norwegian University of Science and  
1010 Technology, 7034 Trondheim, Norway, 126) Biodiversity, Wildlife and Ecosystem Health, Biomedical Sciences, University of Edinburgh,  
1011 Edinburgh, EH8 9JZ, UK, 127) Department of Ecology, Swedish University of Agricultural Sciences, Box 7042, S-750 07 Uppsala, 128) School  
1012 of Biological Sciences, The University of Hong Kong, Pok Fu Lam Road, Hong Kong SAR, China, 129) Department of Theoretical and Applied  
1013 Sciences, Insubria University, Via Dunant 3, 21100 Varese, Italy, 130) CIRAD, UMR Eco&Sols, 34060 Montpellier, France, 131) Eco&Sols,  
1014 Univ Montpellier, CIRAD, INRAE, IRD, Montpellier SupAgro, 34060 Montpellier, France, 132) Senckenberg Research Institute and Natural



1015 History Museum Frankfurt, 63571 Gelnhausen, Germany, 133) Faculty of Biology, University of Duisburg-Essen, 45141 Essen, Germany,  
 1016 134) Institute of Biology / Geobotany and Botanical Garden, Martin Luther University Halle-Wittenberg, Halle (Saale), Germany, 135)  
 1017 Department of Biological Sciences and Bjerknes Centre for Climate Research, University of Bergen, N-5020 Bergen, Norway, 136) Centre  
 1018 for Biodiversity & Taxonomy, Department of Botany, University of Kashmir, Srinagar - 190006, J&K, India, 137) Department of Ecology,  
 1019 University of Innsbruck, 6020 Innsbruck, Austria, 138) INRAE, Univ. Bordeaux, BIOGECO, F-33610 Cestas, France, 139) The Heathland  
 1020 Centre, Alver, Norway, 140) TERRA Teaching and Research Center, Faculty of Gembloux Agro-Bio Tech, University of Liege, Passage des  
 1021 déportés, 2, 5030 Gembloux, Belgium, 141) UK Centre for Ecology & Hydrology, Penicuik, EH26 0QB, Scotland, UK, 142) Vegetation  
 1022 Ecology, Institute of Natural Resource Sciences, ZHAW Zurich University of Applied Sciences, Grüental, 8820 Wädenswil, Switzerland, 143)  
 1023 Institute for Botany, University of Natural Resources and Life Sciences Vienna (BOKU), Gregor-Mendel-Straße 33/I, 1180 Vienna, Austria,  
 1024 144) Centre for Agrometeorological Research (ZAMF), German Meteorological Service (DWD), Bundesallee 33, 38116 Braunschweig,  
 1025 Germany, 145) Dept of Biology, Memorial University, St. John's, NL, A1B 3X9, Canada, 146) Department of Biological Sciences, Simon  
 1026 Fraser University, Burnaby, BC, V5A 1S6, Canada, 147) Department of Geography, University of Zaragoza, Pedro Cerbuna 12, 50009  
 1027 Zaragoza, Spain, 148) Faculty of Resource Management, HAWK University of Applied Sciences and Arts, 37077 Göttingen, Germany, 149)  
 1028 Plant Ecology, Albrecht-von-Haller-Institute for Plant Sciences, Georg-August University of Goettingen, Untere Karspuele 2, 37073  
 1029 Goettingen, Germany, 150) Department of Ecoscience and Arctic Research Centre, Aarhus University, Grenåvej 14, 8410 Rønne, Denmark,  
 1030 151) Department of Geography, Masaryk University, Faculty of Science, Kotlarska 2, 611 37, Brno, Czech Republic, 152) Department of  
 1031 Environmental Science, Shinshu University, Matsumoto, Japan, 153) Department of Ecoscience and Arctic Research Centre, Aarhus  
 1032 University, Frederiksborgvej 399, 4000 Roskilde, Denmark, 154) INRAE, University of Bordeaux, BIOGECO, F-33610 Cestas, France, 155)  
 1033 Department of Forest Ecology and Management, Swedish University of Agricultural Sciences, 90183 Umeå, Sweden, 156) Forest Research  
 1034 Institute, Department of Silviculture and Forest Tree Genetics, Braci Lesnej Street, No 3, Sekocin Stary, 05-090 Raszyn, Poland, 157)  
 1035 Bayreuth Center of Ecology and Environmental Research, 158) ARAID/IPE-CSIC, Pyrenean Institute of Ecology, Avda. Llano de la Victoria,  
 1036 16, Jaca 22700, Spain, 159) Life and Environmental Sciences, University of Iceland, Sturlugata 7, 102 Reykjavik, Iceland, 160) School of  
 1037 Biological Sciences, University of Bristol, Bristol, United Kingdom, 161) Biological and Environmental Sciences, Faculty of Natural Sciences,  
 1038 University of Stirling, Scotland, FK9 4LA, 162) Faculty of Environmental Sciences, Czech University of Life Sciences Prague, Kamýcká 129,  
 1039 165 21 Prague 6 - Suchbát, Czech Republic, 163) Centre for Environmental and Climate Science, Lund University, Sölvegatan 37, 223 62,  
 1040 Lund, Sweden, 164) University of Goettingen, Bioclimatology, Büsgenweg 2, 37077 Göttingen, Germany., 165) Environment Agency  
 1041 Austria, Spittelauer Lände 5, 1090 Vienna, Austria, 166) Centre for Ecological Research, Institute of Ecology and Botany, H-2163 Vácrátót,  
 1042 Alkotmány út 2-4., Hungary, 167) Experimental Plant Ecology, Institute of Botany and Landscape Ecology, University of Greifswald, D-  
 1043 17487 Greifswald, Germany, 168) GLORIA Coordination, Institute for Interdisciplinary Mountain Research, Austrian Academy of Sciences  
 1044 (ÖAW) & Department of Integrative Biology and Biodiversity Research, University of Natural Resources and Life Sciences, Vienna (BOKU),  
 1045 Silbergasse 30/3, 1190 Vienna, Austria, 169) Department of Arctic Biology, The University Centre in Svalbard (UNIS), 9171 Longyearbyen,  
 1046 Svalbard, Norway, 170) Department of Land Resources and Environmental Sciences, Montana State University, Bozeman MT, USA, 59717,  
 1047 171) Climate Impacts Research Centre, Department of Ecology and Environmental Sciences, Umeå University, Vetenskapens väg 38, 98107  
 1048 Abisko, Sweden, 172) Centre for Polar Ecology, Faculty of Science, University of South Bohemia, Na Zlaté Stoe 3, 370 05, České  
 1049 Budějovice, Czech Republic, 173) School of Biological Sciences, Monash University, Victoria 3800, Australia, 174) Terrestrial Ecology Unit,  
 1050 Dept. of Biology, Ghent University, B-9000 Gent, Belgium, 175) Finnish Meteorological Institute, Climate System Research, POB503, 00101  
 1051 Helsinki, Finland, 176) INAR Institute for Atmospheric and Earth System Research/Physics, Faculty of Science, POBox 68 FI-00014  
 1052 University of Helsinki, Finland, 177) Interuniversity Institute for Earth System Research, University of Granada, Granada 18006 Spain, 178)  
 1053 CNR Institute for Agricultural and Forestry Systems in the Mediterranean, P.le Enrico Fermi 1 - Loc. del Granatello, 80055, Portici (Napoli)  
 1054 Italy, 179) Faculty of Forestry, Technical University in Zvolen, T.G.Masaryka 24, 960 01 Zvolen, Slovakia, 180) CNR Institute for Agricultural  
 1055 and Forestry Systems in the Mediterranean, P.le Enrico Fermi 1 - Loc. del Granatello, 80055, Portici (Napoli) Italy, 181) School of Pure &  
 1056 Applied Sciences, Environmental Conservation & Management Programme Open University of Cyprus, PO Box 12794, 2252 Latsia, Nicosia,  
 1057 182) Department of Biology - Aquatic Biology, Aarhus University, Ole Worms Allé 1, 8000 Aarhus C, Denmark, 183) Aarhus Institute of  
 1058 Advanced Studies, AIAS Høegh-Guldbergs Gade 6B, 8000 Aarhus, Denmark, 184) Department of Forest Botany, Dendrology and  
 1059 Geobiocoenology, Faculty of Forestry and Wood Technology, Mendel University in Brno, Zemedelska 1, 613 00 Brno, Czech Republic, 185)  
 1060 Regional Centre for Integrated Environmental Monitoring, Odesa National I.I. Mechnikov University, 7 Mayakovskogo lane, 65082 Odesa,  
 1061 Ukraine, 186) Department of Agroecology, Aarhus University, 20 Blichers Allé, 8830 Tjele, Denmark, 187) NGO New Energy, 11 Bakulina  
 1062 str., 61166 Kharkiv, Ukraine, 188) Biological Dynamics of Forest Fragments Project, Coordenação de Dinâmica Ambiental, Instituto  
 1063 Nacional de Pesquisas da Amazônia, Manaus, AM CEP 69067-375, Brazil., 189) Swiss Federal Institute for Forest, Snow and Landscape  
 1064 Research (WSL), CH-8903 Birmensdorf, Switzerland., 190) Department of Biology, University of Antwerp, Universiteitsplein 1, 2610 Wilrijk,  
 1065 Belgium, 191) Department of Botany and Biodiversity Research Centre, University of British Columbia, Vancouver, BC, Canada, 192)  
 1066 Department of Environment, Province of Antwerp, Koningin Elisabethlei 22, 2018 Antwerpen, Belgium, 193) Institute of Plant and Animal  
 1067 Ecology of Ural Division of Russian Academy of Science, 8 Marta st., 202, Ekaterinburg, Russia, 194) Department of Earth and  
 1068 Environmental Sciences, University of Pavia, Via S. Epifanio 14, Pavia, Italy, 195) Faculty of Science and Technology, Free University of  
 1069 Bolzano, Piazza Università 5, 39100 Bolzano, Italy, 196) Climate Change Unit, Environmental Protection Agency of Aosta Valley, Loc. La  
 1070 Maladière, 48, 11020 Saint-Christophe, Italy, 197) University of Freiburg, Chair of Geobotany, Schänzlestrasse 1, 79104 Freiburg, Germany,  
 1071 198) Environment and Sustainability Institute, University of Exeter, Penryn Campus, Cornwall TR10 9FE, United Kingdom, 199) Centre for  
 1072 Ecosystem Science, School of Biological, Earth and Environmental Sciences, UNSW Sydney, NSW 2052, Sydney, Australia, 200) Department  
 1073 of Plant Biology and Ecology, University of Seville, 41012 Seville, Spain, 201) Department of Biology, Washington University in St. Louis, St.  
 1074 Louis, MO 63130, USA., 202) Department of Animal Biology, Institute of Biology, University of Campinas, Campinas, SP, CEP 13083-862,  
 1075 Brazil, 203) CNR Institute of BioEconomy, Via Gobetti 101, 40129 Bologna, Italy, 204) National Wildlife Research Centre, Environment and  
 1076 Climate Change Canada, Carleton University, 1125 Colonel by Drive, Ottawa, ON K1A 0H3, Canada, 205) School of Life and Environmental  
 1077 Sciences, Deakin University, Burwood, Victoria, Australia, 3125, 206) Institute for Alpine Environment, Eurac Research, Viale Druso 1,  
 1078 39100 Bozen/Bolzano, Italy, 207) Institute of Biology, Dept. of Molecular Botany, University of Hohenheim, 70599 Stuttgart, Germany,  
 1079 208) Instituto de Matemática Aplicada San Luis, IMASL, CONICET and Universidad Nacional de San Luis, Ejército de los Andes 950,  
 1080 D5700HHW San Luis, Argentina, 209) Cátedra de Climatología Agrícola (FCA-UNER), Ruta 11, km 10, Oro Verde, Entre Ríos, Argentina, 210)

1081 Grupo de Ecología de Invasiones, INIBIOMA, CONICET/ Universidad Nacional del Comahue, Av. de los Pioneros 2350, Bariloche 8400,  
 1082 Argentina, 211) CSIC, Global Ecology Unit CREAM- CSIC-UAB, Bellaterra, 08193, Catalonia, Spain., 212) CREAM, E08193, Cerdanyola del  
 1083 Vallès, Catalonia, Spain, 213) Mountains of the Moon University, P.O Box 837, Fort Portal, Uganda, 214) National Agricultural Research  
 1084 Organisation, Mbarara Zonal Agricultural Research and Development Institute, P.O Box 389, Mbarara , Uganda, 215) Laboratory of  
 1085 Meteorology, Department of Construction and Geoengineering, Faculty of Environmental Engineering and Mechanical Engineering,  
 1086 Poznan University of Life Sciences, ul. Piatkowska 94, 60-649, Poznan, Poland, 216) Department of Agroecology, Aarhus University, Blichers  
 1087 Allé 20, 8830 Tjele, Denmark, 217) Department of Biology, Lund University, SE-223 62 Lund, Sweden, 218) Department of Earth and  
 1088 Environmental Sciences, University of Pavia, Via S. Epifanio 14, 27100 Pavia, Italy, 219) Institute of Botany and Landscape Ecology,  
 1089 University Greifswald, D-17487 Greifswald, Germany, 220) V.N. Sukachev Institute of Forest SB RAS, Krasnoyarsk, Russia, 221) Institute of  
 1090 Ecology and Earth Sciences, University of Tartu, Liivi 2, Tartu 50409, Estonia, 222) Department of Biology , Aarhus University, Ole Worms  
 1091 Allé 1, 8000 Aarhus C, Denmark, 223) Department of Biology and Ecology Center, Utah State University, 5305 Old Main Hill, Logan, UT  
 1092 84322, USA, 224) Department of Life Sciences, Imperial College, Silwood Park Campus, Ascot, Berkshire SL5 7PY, UK, 225) Landscape  
 1093 Ecology, Institute of Terrestrial Ecosystems, Department of Environmental Systems Science, ETH Zürich, 8092 Zürich, Switzerland, 226)  
 1094 Unit of Land Change Science, Swiss Federal Research Institute WSL, 8903 Birmensdorf, Switzerland, 227) Department of Biology,  
 1095 Washington University in St. Louis, Campus Box 1137, 1 Brookings Drive, St. Louis, MO 63130 USA, 228) CREAM, Cerdanyola del Vallès  
 1096 08193, Catalonia, Spain, 229) School of Ecology and Environment Studies, Nalanda University, Rajgir, India, 230) School of Biosciences,  
 1097 University of Sheffield, Western Bank, Sheffield, S10 2TN, U.K., 231) CESAM & Department of Environment, University of Aveiro, 3810-193  
 1098 Aveiro, Portugal, 232) Department of Agronomy, Food, Natural resources, Animals and Environment - University of Padua, 35020 Legnaro,  
 1099 Italy, 233) Univ. Savoie Mont Blanc, CNRS, Univ. Grenoble Alpes, EDYTEM, F-73000 Chambéry, France, 234) Universitat Autònoma de  
 1100 Barcelona, E08193 Bellaterra (Cerdanyola del Vallès), Catalonia, Spain, 235) Department of Ecology and Biogeography, Faculty of  
 1101 Biological and Veterinary Sciences, Nicolaus Copernicus University, Toruń, Poland, 236) Centre for Climate Change Research, Nicolaus  
 1102 Copernicus University, Toruń, Poland, 237) A. Borza Botanic Garden, Babeş-Bolyai University, Cluj-Napoca, Romania, 238) Faculty of  
 1103 Biology and Geology, Department of Taxonomy and Ecology, Babeş-Bolyai University, Cluj-Napoca, Romania, 239) E. G. Racoviță Institute,  
 1104 Babeş-Bolyai University, Cluj-Napoca, Romania, 240) Centre for Sustainable Ecosystem Solutions, School of Earth, Atmospheric and Life  
 1105 Sciences, University of Wollongong, Wollongong, New South Wales, 2522, Australia, 241) University of Applied Sciences Trier,  
 1106 Environmental Campus Birkenfeld, 55761 Birkenfeld, Germany, 242) Institut Universitaire de France, 1 Rue Descartes, 75231 Paris cedex  
 1107 05, France, 243) Swiss Federal Institute for Forest, Snow and Landscape Research WSL, Zuercherstrasse 111, 8903 Birmensdorf,  
 1108 Switzerland, 244) Securing Antarctica's Environmental Future, School of Earth, Atmospheric and Life Sciences, University of Wollongong,  
 1109 2522 Australia, 245) Aquatic Ecology & Environmental Biology, Radboud Institute for Biological and Environmental Sciences Water and  
 1110 Wetland Research, Faculty of Science, Radboud University Nijmegen, 6525 NJ Nijmegen, The Netherlands., 246) University of Notre Dame,  
 1111 Department of Biological Sciences and the Environmental Change Initiative, 247) Swiss National Park, Chastè Planta-Wildenberg, 7530  
 1112 Zerne, Switzerland, 248) Remote Sensing Laboratories, Dept. of Geography, University of Zurich, Winterthurerstrasse 190, 8057 Zurich,  
 1113 Switzerland, 249) CIRAD, UMR Eco&Sols, BP1386, CP18524, Dakar, Senegal, 250) Eco&Sols, Univ Montpellier, CIRAD, INRAE, IRD, Institut  
 1114 Agro, Montpellier, France, 251) LMI IESOL, Centre IRD-ISRA de Bel Air, BP1386, CP18524, Dakar, Senegal, 252) Parc national des Ecrins -  
 1115 Domaine de Charance - 05000 GAP - France, 253) Universidad Nacional de San Antonio Abad del Cusco, Cusco, Perú, 254) Centro de  
 1116 Investigación de la Biodiversidad Wilhelm L. Johannsen, Cusco, Perú, 255) Biological Dynamics of Forest Fragments Project, PDBFF,  
 1117 Instituto Nacional de Pesquisas da Amazônia, Av. André Araujo, 2936 - Petrópolis, Manaus, Amazonas, 69067-375, Brazil, 256) Department  
 1118 of Ecology and Environmental Science, Umeå University, 901 87 Umeå, Sweden, 257) Institute of Bio- and Geosciences (IBG-3):  
 1119 Agrosphere, Forschungszentrum Jülich GmbH, Jülich, Germany, 258) Chair of Soil Science and Geomorphology, Department of  
 1120 Geosciences, University of Tuebingen, 72070 Tuebingen, Germany, 259) Department of Geography, The University of British Columbia,  
 1121 Vancouver, BC V6T 1Z2, 260) Department of Botany and Biodiversity Research, Rennweg 14, 1030 Vienna, 261) Princeton School of Public  
 1122 and International Affairs, Princeton University, Princeton, NJ 08540, USA, 262) Université de Lorraine, AgroParisTech, INRAE, Silva, 54000  
 1123 Nancy, France., 263) Department of Soil Science and Landscape Management, Faculty of Earth Sciences and Spatial Management, Nicolaus  
 1124 Copernicus University, Toruń, Poland, 264) Terra Nova National Park, Parks Canada Agency, Glovertown NL, A0G3Y0, 265) Universidade  
 1125 Estadual do Norte Fluminense Darcy Ribeiro, Campos dos Goytacazes, Rio de Janeiro, Brazil, 266) National Forest Centre, Forest Research  
 1126 Institute Zvolen, T. G. Masaryka 22, 96001 Zvolen, Slovakia, 267) Department of Biology, Norwegian University of Science and Technology,  
 1127 7491 Trondheim, Norway, 268) Department of Physical Geography, Stockholm University, 106 91 Stockholm, Sweden, 269) Department of  
 1128 Geography, University of British Columbia, 1984 West Mall, Vancouver, BC V6T 1Z2, 270) Department of Earth and Environmental  
 1129 Sciences, Celestijnenlaan 200E, 3001 Leuven, Belgium, 271) Soil Science Department, Federal University of Viçosa, Prof. Peter Henry Rolfs  
 1130 Ave., 36570-900, Viçosa-MG, Brazil, 272) Universidade Federal da Paraíba, Departamento de Geociências. Cidade Universitária, João  
 1131 Pessoa - PB, CEP 58051-900, Brasil, 273) Goethe-Universität Frankfurt, Department of Physical Geography, Altenhöferallee 1, 60438  
 1132 Frankfurt am Main, Germany, 274) Department of Evolution, Ecology, and Organismal Biology, University of California Riverside, Riverside,  
 1133 CA, 92521, USA, 275) Department of Natural History, NTNU University Museum, Norwegian University of Science and Technology, NO-  
 1134 7491 Trondheim Norway, 276) UMR 7058 CNRS 'Ecologie et Dynamique des Systèmes Anthropisés' (EDYSAN), Univ. de Picardie Jules  
 1135 Verne, Amiens, France, 277) EnvixLab, Dipartimento di Bioscienze e Territorio, Università degli Studi del Molise, Via Duca degli Abruzzi  
 1136 s.n.c., 86039 Termoli, Italy, 278) Institute of Meteorology and Climate Research (IMK), Department of Atmospheric Environmental  
 1137 Reserach (IFU), Karlsruhe Institute of Technology (KIT), Kreuzteckbahn Straße 19, 82467 Garmisch-Partenkirchen, Germany, 279) Swedish  
 1138 University of Agricultural Sciences, SLU Swedish Species Information Centre, Almas allé 8 E, 75651 Uppsala, Sweden, 280) University  
 1139 Duisburg-Essen, Faculty for Biology, Universitätsstr. 5, 45141 Essen, Germany, 281) Department of Geosciences and Natural Resource  
 1140 Management, University of Copenhagen, Øster Voldgade 10, DK-1350 Copenhagen, Denmark, 282) Experimental Plant Ecology, Institute  
 1141 of Botany and Landscape Ecology, University of Greifswald, partner in the Greifswald Mire Centre, D-17487 Greifswald, Germany, 283)  
 1142 Fondation J.-M. Aubert, 1938 Champex-Lac, Switzerland, 284) Département de Botanique et Biologie végétale, Université de Genève, Case  
 1143 postale 71, CH-1292 Chambésy, Switzerland, 285) Department of Geography and Earth Sciences, Aberystwyth University, Wales, UK, 286)  
 1144 Center for Systematic Biology, Biodiversity and Bioresources - 3B, Babeş-Bolyai University, Cluj-Napoca, Romania, 287) Northern  
 1145 Environmental Geoscience Laboratory, Department of Geography and Planning, Queen's University, 288) Finnish Meteorological Inst., P.O.  
 1146 Box 503, FI-00101 Helsinki, Finland, 289) Graduate School of Life and Environmental Sciences, Osaka Prefecture University, 599-8531,

1147 Japan, 290) Nature Research Centre, Akademijos 2, 08412 Vilnius, Lithuania, 291) Institute of Biological Research Cluj-Napoca, National  
1148 Institute of Research and Development for Biological Sciences, Bucharest, Romania, 292) CNR Institute for BioEconomy, Via Giovanni  
1149 Caproni, 50144 Firenze, Italy, 293) The Ecosystem Management Research Group (ECOBE), University of Antwerp, 2610 Wilrijk  
1150 (Antwerpen), Belgium, 294) Plant Conservation and Population Biology, Department of Biology, KU Leuven, Kasteelpark Arenberg 31, 3001  
1151 Heverlee, Belgium, 295) A.N. Severtsov Institute of Ecology and Evolution, Russian Academy of Sciences, 119071, Leninsky pr.33, Moscow,  
1152 Russia, 296) Netherlands Institute of Ecology, Droevendaalsesteeg 10, 6708 PB, Wageningen, the Netherlands, 297) Plant Ecology &  
1153 Nature Conservation Group Wageningen University, Droevendaalse Steeg 3a 6708 PB Wageningen, 298) Centre for Integrative Ecology,  
1154 School of Life and Environmental Sciences, Deakin University, Burwood, Victoria, Australia, 3125, 299) CAVElab - Computational and  
1155 Applied Vegetation Ecology, Department of Environment, Ghent University, Coupure Links 653, 9000 Gent, Belgium, 300) Earth Surface  
1156 Processes Team, Centre for Environmental and Marine Studies (CESAM), Dept. Environment and Planning, University of Aveiro, 3810-193,  
1157 Aveiro, Portugal, 301) Instituto Pirenaico de Ecología, IPE-CSIC. Av. Llano de la Victoria, 16. 22700 Jaca (Huesca) Spain, 302) CNR - Institute  
1158 for Agricultural and Forestry Systems in the Mediterranean, P.le Enrico Fermi 1- Loc. del Granatello, 80055, Portici, (Napoli), Italy, 303)  
1159 Institute of Earth Surface Dynamics, Faculty of Geosciences and Environment, University of Lausanne, Géopolis, 1015 Lausanne,  
1160 Switzerland, 304) Climate Impacts Research Centre, Department of Ecology and Environmental Sciences, Umeå University, Abisko,  
1161 Sweden, 305) Forest Research, Northern Research Station, Roslin, EH25 9SY, UK, 306) Institute of Mountain Hazards and Environment,  
1162 Chinese Academy of Sciences, Chengdu, P.R. China, 307) MOE Key Laboratory of Geographical Processes and Ecological Security in  
1163 Changbai Mountains, School of Geographical Sciences, Northeast Normal University, Changchun, Jilin 130024, China, 308) Department of  
1164 Earth and Environmental Sciences, Lehigh University, Bethlehem, PA 18015, United States, 309) High Meadows Environmental Institute,  
1165 Princeton University, NJ 08544, USA, 310) Zhejiang Tiantong Forest Ecosystem National Observation and Research Station, School of  
1166 Ecological and Environmental Sciences, East China Normal University, Shanghai 200241, China, 311) University of Bayreuth, Ecological-  
1167 Botanical Gardens, Universitaetsstr. 30, Bayreuth, Germany, 312) Key Laboratory of Geographical Processes and Ecological Security in  
1168 Changbai Mountains, Ministry of Education, School of Geographical Sciences, Northeast Normal University, Changchun 130024, China.







1365 0002-4618-2407. Olivier Roupsard: <https://orcid.org/0000-0002-1319-142X>. Jhonatan Sallo Bravo: <https://orcid.org/0000-0001-9007-4959>. Julia Seeber: <https://orcid.org/0000-0003-0189-7377>. Laura Siegwart Collier: <https://orcid.org/0000-0003-0985-9615>. Stuart W. Smith: <https://orcid.org/0000-0001-9396-6610>. Arildo Souza Dias: <https://orcid.org/0000-0002-5495-3435>. Stefan Stoll: <https://orcid.org/0000-0002-3656-417X>. Torbern Tagesson: <https://orcid.org/0000-0003-3011-1775>. Jean-Paul Theurillat: <https://orcid.org/0000-0002-1843-5809>. Urs Albert Treier: <https://orcid.org/0000-0003-4027-739X>. Pavel Dan Turtureanu: <https://orcid.org/0000-0002-7422-3106>. Vilna A. Tyystjärvi: <https://orcid.org/0000-0002-1175-5463>. Josef Urban: <https://orcid.org/0000-0003-1730-947X>. Jonathan von Oppen: <https://orcid.org/0000-0001-6346-2964>. Jan Wild: <https://orcid.org/0000-0003-3007-4070>. Sonja Wipf: <https://orcid.org/0000-0002-3492-1399>. Zicheng Yu: <https://orcid.org/0000-0003-2358-2712>. Jian Zhang: <https://orcid.org/0000-0003-0589-6267>. Reiner Zimmermann: <https://orcid.org/0000-0002-8724-941x>. Jürgen Dengler: <https://orcid.org/0000-0003-3221-660X>. Esther R. Frei: <https://orcid.org/0000-0003-1910-7900>. Eduardo Fuentes-Lillo: <https://orcid.org/0000-0001-5657-954X>. Paraskevi Manolaki: <https://orcid.org/0000-0003-3958-0199>. Sergiy Medinets: <https://orcid.org/0000-0001-5980-1054>. Joseph Okello: <https://orcid.org/0000-0003-4462-3923>. Matteo Petit Bon: <https://orcid.org/0000-0001-9829-8324>. Mihai Pușcaș: <https://orcid.org/0000-0002-2632-640X>. Olivier Roupsard: <https://orcid.org/0000-0002-1319-142X>. Pavel Dan Turtureanu: <https://orcid.org/0000-0002-7422-3106>

## 1379 References

1380 Abatzoglou JT, Dobrowski SZ, Parks SA, Hegewisch KC (2018) TerraClimate, a high-resolution global  
1381 dataset of monthly climate and climatic water balance from 1958–2015. *Scientific data*, **5**,  
1382 170191.

1383 Amatulli G, Domisch S, Tuanmu M-N, Parmentier B, Ranipeta A, Malczyk J, Jetz W (2018) A suite of  
1384 global, cross-scale topographic variables for environmental and biodiversity modeling.  
1385 *Scientific data*, **5**, 180040.

1386 Antão LH, Bates AE, Blowes SA, Waldock C, Supp SR, Magurran AE, Dornelas M, Schipper AM (2020)  
1387 Temperature-related biodiversity change across temperate marine and terrestrial systems.  
1388 *Nature ecology & evolution*, **4**, 927-933.

1389 Ashcroft MB, Cavanagh M, Eldridge MDB, Gollan JR (2014) Testing the ability of topoclimatic grids of  
1390 extreme temperatures to explain the distribution of the endangered brush-tailed rock-  
1391 wallaby (*Petrogale penicillata*). *Journal of biogeography*, **41**, 1402-1413.

1392 Ashcroft MB, Chisholm LA, French KO (2008) The effect of exposure on landscape scale soil surface  
1393 temperatures and species distribution models. *Landscape Ecology*, **23**, 211-225.

1394 Ashcroft MB, Gollan JR (2012) Fine-resolution (25 m) topoclimatic grids of near-surface (5 cm)  
1395 extreme temperatures and humidities across various habitats in a large (200 x 300 km) and  
1396 diverse region. *International Journal of Climatology*, **32**, 2134-2148.

1397 Barnes R, Sahr K, Evenden G, Johnson A, Warmerdam F (2017) dggridR: discrete global grids for R. R  
1398 package version 0.1.12.

1399 Bergstrom DM, Wienecke BC, Van Den Hoff J, Hughes L, Lindenmayer DB, Ainsworth TD, Baker CM,  
1400 Bland L, Bowman DM, Brooks ST (2021) Combating ecosystem collapse from the tropics to  
1401 the Antarctic. *Global change biology*, **27**, 1692-1703.

1402 Berner LT, Massey R, Jantz P, Forbes BC, Macias-Fauria M, Myers-Smith I, Kumpula T, Gauthier G,  
1403 Andreu-Hayles L, Gaglioti BV (2020) Summer warming explains widespread but not uniform  
1404 greening in the Arctic tundra biome. *Nature Communications*, **11**, 1-12.

1405 Bond-Lamberty B, Thomson A (2018) A Global Database of Soil Respiration Data, Version 4.0. ORNL  
1406 DAAC.

1407 Booth TH, Nix HA, Busby JR, Hutchinson MF (2014) BIOCLIM: the first species distribution modelling  
1408 package, its early applications and relevance to most current MAXENT studies. *Diversity and  
1409 Distributions*, **20**, 1-9.

1410 Bramer I, Anderson B, Bennie J, Bladon A, De Frenne P, Hemming D, Hill RA, Kearney MR, Körner C,  
1411 Korstjens AH, Lenoir J, Maclean IMD, Marsh CD, Morecroft MD, Ohlemüller R, Slater HD,  
1412 Suggitt AJ, Zellweger F, Gillingham PK (2018) Advances in monitoring and modelling climate  
1413 at ecologically relevant scales. *Advances in Ecological Research*, **58**, 101-161.

1414 Breiman L (2001) Random forests. *Machine learning*, **45**, 5-32.

1415 Bruelheide H, Dengler J, Purschke O, Lenoir J, Jiménez-Alfaro B, Hennekens SM, Botta-Dukát Z,  
1416 Chytrý M, Field R, Jansen F (2018) Global trait–environment relationships of plant  
1417 communities. *Nature ecology & evolution*, **2**, 1906.

1418 Bütikofer L, Anderson K, Bebbler DP, Bennie JJ, Early RI, Maclean IM (2020) The problem of scale in  
1419 predicting biological responses to climate. *Global change biology*, **26**, 6657-6666.

1420 Chen L, Aalto J, Luoto M (2021) Significant shallow–depth soil warming over Russia during the past  
1421 40 years. *Global and Planetary Change*, **197**, 103394.

1422 Cooper EJ (2014) Warmer shorter winters disrupt Arctic terrestrial ecosystems. *Annual Review of*  
1423 *Ecology, Evolution, and Systematics*, **45**, 271-295.

1424 Copernicus Climate Change Service (C3s) (2019) C3S ERA5-Land reanalysis. (ed Copernicus Climate  
1425 Change Service).

1426 Coûteaux M-M, Bottner P, Berg B (1995) Litter decomposition, climate and litter quality. *Trends in*  
1427 *ecology & evolution*, **10**, 63-66.

1428 Crowther TW, Todd-Brown KE, Rowe CW, Wieder WR, Carey JC, Machmuller MB, Snoek B, Fang S,  
1429 Zhou G, Allison SD (2016) Quantifying global soil carbon losses in response to warming.  
1430 *Nature*, **540**, 104-108.

1431 Daly C (2006) Guidelines for assessing the suitability of spatial climate data sets. *International*  
1432 *Journal of Climatology*, **26**, 707-721.

1433 Davis E, Trant A, Hermanutz L, Way RG, Lewkowicz AG, Collier LS, Cuerrier A, Whitaker D (2020)  
1434 Plant–Environment Interactions in the Low Arctic Torngat Mountains of Labrador.  
1435 *Ecosystems*, 1-21.

1436 De Frenne P, Lenoir J, Luoto M, Scheffers BR, Zellweger F, Aalto J, Ashcroft M, Christiansen D,  
1437 Decocq G, De Pauw K, Govaert S, Greiser C, Gril E, Hampe A, Jucker T, Klings D, Koelemeijer  
1438 I, Lembrechts J, Marrec R, Meeussen C, Ogee J, Tyystjarvi V, Vangansbeke P, Hylander K  
1439 (2021) Forest microclimates and climate change: importance, drivers and future research  
1440 agenda. *Global change biology*, **In press**.

1441 De Frenne P, Rodríguez-Sánchez F, Coomes DA, Baeten L, Verstraeten G, Vellend M, Bernhardt-  
1442 Römermann M, Brown CD, Brunet J, Cornelis J (2013) Microclimate moderates plant  
1443 responses to macroclimate warming. *Proceedings of the National Academy of Sciences*, **110**,  
1444 18561-18565.

1445 De Frenne P, Zellweger F, Rodríguez-Sánchez F, Scheffers BR, Hylander K, Luoto M, Vellend M,  
1446 Verheyen K, Lenoir J (2019) Global buffering of temperatures under forest canopies. *Nature*  
1447 *ecology & evolution*, **3**, 744-749.

1448 Dinerstein E, Olson D, Joshi A, Vynne C, Burgess ND, Wikramanayake E, Hahn N, Palminteri S, Hedao  
1449 P, Noss R (2017) An ecoregion-based approach to protecting half the terrestrial realm.  
1450 *BioScience*, **67**, 534-545.

1451 Du E, Terrer C, Pellegrini AF, Ahlström A, Van Lissa CJ, Zhao X, Xia N, Wu X, Jackson RB (2020) Global  
1452 patterns of terrestrial nitrogen and phosphorus limitation. *Nature Geoscience*, **13**, 221-226.

1453 Fick SE, Hijmans RJ (2017) WorldClim 2: new 1-km spatial resolution climate surfaces for global land  
1454 areas. *International Journal of Climatology*, **37**, 4302-4315.

1455 Geiger R (1950) *The climate near the ground*, Cambridge, Massachusetts, USA, Harvard University  
1456 Press.

1457 Gistemp Team (2021) GISS Surface Temperature Analysis (GISTEMP), version 4. NASA Goddard  
1458 Institute for Space Studies.

1459 Gorelick N, Hancher M, Dixon M, Ilyushchenko S, Thau D, Moore R (2017) Google Earth Engine:  
1460 Planetary-scale geospatial analysis for everyone. *Remote Sensing of Environment*, **202**, 18-  
1461 27.

1462 Gottschall F, Davids S, Newiger-Dous TE, Auge H, Cesarz S, Eisenhauer N (2019) Tree species identity  
1463 determines wood decomposition via microclimatic effects. *Ecology and evolution*, **9**, 12113-  
1464 12127.

1465 Graae BJ, Vandvik V, Armbruster WS, Eiserhardt WL, Svenning J-C, Hylander K, Ehrlén J, Speed JD,  
1466 Klanderud K, Bråthen KA, Milbau A, Opedal OH, Alsos IG, Ejrnaes R, Bruun HH, Birks HJB,  
1467 Westergaard KB, Birks HH, Lenoir J (2018) Stay or go—how topographic complexity influences



1468 alpine plant population and community responses to climate change. *Perspectives in plant*  
1469 *ecology, evolution and systematics*, **30**, 41-50.

1470 Greiser C, Meineri E, Luoto M, Ehrlén J, Hylander K (2018) Monthly microclimate models in a  
1471 managed boreal forest landscape. *Agricultural and Forest Meteorology*, **250**, 147-158.

1472 Grünberg I, Wilcox EJ, Zwieback S, Marsh P, Boike J (2020) Linking tundra vegetation, snow, soil  
1473 temperature, and permafrost. *Biogeosciences*, **17**, 4261-4279.

1474 Grundstein A, Todhunter P, Mote T (2005) Snowpack control over the thermal offset of air and soil  
1475 temperatures in eastern North Dakota. *Geophysical Research Letters*, **32**.

1476 Hall DK, Riggs GA, Salomonson VV, Digirolamo NE, Bayr KJ (2002) MODIS snow-cover products.  
1477 *Remote Sensing of Environment*, **83**, 181-194.

1478 Hengl T, De Jesus JM, Heuvelink GB, Gonzalez MR, Kilibarda M, Blagotić A, Shangguan W, Wright  
1479 MN, Geng X, Bauer-Marschallinger B (2017) SoilGrids250m: Global gridded soil information  
1480 based on machine learning. *Plos One*, **12**, e0169748.

1481 Hengl T, Nussbaum M, Wright MN, Heuvelink GB, Gräler B (2018) Random forest as a generic  
1482 framework for predictive modeling of spatial and spatio-temporal variables. *PeerJ*, **6**, e5518.

1483 Hennon PE, D'amore DV, Witter DT, Lamb MB (2010) Influence of forest canopy and snow on  
1484 microclimate in a declining yellow-cedar forest of Southeast Alaska. *Northwest Science*, **84**,  
1485 73-87.

1486 Holden ZA, Klene AE, Keefe RF, Moisen GG (2013) Design and evaluation of an inexpensive radiation  
1487 shield for monitoring surface air temperatures. *Agricultural and Forest Meteorology*, **180**,  
1488 281-286.

1489 Hursh A, Ballantyne A, Cooper L, Maneta M, Kimball J, Watts J (2017) The sensitivity of soil  
1490 respiration to soil temperature, moisture, and carbon supply at the global scale. *Global*  
1491 *change biology*, **23**, 2090-2103.

1492 Jian J, Steele MK, Zhang L, Bailey VL, Zheng J, Patel KF, Bond-Lamberty BP (2021) On the use of air  
1493 temperature and precipitation as surrogate predictors in soil respiration modelling.  
1494 *European Journal of Soil Science*.

1495 Johnston AS, Meade A, Ardö J, Arriga N, Black A, Blanken PD, Bonal D, Brümmer C, Cescatti A, Dušek  
1496 J (2021) Temperature thresholds of ecosystem respiration at a global scale. *Nature ecology*  
1497 *& evolution*, **5**, 487-494.

1498 Karger DN, Conrad O, Böhner J, Kawohl T, Kreft H, Soria-Auza RW, Zimmermann NE, Linder HP,  
1499 Kessler M (2017a) Climatologies at high resolution for the earth's land surface areas.  
1500 *Scientific data*, **4**, 170122.

1501 Karger DN, Conrad O, Böhner J, Kawohl T, Kreft H, Soria-Auza RW, Zimmermann NE, Linder HP,  
1502 Kessler M (2017b) Data from: Climatologies at high resolution for the earth's land surface  
1503 areas. In: *Dryad Digital Repository*.

1504 Kattge J, Bönisch G, Diaz S, Lavorel S, Prentice IC, Leadley P, Tautenhahn S, Werner G, Günther A  
1505 (2019) TRY plant trait database-enhanced coverage and open access. *Global change biology*,  
1506 **26**, 119-188.

1507 Kearney M, Porter W (2009) Mechanistic niche modelling: combining physiological and spatial data  
1508 to predict species' ranges. *Ecology letters*, **12**, 334-350.

1509 Kearney M, Shine R, Porter WP (2009) The potential for behavioral thermoregulation to buffer "cold-  
1510 blooded" animals against climate warming. *Proceedings of the National Academy of*  
1511 *Sciences*, **106**, 3835-3840.

1512 Kearney MR, Gillingham PK, Bramer I, Duffy JP, Maclean IM (2019) A method for computing hourly,  
1513 historical, terrain-corrected microclimate anywhere on Earth. *Methods in Ecology and*  
1514 *Evolution*, **11**, 38-43.

1515 Kissling WD, Walls R, Bowser A, Jones MO, Kattge J, Agosti D, Amengual J, Basset A, Van Bodegom  
1516 PM, Cornelissen JH (2018) Towards global data products of Essential Biodiversity Variables  
1517 on species traits. *Nature ecology & evolution*, **2**, 1531-1540.

1518 Körner C, Hiltbrunner E (2018) The 90 ways to describe plant temperature. *Perspectives in plant*  
1519 *ecology, evolution and systematics*, **30**, 16-21.

1520 Körner C, Paulsen J (2004) A world-wide study of high altitude treeline temperatures. *Journal of*  
1521 *biogeography*, **31**, 713-732.

1522 Lembrechts J, Aalto J, Ashcroft M, De Frenne P, Kopecký M, Lenoir J, Luoto M, Maclean IM,  
1523 Consortium S, Nijs I (2020) SoilTemp: call for data for a global database of near-surface  
1524 temperature. *Global change biology*, **26**, 6616-6629.

1525 Lembrechts J, Lenoir J, Scheffers BR, De Frenne P (2021) Time for countrywide microclimate  
1526 networks. *Global Ecology and Biogeography*.

1527 Lembrechts JJ, Lenoir J (2019) Microclimatic conditions anywhere at any time! *Global change*  
1528 *biology*.

1529 Lembrechts JJ, Lenoir J, Roth N, Hattab T, Milbau A, Haider S, Pellissier L, Pauchard A, Ratier Backes  
1530 A, Dimarco RD (2019) Comparing temperature data sources for use in species distribution  
1531 models: From in-situ logging to remote sensing. *Global Ecology and Biogeography*, **28**, 1578-  
1532 1596.

1533 Lembrechts JJ, Nijs I (2020) Microclimate shifts in a dynamic world. *Science*, **368**, 711-712.

1534 Lenoir J, Bertrand R, Comte L, Bourgeaud L, Hattab T, Murielle J, Grenouillet G (2020) Species  
1535 better track climate warming in the oceans than on land. *Nature ecology & evolution*, **4**,  
1536 1044-1059.

1537 Luojus K, Pulliainen J, Takala M, Derksen C, Rott H, Nagler T, Solberg R, Wiesmann A, Metsamaki S,  
1538 Malnes E (2010) Investigating the feasibility of the GlobSnow snow water equivalent data for  
1539 climate research purposes. In: *2010 IEEE International Geoscience and Remote Sensing*  
1540 *Symposium*. IEEE.

1541 Maclean IM, Duffy JP, Haesen S, Govaert S, De Frenne P, Vanneste T, Lenoir J, Lembrechts JJ, Rhodes  
1542 MW, Van Meerbeek K (2021) On the measurement of microclimate. *Methods in Ecology and*  
1543 *Evolution*.

1544 Maclean IM, Klings DH (2021) Microclimc: A mechanistic model of above, below and within-canopy  
1545 microclimate. *Ecological Modelling*, **451**, 109567.

1546 Maclean IM, Mosedale JR, Bennie JJ (2019) Microclima: An r package for modelling meso-and  
1547 microclimate. *Methods in Ecology and Evolution*, **10**, 280-290.

1548 Myers-Smith IH, Kerby JT, Phoenix GK, Bjerke JW, Epstein HE, Assmann JJ, John C, Andreu-Hayles L,  
1549 Angers-Blondin S, Beck PS (2020) Complexity revealed in the greening of the Arctic. *Nature*  
1550 *Climate Change*, **10**, 106-117.

1551 Niittynen P, Heikkinen RK, Aalto J, Guisan A, Kemppinen J, Luoto M (2020) Fine-scale tundra  
1552 vegetation patterns are strongly related to winter thermal conditions. *Nature Climate*  
1553 *Change*, **10**, 1143-1148.

1554 Niittynen P, Luoto M (2018) The importance of snow in species distribution models of arctic  
1555 vegetation. *Ecography*, **41**, 1024-1037.

1556 O'donnell MS, Ignizio DA (2012) Bioclimatic predictors for supporting ecological applications in the  
1557 conterminous United States. *US Geological Survey Data Series*, **691**, 4-9.

1558 Obu J, Westermann S, Bartsch A, Berdnikov N, Christiansen HH, Dashtseren A, Delaloye R, Elberling  
1559 B, Etzelmüller B, Kholodov A (2019) Northern Hemisphere permafrost map based on TTOP  
1560 modelling for 2000–2016 at 1 km<sup>2</sup> scale. *Earth-Science Reviews*, **193**, 299-316.

1561 Olden JD, Lawler JJ, Poff NL (2008) Machine learning methods without tears: a primer for ecologists.  
1562 *The Quarterly review of biology*, **83**, 171-193.

1563 Opedal OH, Armbruster WS, Graae BJ (2015) Linking small-scale topography with microclimate, plant  
1564 species diversity and intra-specific trait variation in an alpine landscape. *Plant Ecology &*  
1565 *Diversity*, **8**, 305-315.

1566 Overland JE, Wang M, Walsh JE, Stroeve JC (2014) Future Arctic climate changes: Adaptation and  
1567 mitigation time scales. *Earth's Future*, **2**, 68-74.

1568 Pastorello G, Papale D, Chu H, Trotta C, Agarwal D, Canfora E, Baldocchi D, Torn M (2017) A new data  
1569 set to keep a sharper eye on land-air exchanges. *Eos, Transactions American Geophysical*  
1570 *Union (Online)*, **98**.

1571 Perera-Castro AV, Waterman MJ, Turnbull JD, Ashcroft MB, Mckinley E, Watling JR, Bramley-Alves J,  
1572 Casanova-Katny A, Zuniga G, Flexas J (2020) It is hot in the sun: Antarctic mosses have high  
1573 temperature optima for photosynthesis despite cold climate. *Frontiers in Plant Science*, **11**,  
1574 1178.

1575 Pincebourde S, Murdock CC, Vickers M, Sears MW (2016) Fine-scale microclimatic variation can  
1576 shape the responses of organisms to global change in both natural and urban environments.  
1577 *Integrative and Comparative Biology*, **56**, 45-61.

1578 Pleim JE, Gilliam R (2009) An indirect data assimilation scheme for deep soil temperature in the  
1579 Pleim–Xiu land surface model. *Journal of Applied Meteorology and Climatology*, **48**, 1362-  
1580 1376.

1581 Portillo-Estrada M, Pihlatie M, Korhonen JFJ, Levula J, Frumau AKF, Ibrom A, Lembrechts JJ, Morillas  
1582 L, Horvath L, Jones SK, Niinemets U (2016) Climatic controls on leaf litter decomposition  
1583 across European forests and grasslands revealed by reciprocal litter transplantation  
1584 experiments. *Biogeosciences*, **13**, 1621-1633.

1585 Potter KA, Woods HA, Pincebourde S (2013) Microclimatic challenges in global change biology.  
1586 *Global change biology*, **19**, 2932-2939.

1587 R Core Team (2020) R: a language and environment for statistical computing, R Foundation for  
1588 Statistical Computing.

1589 Richardson LF (1922) *Weather prediction by numerical process*, Cambridge university press.

1590 Rosenberg NJ, Kimball B, Martin P, Cooper C (1990) From climate and CO2 enrichment to  
1591 evapotranspiration. *Climate change and US water resources.*, 151-175.

1592 Santoro M (2018) GlobBiomass—Global datasets of forest biomass. *PANGAEA10*, **1594**.

1593 Scherrer D, Schmid S, Körner C (2011) Elevational species shifts in a warmer climate are  
1594 overestimated when based on weather station data. *International journal of*  
1595 *Biometeorology*, **55**, 645-654.

1596 Schimel DS, Braswell B, Mckeown R, Ojima DS, Parton W, Pulliam W (1996) Climate and nitrogen  
1597 controls on the geography and timescales of terrestrial biogeochemical cycling. *Global*  
1598 *Biogeochemical Cycles*, **10**, 677-692.

1599 Schimel JP, Bilbrough C, Welker JM (2004) Increased snow depth affects microbial activity and  
1600 nitrogen mineralization in two Arctic tundra communities. *Soil Biology and Biochemistry*, **36**,  
1601 217-227.

1602 Senior RA, Hill JK, Edwards DP (2019) Global loss of climate connectivity in tropical forests. *Nature*  
1603 *Climate Change*, **9**, 623-626.

1604 Smith M, Riseborough D (1996) Permafrost monitoring and detection of climate change. *Permafrost*  
1605 *and Periglacial Processes*, **7**, 301-309.

1606 Smith M, Riseborough D (2002) Climate and the limits of permafrost: a zonal analysis. *Permafrost*  
1607 *and Periglacial Processes*, **13**, 1-15.

1608 Soudzilovskaia NA, Douma JC, Akhmetzhanova AA, Van Bodegom PM, Cornwell WK, Moens EJ,  
1609 Treseder KK, Tibbett M, Wang YP, Cornelissen JH (2015) Global patterns of plant root  
1610 colonization intensity by mycorrhizal fungi explained by climate and soil chemistry. *Global*  
1611 *Ecology and Biogeography*, **24**, 371-382.

1612 Stefan V, Levin S (2018) Plotbiomes: Plot Whittaker biomes with ggplot2. R package version 0.0.  
1613 0.9001.

1614 Steidinger BS, Crowther TW, Liang J, Van Nuland ME, Werner GD, Reich PB, Nabuurs G-J, De-Miguel  
1615 S, Zhou M, Picard N (2019) Climatic controls of decomposition drive the global biogeography  
1616 of forest-tree symbioses. *Nature*, **569**, 404-408.

- 1617 Terando AJ, Youngsteadt E, Meineke EK, Prado SG (2017) Ad hoc instrumentation methods in  
 1618 ecological studies produce highly biased temperature measurements. *Ecology and evolution*,  
 1619 **7**, 9890-9904.
- 1620 Van Den Hoogen J, Geisen S, Routh D, Ferris H, Traunspurger W, Wardle DA, De Goede RG, Adams  
 1621 BJ, Ahmad W, Andriuzzi WS (2019) Soil nematode abundance and functional group  
 1622 composition at a global scale. *Nature*, **572**, 194-198.
- 1623 Van Den Hoogen J, Robmann N, Routh D, Lauber T, Van Tiel N, Danylo O, Crowther TW (2021) A  
 1624 geospatial mapping pipeline for ecologists. *bioRxiv*,  
 1625 <https://doi.org/10.1101/2021.07.07.451145>.
- 1626 Wang K, Dickinson RE (2012) A review of global terrestrial evapotranspiration: Observation,  
 1627 modeling, climatology, and climatic variability. *Reviews of Geophysics*, **50**.
- 1628 Way RG, Lewkowicz AG (2018) Environmental controls on ground temperature and permafrost in  
 1629 Labrador, northeast Canada. *Permafrost and Periglacial Processes*, **29**, 73-85.
- 1630 White HJ, León-Sánchez L, Burton VJ, Cameron EK, Caruso T, Cunha L, Dirilgen T, Jurburg SD, Kelly R,  
 1631 Kumaresan D (2020) Methods and approaches to advance soil macroecology. *Global Ecology  
 1632 and Biogeography*, **29**, 1674-1690.
- 1633 Whiteman CD (1982) Breakup of temperature inversions in deep mountain valleys: Part I.  
 1634 Observations. *Journal of Applied Meteorology*, **21**, 270-289.
- 1635 Wild J, Kopecký M, Macek M, Šanda M, Jankovec J, Haase T (2019) Climate at ecologically relevant  
 1636 scales: A new temperature and soil moisture logger for long-term microclimate  
 1637 measurement. *Agricultural and Forest Meteorology*, **268**, 40-47.
- 1638 Wood S (2012) mgcv: Mixed GAM Computation Vehicle with GCV/AIC/REML smoothness estimation.  
 1639 World Meteorological Organization (2008) *Guide to Meteorological Instruments and Methods of  
 1640 Observation*, Geneva, WMO-No. 8.
- 1641 Xu T, Hutchinson M (2011) ANUCLIM version 6.1 user guide. The Australian National University,  
 1642 Fenner School of Environment and Society, Canberra.
- 1643 Xu Y, Ramanathan V, Victor DG (2018) Global warming will happen faster than we think. *Nature*.  
 1644 Zellweger F, De Frenne P, Lenoir J, Vangansbeke P, Verheyen K, Bernhardt-Römermann M, Baeten L,  
 1645 Hédli R, Berki I, Brunet J, Van Calster H, Chudomelová M, Decocq G, Dirnböck T, Durak T,  
 1646 Heinken T, Jaroszewicz B, Kopecký M, Malis F, Macek M, Marek M, Naaf T, Nagel TA,  
 1647 Ortman-Ajkai A, Petrik P, Pielech R, Reczynska K, Schmidt W, Standovár T, Swierkosz K,  
 1648 Teleki B, Vild O, Wulf M, Coomes D (2020) Forest microclimate dynamics drive plant  
 1649 responses to warming. *Science*, **368**, 772-775.
- 1650 Zhang Y, Sherstiukov AB, Qian B, Kokelj SV, Lantz TC (2018) Impacts of snow on soil temperature  
 1651 observed across the circumpolar north. *Environmental Research Letters*, **13**, 044012.
- 1652 Zhang Y, Wang S, Barr AG, Black T (2008) Impact of snow cover on soil temperature and its  
 1653 simulation in a boreal aspen forest. *Cold Regions Science and Technology*, **52**, 355-370.
- 1654 Zhou S, Williams AP, Lintner BR, Berg AM, Zhang Y, Keenan TF, Cook BI, Hagemann S, Seneviratne SI,  
 1655 Gentile P (2021) Soil moisture–atmosphere feedbacks mitigate declining water availability  
 1656 in drylands. *Nature Climate Change*, 1-7.
- 1657 Zomer RJ, Trabucco A, Bossio DA, Verchot LV (2008) Climate change mitigation: A spatial analysis of  
 1658 global land suitability for clean development mechanism afforestation and reforestation.  
 1659 *Agriculture, ecosystems & environment*, **126**, 67-80.

1660  
 1661  
 1662  
 1663  
 1664



1666 **Tables**

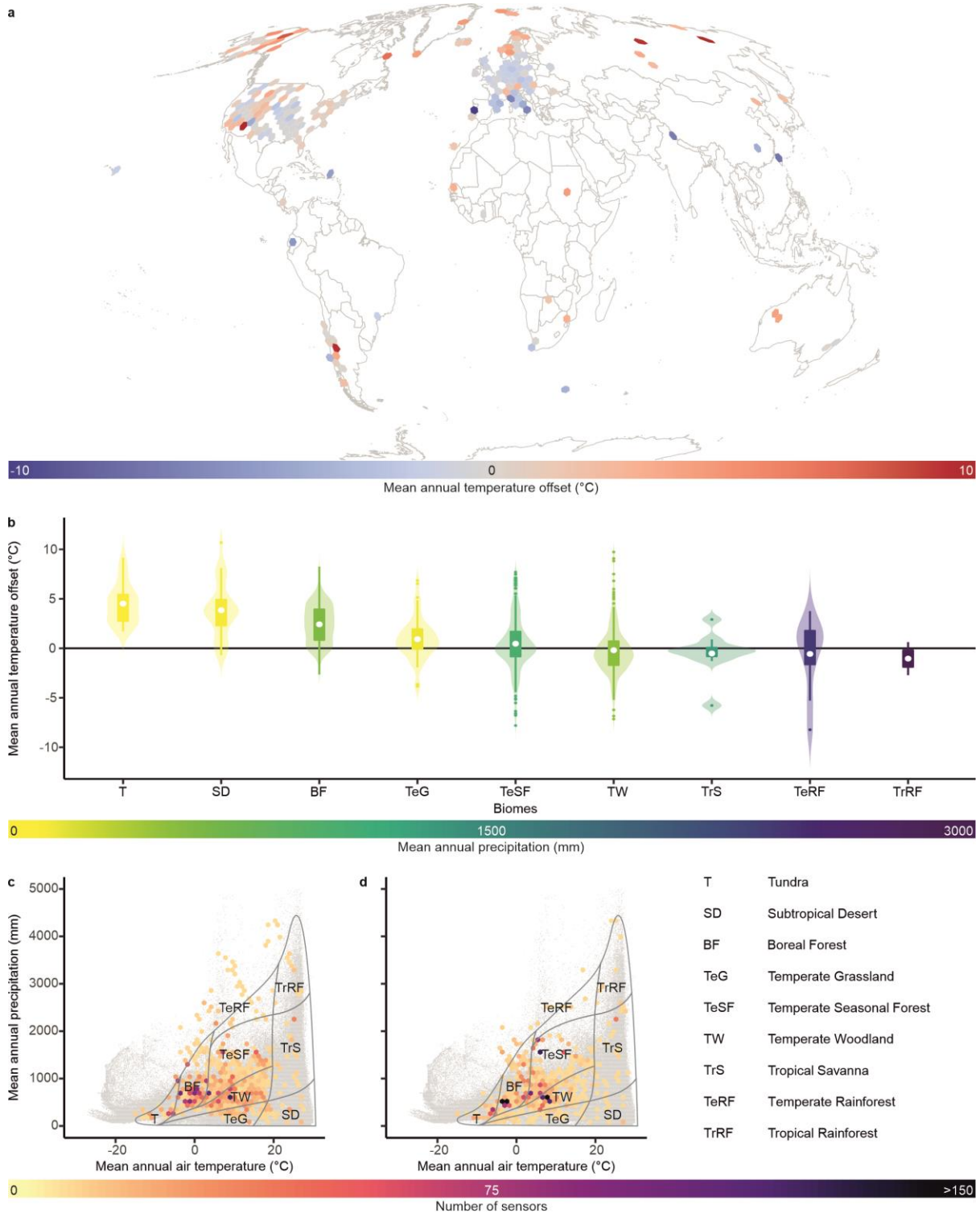
1667 **Table 1:** Overview of soil bioclimatic variables as calculated in this study.

<b>Bioclimatic variable</b>	<b>Meaning</b>
SBIO1	annual mean temperature
SBIO2	mean diurnal range (mean of monthly (max temp - min temp))
SBIO3	isothermality (SBIO2/SBIO7) (×100)
SBIO4	temperature seasonality (standard deviation ×100)
SBIO5	max temperature of warmest month
SBIO6	min temperature of coldest month
SBIO7	temperature annual range (SBIO5-SBIO6)
SBIO8	mean temperature of wettest quarter
SBIO9	mean temperature of driest quarter
SBIO10	mean temperature of warmest quarter
SBIO11	mean temperature of coldest quarter

1668

1669

1670



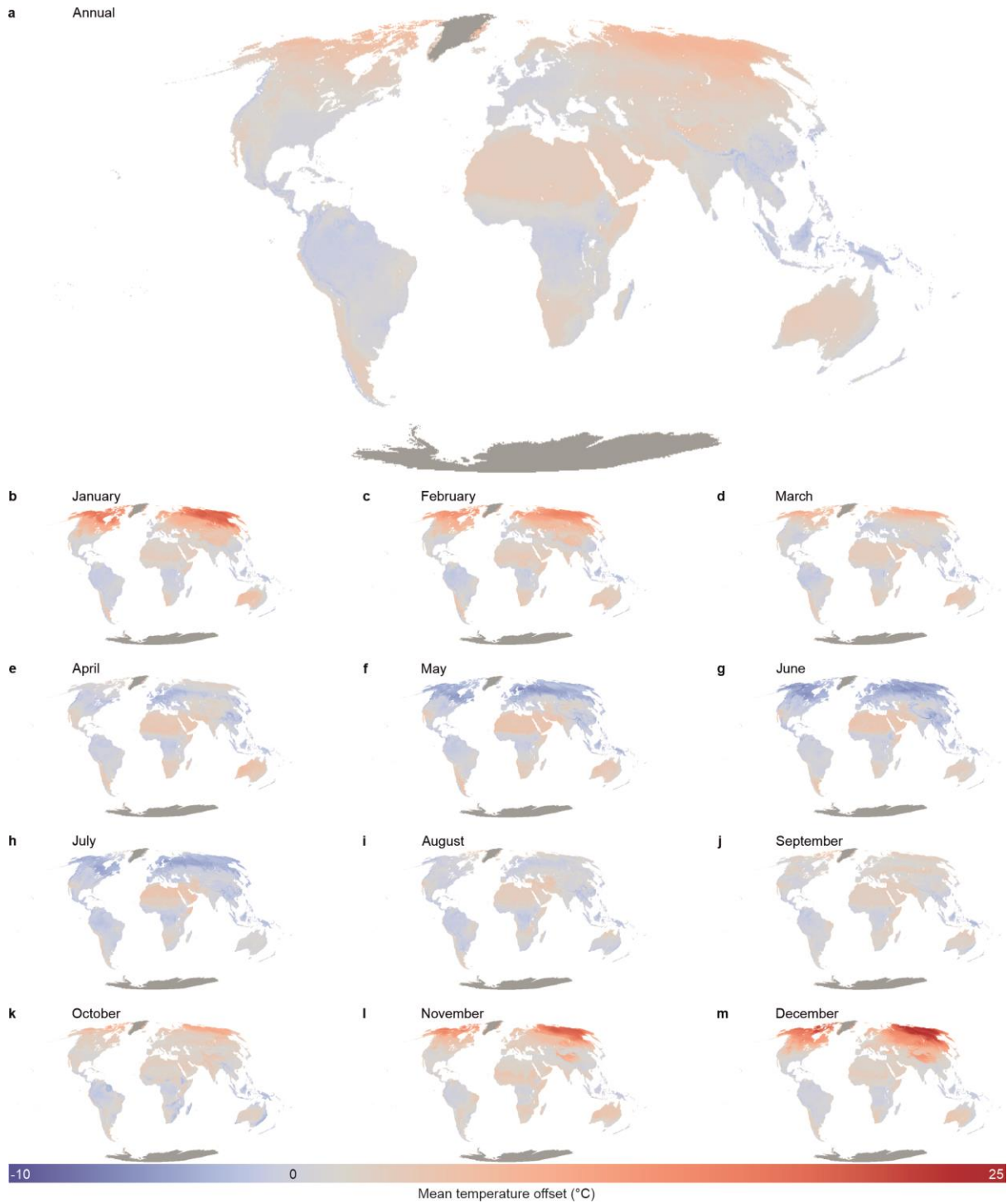
1672

1673 **Figure 1: Temperature offsets between soil and air temperature differed significantly among**  
 1674 **biomes.** (a) Distribution of in-situ measurement locations across the globe, coloured by the mean  
 1675 annual temperature offset (in °C) between in situ measured soil temperature (topsoil, 0–5 cm depth)  
 1676 and gridded air temperature (ERA5L). Offsets were averaged per hexagon, each with a size of  
 1677 approximately 70,000 km<sup>2</sup>. Mollweide projection. (b) Mean annual temperature offsets per Whittaker  
 1678 biome (adapted from Whittaker 1970, based on geographic location of sensors averaged at 1 km<sup>2</sup>; 0–  
 1679 5 cm depth), ordered by mean temperature offset and coloured by mean annual precipitation. (c–d)

1680 *Distribution of sensors in 2D climate space for the topsoil (c, 0–5 cm depth, N = 4530) and the second*  
1681 *layer (d, 5–15 cm depth, N = 3989). Colours of hexagons indicate the number of sensors at each climatic*  
1682 *location, with a 40 × 40 km resolution. Grey dots in the background represent the global variation in*  
1683 *climatic space (obtained by sampling 1,000,000 random locations from the CHELSA world maps).*  
1684 *Overlay with grey lines depicts a delineation of Whittaker biomes.*

1685



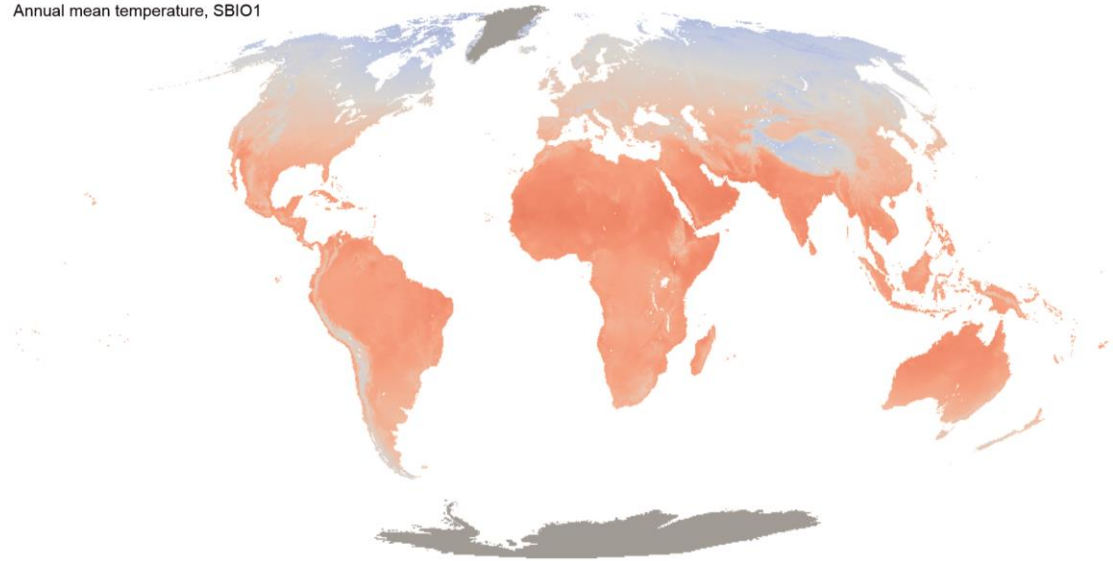


1687

1688 **Figure 2: Global modelled temperature offsets between soil and air temperature show strong**  
 1689 **spatiotemporal variation across months.** Modelled annual (a) and monthly (b–m) temperature  
 1690 offset (in °C) between in situ measured soil temperature (topsoil, 0–5 cm) and gridded air  
 1691 temperature. Positive (red) values indicate soils that are warmer than the air. Dark grey represents  
 1692 regions outside the modelling area.

1693

a Annual mean temperature, SBIO1



b Mean Diurnal Range  
Mean of monthly (max - min), SBIO2



c Max Temperature of  
Warmest Month, SBIO5



d Min Temperature of  
Coldest Month, SBIO6



e Temperature Annual Range  
SBIO5 - SBIO6 = SBIO7



f Mean Temperature of  
Wettest Quarter, SBIO8



g Mean Temperature of  
Driest Quarter, SBIO9



h Mean Temperature of  
Warmest Quarter, SBIO10



i Mean Temperature of  
Coldest Quarter, SBIO11



j Isothermality  
SBIO2 / SBIO7 (×100) = SBIO3



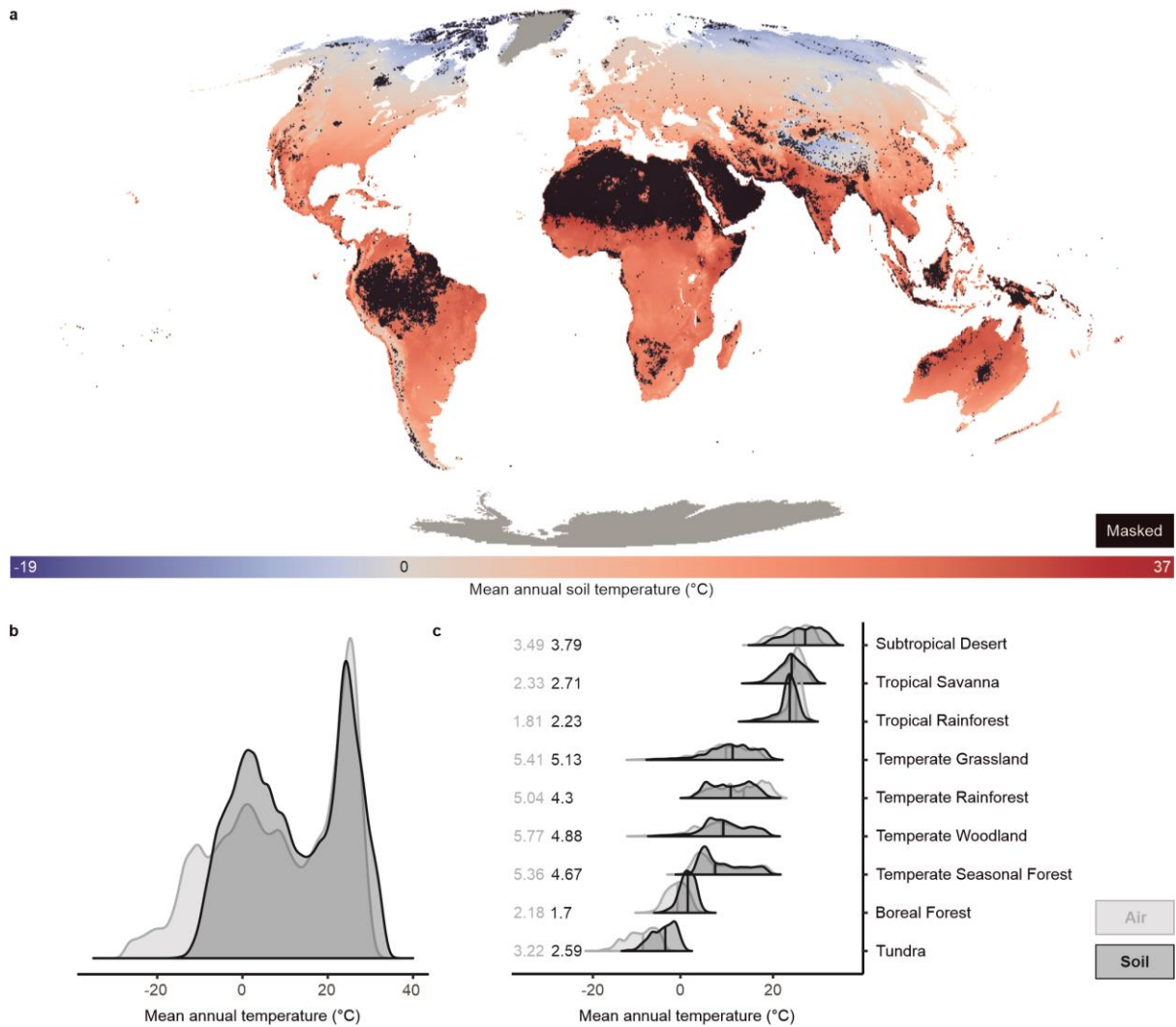
k Temperature Seasonality  
Standard deviation (×100), SBIO4



1694  
1695  
1696  
1697

**Figure 3: Soil bioclimatic variables.** Global maps of bioclimatic variables for topsoil (0–5 cm depth) climate, calculated using the maps of monthly soil climate (see Fig. 2), and the bioclimatic variables for air temperature from CHLSA.

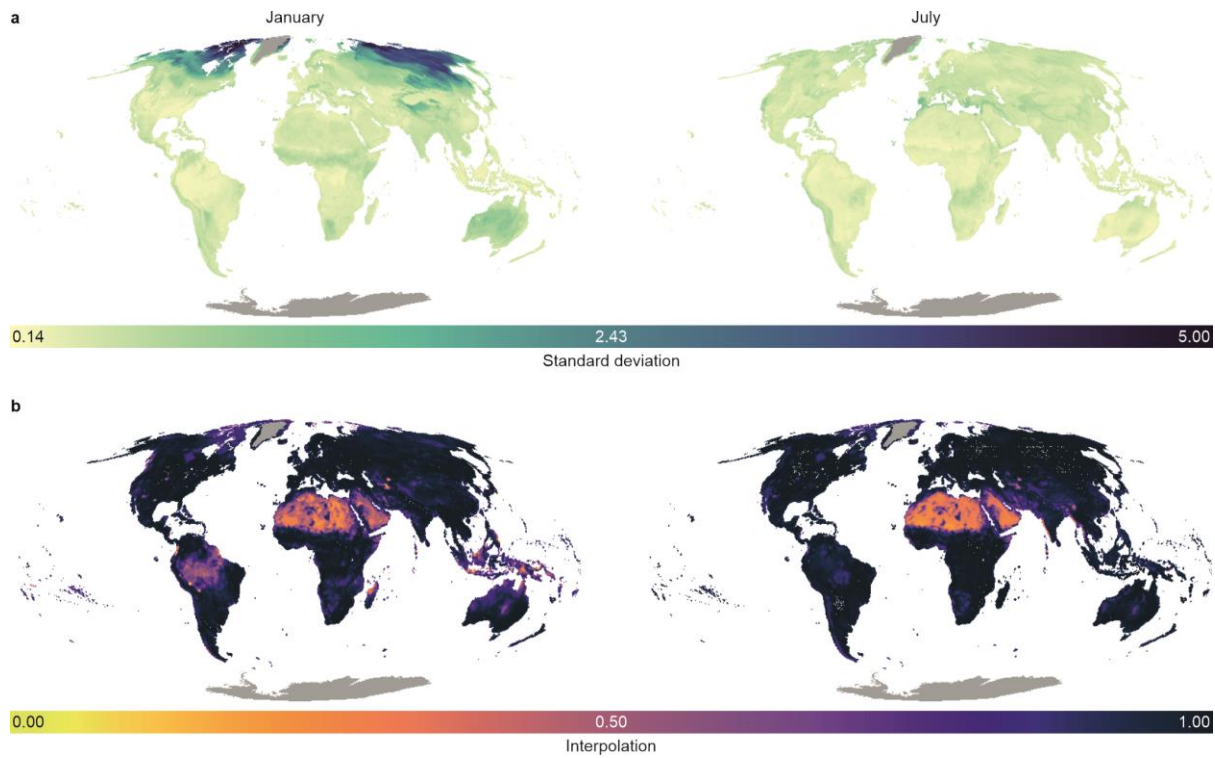
1698



1699

1700 **Figure 4: Mean annual soil temperature shows significantly lower spatial variability than air**  
 1701 **temperature.** (a) Global map of mean annual topsoil temperature (SBIO1, 0–5 cm depth, in °C), created  
 1702 by adding the monthly offset between soil and air temperature for the period 2000–2020 (Fig. 2) to  
 1703 the monthly air temperature from CHELSA. A black mask is used to exclude regions where our models  
 1704 are extrapolating (i.e., interpolation values in Fig. 5 are < 0.9, 18% of pixels). Dark grey represents  
 1705 regions outside the modelling area. (b–c) Density plots of mean annual soil temperature across the  
 1706 globe (b) and for each Whittaker biome separately (c) for SBIO1 (dark grey, soil temperature),  
 1707 compared with BIO1 from CHELSA (light grey, air temperature), created by extracting 1 000 000  
 1708 random points from the 1-km<sup>2</sup> gridded bioclimatic products. The numbers in (c) represent the standard  
 1709 deviations of air temperature (light grey) and soil temperature (dark grey). Biomes are ordered  
 1710 according to the median annual soil temperature values (vertical black line) from the highest  
 1711 temperature (subtropical desert) to the lowest (tundra).

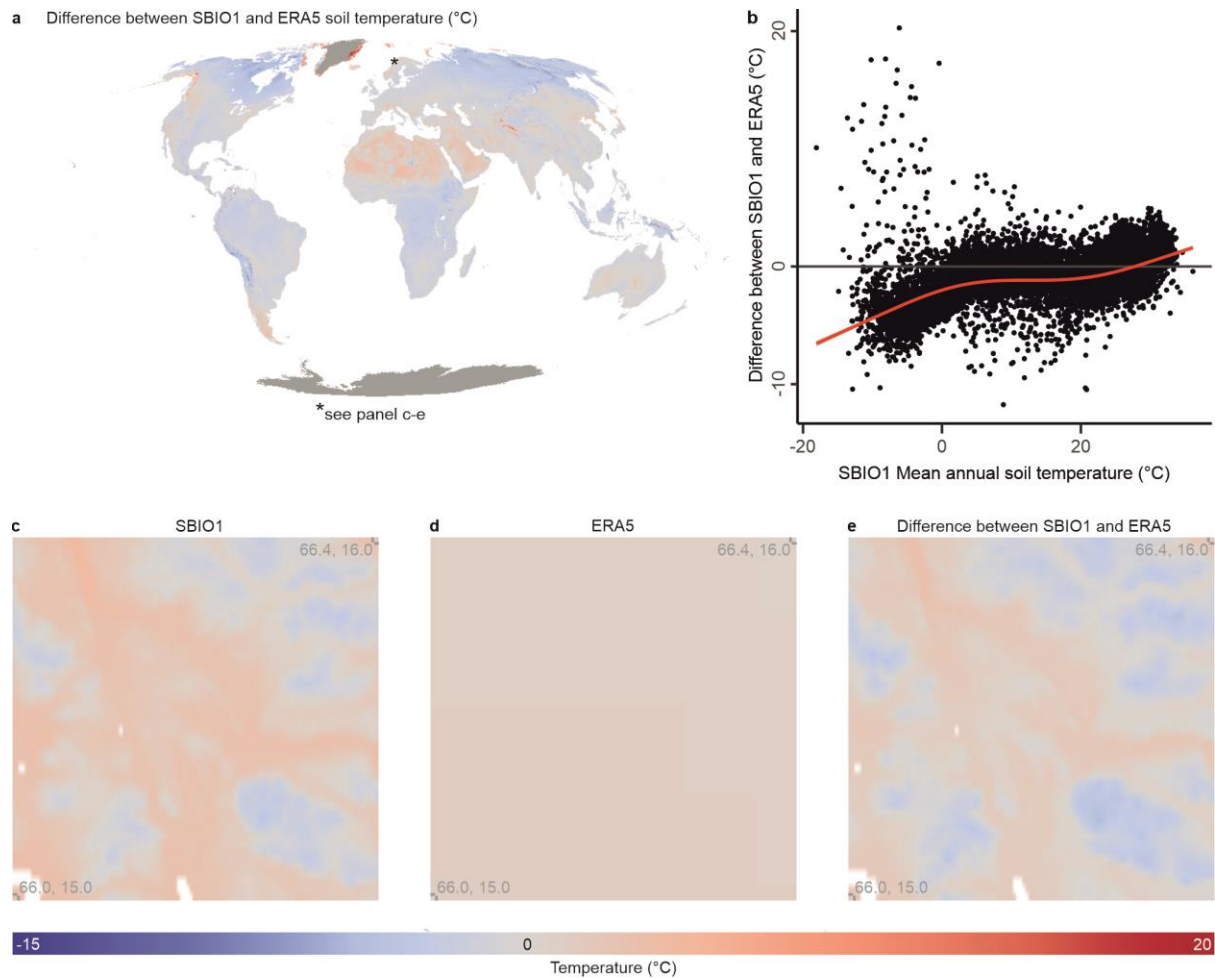
1712



1713

1714 **Figure 5: Models of the temperature offset between soil and air temperature have low standard**  
 1715 **deviations and good global coverage.** Analyses for the temperature offset between in situ measured  
 1716 topsoil (0–5 cm depth) temperature and gridded air temperature. (a) Standard deviation (in °C) over  
 1717 the predictions from a cross-validation analysis that iteratively varied the set of covariates  
 1718 (explanatory data layers) and model hyperparameters across 100 models and evaluated model  
 1719 strength using 10-fold cross-validation, for January (left) and July (right), as examples of the two most  
 1720 contrasting months. (b) The fraction of axes in the multidimensional environmental space for which  
 1721 the pixel lies inside the range of data covered by the sensors in the database. Low values indicate  
 1722 increased extrapolation.

1723



1724

1725 **Figure 6: The mean annual soil temperature (SBIO1, 1 x 1 km resolution) modelled here is**  
 1726 **consistently cooler than ERA5L (9 x 9 km) soil temperature in forested areas.** (a) Spatial  
 1727 representation of the difference between SBIO1 based on our model and based on ERA5L soil  
 1728 temperature data. Negative values (blue colours) indicate areas where our model predicts cooler soil  
 1729 temperature. Dark grey areas (Greenland and Antarctica) are excluded from our models. Asterisk in  
 1730 Scandinavia indicates the highlighted area in panels d to f (see below). (b) Distribution of the difference  
 1731 between SBIO1 and ERA5L along the macroclimatic gradient (represented by SBIO1 itself) based on a  
 1732 random subsample of 50 000 points from the map in a). Red line from a Generalized Additive Model  
 1733 (GAM) with  $k=4$ . (c-e) High-resolution zoomed panels of an area of high elevational contrast in Norway  
 1734 (from 66.0-66.4° N, 15.0-16.0° E) visualizing SBIO1 (c), ERA5L (d) and their difference (e), to highlight  
 1735 the higher spatial resolution as obtained with SBIO1.

1736